CRCLEME

Cooperative Research Centre for
Landscape Environments
and Mineral Exploration

OPEN FILE
REPORT
SERIES

GEOPHYSICAL AND REMOTE SENSING METHODS FOR REGOLITH EXPLORATION

Edited by
Eva Papp

CRC LEME OPEN FILE REPORT 144

July 2002

CRCLEME

CRC LEME is an unincorporated joint venture between CSIRO-Exploration & Mining, and Land & Water, The Australian National University, Curtin University of Technology, University of Adelaide, University of Canberra, Geoscience Australia, Bureau of Rural Sciences, Primary Industries and Resources SA, NSW Department of Mineral Resources-Geological Survey and Minerals Council of Australia, established and supported under the Australian Government's Cooperative Research Centres Program.

CRC
AUSTRALIA

GEOPHYSICAL AND REMOTE SENSING METHODS FOR REGOLITH EXPLORATION

Edited by
Eva Papp

CRC LEME OPEN FILE REPORT 144

July2002

CRC LEME is an unincorporated joint venture between CSIRO-Exploration & Mining, and Land & Water, The Australian National University, Curtin University of Technology, University of Adelaide, University of Canberra, Geoscience Australia, Bureau of Rural Sciences, Primary Industries and Resources SA, NSW Department of Mineral Resources-Geological Survey and Minerals Council of Australia.
Headquarters: CRC LEME c/o CSIRO Exploration and Mining, PO Box 1130, Bentley WA 6102, Australia

This report presents a collection of brief articles on geophysical and remote sensing methodologies suitable for regolith exploration, brought together by staff from the CRC for Landscape Environments and Mineral Exploration. The work is unencumbered by any confidentiality agreements.

Copies of this publication can be obtained from:
The Publications Officer, c/- CRC LEME, CSIRO Exploration and Mining, PO Box 1130, Bentley, WA 6102, Australia. Information on other publications in this series may be obtained from the above, or from http://crcleme.org.au/
Cataloguing-in-publication:
Papp, E. (Ed.)
Geophysical and Remote Sensing Methods for Regolith Exploration
ISBN 0 643 06844 9
1. Regolith – Australia, 2. Geophysics, 3. Remote sensing
I. Title
CRC LEME Open File Report 144.
ISSN 1329-4768

Editors affiliation and address:

Éva Papp: Cooperative Research Centre for
Landscape Environments and Mineral Exploration (CRC LEME).
Department of Geology
Australian National University
Canberra, ACT 0200.
Ph: 02 6238 2114.
E-mail: Eva.Papp@ga.gov.au

PREFACE

The purpose of the volume is to provide source material for students, geologists and geophysicists in the form of a collection of brief articles on geophysical and remote sensing methodologies suitable for regolith exploration. The articles do not contain detailed information on how each method works, but are rather intended as a guide to selecting the appropriate method for a particular exploration or environmental problem.

A number of factors contributed to the initiation of this project. Firstly, a realisation that there is very little material available on regolith geophysics that could be used by mineral exploration professionals to make important decisions about the application or deterrence of certain geophysical or remote sensing techniques. Secondly, the scarcity of material on this topic that can be used for teaching purposes at undergraduate university level. Thirdly, the success of Brad Pillans' booklet titled "Regolith dating methods", a CRC LEME publication, showed that there is a lot of interest among the professional community in practical, off-the-shelf material in regolith exploration methodologies.

The booklet contains twelve articles. Each article describes a remote sensing or a geophysical technique suitable for regolith exploration. The papers are organised in a similar structure, with the intention of aiding the reader in the comparison of the methods. After a brief general description, the advantages and pitfalls of each method are presented, as well as the likely product of a survey. This is followed by one or more case histories, the organisational requirements of a field survey, the likely costs, and finally addresses of the main organisations providing the service.

We believe that with this volume CRCLEME is providing a service to the exploration and environmental geophysics community as well as providing a valuable aid for teaching mineral exploration students.

Éva Papp
Editor

CONTENTS

LIST OF FIGURES

Airborne and Ground Magnetics

Airborne Gamma-ray Spectrometry

Ground and Airborne Electromagnetic Methods

Ground Penetrating Radar

Ground Acoustic Penetration

Seismic surveys for imaging the regolith

Gravity

Geophysical well logging

VERTICAL AERIAL PHOTOGRAPHY

Mike Craig
Cooperative Research Centre for Landscape Environments and Mineral Exploration, Geoscience Australia. PO Box 378, Canberra, ACT 2601. E-mail: mike.craig@ga.gov.au

1. DESCRIPTION

Aerial photographs (sometimes called airphotos) are often the first choice of imagery datasets available to help interpret regolith landform characteristics especially for mineral exploration. Aerial photographs are easy to use, especially for lesser-experienced interpreters. Photographs are often more widely applicable because they are based on the visible portion of the spectrum and can provide more easily identifiable ground features with which to work. The use of ordinary photographs, mostly as contact prints either black and white or often colour, is a widely practiced and well known technique for obtaining geological information otherwise not readily available. Regolith is part of that geological information, and can be interpreted from photographs. Regolith characteristics are closely related to landform characteristics and landform evolution. Regolith and landform attributes are more easily recognised by interpreters with training in geomorphology.

Vertical aerial photographs are taken with the camera pointing vertically towards the ground surface. Other orientations are possible such as high angle oblique where the tilt of the camera includes the horizon or low angle oblique where the tilt of the camera is insufficient to include the horizon. The major advantage in the use of vertical aerial photographs comes from their ability to show the landscape and its features in three dimensions as a stereomodel. Stereomodels are usually seen with the aid of a stereoscopic viewer to view two photographs simultaneously. The photographs are taken usually in the visible light spectrum in an overlapping arrangement that permits scene duplication on at least two successive frames. This duplication is known as stereoscopic overlap. Often the overlap between photographs is optimised at 60% in the forward direction forward-lap and 30% as sidelap. With this arrangement, every second photo is sufficient to provide a satisfactory stereomodel. The complete suite therefore can be divided into an alternate set, a conjugate set, and either set can be used for interpretation.

Regardless of whether sequential photos or alternate photos are used to establish and view a stereomodel there is an element of vertical exaggeration introduced into the vertical scale of the model. This is due to the vertical scale being greater than the horizontal scale. The degree of exaggeration present in the model is related to the separation of the photo centres (ie. principal points) and the geometry of the viewing apparatus. The exaggeration that stereoscopic viewing of photos in alternate number sets induces is double the vertical exaggeration of photos viewed in sequential number order. (As a rough rule of thumb the vertical exaggeration seen in the 3D model from stereoscopic viewing of normal sequential 60% overlap photography, is between 3-4 times the horizontal scale).

Contained on each aerial photographic print is a strip of information known as the title strip. The title strip is usually located on one edge of each individual photograph and contains details relevant to that photograph. The title strip typically includes: the name of the geographic sheet, or of the local area on the ground, over which the photograph was taken, a number specific to that photo (identifying the order of acquisition within the flight line), flying altitude (above sea level) at time of photography, the identity number of the negative on which the photo occurs, the focal length of the lens on the camera used (the nominal photo scale is derived by determining the ratio of the focal length of the camera lens divided by the flying altitude – all in common units), a designator of the camera type (eg. RC 9), and an arrow indicating the general direction of North.

In Papp, É. (Editor), 2002, *Geophysical and Remote Sensing Methods for Regolith Exploration*, CRCLEME Open File Report 144, pp 1-5.

There are possible errors introduced at the time of acquiring aerial photography. It is best to be aware of these errors because they can make using aerial photos more awkward. The error caused by plane drift during photo acquisition is characterised by the photo edges being parallel but not collinear within one flight line (also known as a run). Between successive flight lines, drift can cause the sidelap to be highly variable or sometimes non-existent. Crab error on the other hand results in twisting of the photo orientation so that the photo edges are not parallel with the flight line. Usually, crab results from an effort to correct drift without the necessary correction to aircraft heading. Aircraft induced pitch, yaw and roll errors can also be incorporated into vertical aerial photographs and may need to be removed in particular circumstances. These errors will not be discussed here.

Runs of airphotographs may be arranged to form a complete coverage of a designated area. They can be assembled in ways to reduce feature mismatch, further manipulated to reduce tonal differences or just assemble without modification. Print laydowns are assemblages of sequences of aerial photos, usually every second print in their correct relative positions to provide an approximate unrectified map. This may be rephotographed and form a photoindex. The prints may be cut to eliminate the distorted portions and then these parts fitted together along fencelines, roads, rivers and ridge crests for example to form a jigsaw puzzle like map. It is still not geographically correct and is said to be an uncontrolled photomosaic. If careful correction of differences in scale, tone, tilt of each print is carried out, a controlled photomosaic can be produced. These may be sold by the various agencies. They may cost many tens of dollars, depending on the area required and scales involved. Digital photogrammetry is now more readily available through contractors and is increasingly used to produce such products. The cost is sometimes a little less and may be already produced in areas of significant exploration activity. Sometimes digital elevation models are a by-product of this work and may be available at affordable prices. They can be important additional datasets to help with interpretations.

2. FIELD PROCEDURES

Preliminary interpretation may be made prior to visiting the field. Ultimately though the interpreter reaches a point where experience fails to resolve uncertainties in interpretation. Field calibration of photographic images is usually required by the interpreter to resolve uncertainties. Once the relief patterns, tones, textures, and perhaps colours in the photopatterns are understood a more reliable interpretation can result. Calibration may sometimes be possible and be based only on the interpreters prior experience. There are no hard and fast rules; each case is different. Photopatterns are calibrated by collecting attributes describing the regolith materials and landform characteristics. All attribute descriptions are usually linked to the observation point marked on the photographs. These represent the calibration points and form part of the more general site descriptions recorded during fieldwork. The points should be spatially located by way of some form of geographic coordinate for later more accurate construction of maps whether hard copy or digital.

3. DATA PROCESSING

Mostly processing of aerial photographs, because they are from the visible spectrum, is done through the eyes (with the aid of optical instruments) of trained experienced interpreters. Aerial photographs can be reprocessed by computer manipulation using specialised software packages. This should only be undertaken by experienced interpreters with the required computing skills. The "black-box" approach can be a trap for the inexperienced.

4. DATA INTERPRETATION

Interpretation is mostly experience-based because of the complexity of photopatterns and the variability of problems encountered. Many of the regolith landform features outlined in RTMAP (Pain, et al., 1991) can be recognised to varying degrees. Training in geomorphology makes the task of interpretation of regolith landform features from aerial photographs and in the field much easier.

Potential mappers and interpreters should at least read the RTMAP guidelines if they lack basic training in geomorphology or have little field experience.

Some more basic interpretative techniques eventually may be available in the future through automated computer analysis using knowledge-based rule systems; but this is not yet routinely used. Interpreters using aerial photographs will usually have to rely on their knowledge of relief, patterns, tones, textures, and colours present in the photopatterns. Ideally, interpreter experience and reliability will be improved by repeated comparisons with numerous stereomodel characteristics and actual ground surface features.

5. APPLICATIONS

Geology, regolith, land-use, soils, forestry, engineering, urban planning, natural hazards are a few examples of studies where aerial photographs may be used to help provide interpretations.

6. PROBLEMS AND LIMITATIONS

Photographs may not necessarily show all the features you may hope to identify or distinguish and therefore other forms of remotely sensed imagery may be needed eg. satellite thematic mapper; radar; magnetics; EM; radiometric; to name a few. The lack of tonal contrast can be a problem with photographic prints from time to time. This can sometimes be overcome by reprocessing scanned images by computer image-manipulation software. Care must be taken to scan them at sufficiently high resolution so that their usefulness is not severely reduced. Resolution is usually not a problem with reasonable quality commercial aerial photographic prints. Sometimes the scale may not suit your purpose but you may have to adapt if other scales are not available and you cannot afford to have custom photographs generated commercially. There is often an exaggeration factor (2x to 3x) using aerial photographs and stereoscopic viewers.

7. SURVEY ORGANISATIONS

Suppliers of aerial photography range from government departments to private contractors. Private contractors are sometimes used by the government departments as well. The national survey organisation is probably the best place to start inquiries for obtaining aerial photographs. In Australia, this Department is currently known as AUSLIG. AUSLIG staff can tell you who is its current outsourced supplier for aerial photographs are for much of Australia. These photos may not be at the scale you require. They may not cover the specific area of your interest and therefore you may need to direct your inquiries to the State Government Survey responsible for Lands or Mapping -they may have an outsourced supplier as well. Commonwealth Government generated photography goes back many years - as early as the 1920's but more significantly in the late 1940's.

The first aerial photography from which a map (photomap) was made in Australia was carried out in 1922 and scattered localised coverages were acquired in the following years. In 1924, the first systematic aerial photography of a mining field was at Mt Isa. However, it was not until after World War 2 that a concerted program of systematic regional coverage was implemented utilising the RAAF aerial photographic squadron's capability. This program was subsequently expanded using commercial operators and State agencies to produce the "K17" regional coverage over most of Australia. This comprised panchromatic photography at a nominal scale of 1:50,000 with a forward overlap between photographs of 60%. The photography name ie. K17 is derived from the designation of the camera used.

In 1960, a program of photography at a nominal scale of 1:84,000 was developed using the RC9 super wide-angle camera that produced a flight-line coverage with an 80% forward overlap. The K17 and RC9 photography represent the only near complete nationally consistent coverages flown in Australia. Many other coverages of local and regional areas are available at different scales and photo types (panchromatic, colour, high altitude etc.) through government and commercial agencies (Lines, 1992). Photographs at 1:50,000 scale are often obtainable from State Lands Survey Offices or their outsourced agents. Currently, no simple accurate guidelines for suppliers can be provided. The circumstances now change over time. You can currently view the flight line diagrams for Commonwealth generated photography at: http://www.ga.gov.au/products/photos. From that site, you may be able to follow links to other outsourced suppliers and State Government agencies.

8. COSTS

Each organisation has its own costing arrangements. Therefore it would not be instructive to quote current costs but suffice to say that the unit cost for small numbers of prints is usually much higher than for large numbers of prints. Prices in the past have been around twenty dollars for low number individual prints. There is often an access or retrieval cost if films are archived and that fee may be around thirty dollars. This access fee is usually built into the overall cost structure for large orders. Costs also vary depending on if you require positive prints or transparencies ie. diapositives. Other cost factors would depend on whether colour or black and white photos were required, the number of duplicates or even single prints you require from the same roll of film. Single prints from many different films are often a costly purchase.

9. EXAMPLE INTERPRETATION

Figure 1 shows an example of an area near Higginsville, south of Kambalda, in the Eastern Goldfields of Western Australia where aerial photography has been used to assist in the generation of a regolith landform map. The regolith polygon interpretations can be seen on the black and white aerial photographic basemap. An extract of the final map now replaces the corresponding area on the basemap. This example shows the progression from aerial photographic polygon interpretation through to selected portion of the final map.

REFERENCES

Lines, J. D., 1992. Australia on Paper. The Story of Australian Mapping. Fortune Publications, Box Hill, Victoria, 343 pp.

Lintern, M. J., Craig, M. A., Walsh, D. M., and Sheridan, N. C., 1996. The Distribution of Gold and Other Elements in Surficial Materials from the Higginsville Palaeochannel Gold Deposits, Norseman, Western Australia. CRCLEME AMIRA Project 409. CRC LEME restricted report 28R. 38 pp. and 66 pp.

Pain, C. F., Chan, R. A., Craig M. A., Hazell, M., Kamprad, J. and Wilford, J., 1991. RTMAP, BMR regolith database field handbook. Minerals and Landuse Program, Series 1. Bureau of Mineral Resources Geology and Geophysics, Record 1991/29. 125 pp.

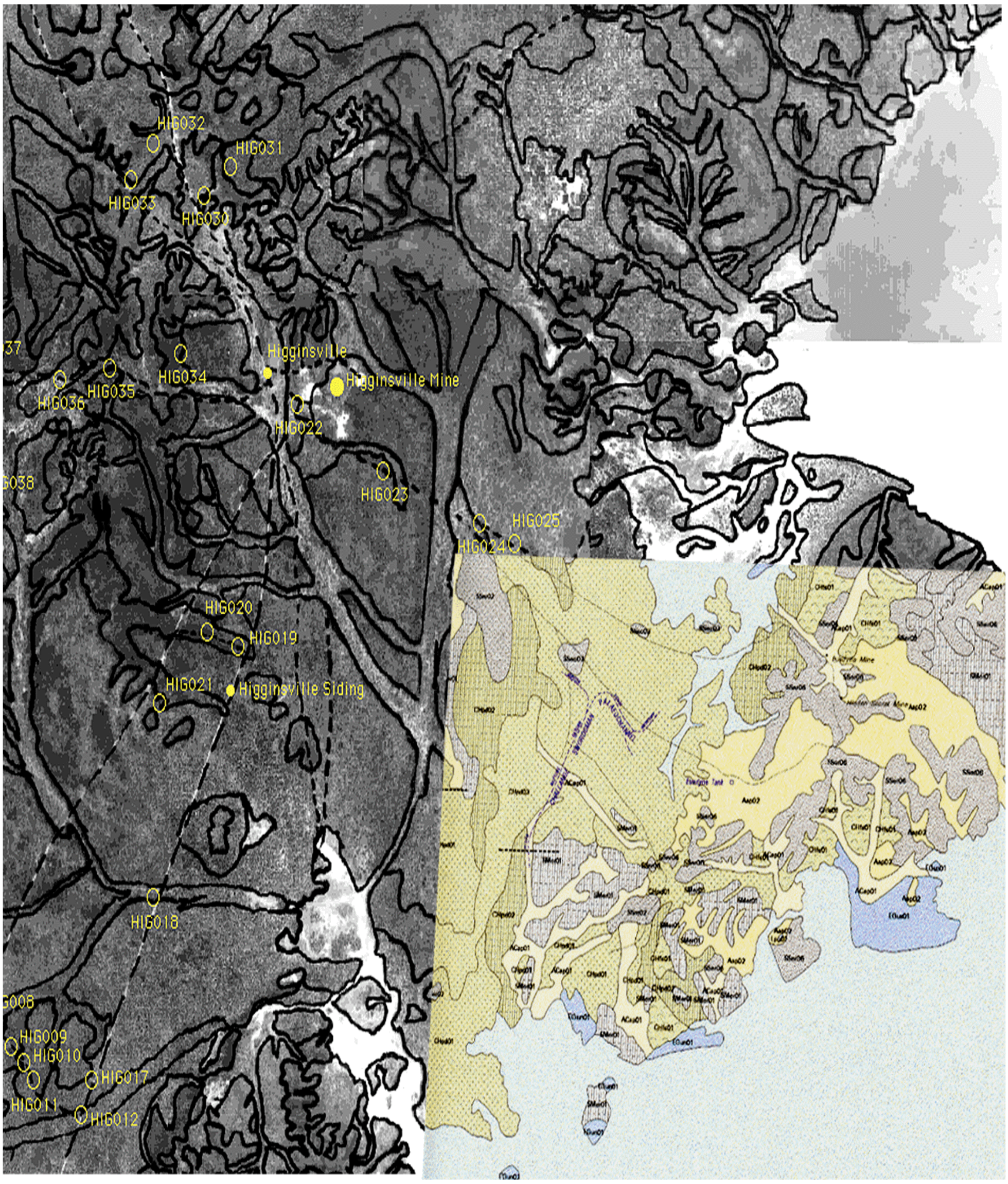

Figure 1. Higginsville regolith base map (Lintern, et al., 1996), compiled by Mike Craig on RC9 aerial photographs. The map shows regolith polygons, side localities and place names. A final regolith map extract is shown at the bottom right to indicate the relationships between the airphoto interpretation and the final map. From AMIRA Project P409

LANDSAT THEMATIC MAPPER

John Wilford[1] and John Creasey[2]

[1] Cooperative Research Centre for Landscape Environments and Mineral Exploration, Geoscience Australia. PO Box 378, Canberra, ACT 2601. E-mail: john.wilford@ga.gov.au

[2] Geoscience Australia. PO Box 378, Canberra, ACT 2601. E-mail: john.creasey@ga.gov.au

1. INTRODUCTION

The first Landsat satellite was launched in July 1972. Of the sensors carried, the Multispectral Scanner (MSS) with 80 metre pixels and four spectral bands was found to provide information of unforeseen value. In July 1982, the launch of Landsat 4 saw the inclusion of the Thematic Mapper (TM) sensor with a 30 metre resolution and 7 spectral bands. Both sensors are on Landsat 5.

The newest in this series of remote sensing satellites is Landsat 7. Launched on 15 April 1999, Landsat 7 has the new Enhanced Thematic Mapper Plus (ETM+) sensor. This sensor has the same 7 spectral bands as its predecessor, TM, but has an added panchromatic band with 15 metre resolution and a higher resolution thermal band of 60 metres.

The radiance measured by the Landsat sensor is a measure of the integration of soil, rock and vegetation characteristics. A processed Landsat TM image should, therefore, show a high degree of correspondence to a regolith-landform map and show that spectrally homogeneous units can be equated with terrain units and therefore named and described.

The use of Landsat TM data for geological mapping is well known (Drury and Hunt, 1989, Drury, 1993, Podwysocki, et al., 1985). How it is used to help construct a regolith-landform map is generally less widely understood. The results of a study of Landsat TM data in the North-eastern Goldfields region of Western Australia by Tapley and Gozzard (1992) and Gozzard and Tapley (1992) indicated that most units interpreted on 1:25,000-scale air photos could be identified on enhancements of the TM data. In addition, the TM data revealed considerably more detail about the compositional variability within the terrain units, especially those within the erosional and depositional regimes. The effectiveness of the data can be attributed to the spectral resolution of the TM data, particularly the ability to detect features related to the absorption of Fe oxides (band 4) and the absorption of clay minerals in band 7.

Spectral characteristics of common surface materials including vegetation, bedrock and regolith materials that can be resolved in the visible and near infrared range of the electromagnetic spectrum when using Landsat TM data are shown in Figure 1 and Table 1.

In Papp, É. (Editor), 2002, *Geophysical and Remote Sensing Methods for Regolith Exploration*, CRCLEME Open File Report 144, pp 6-12.

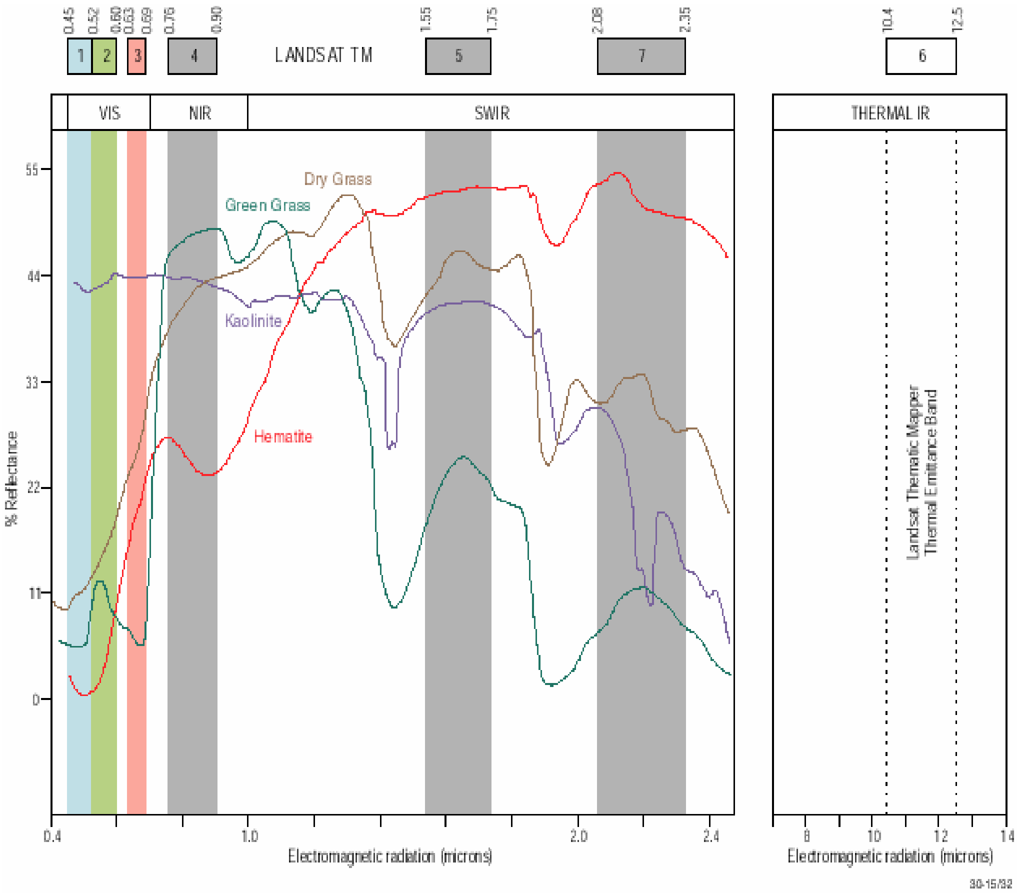

Figure 1. Spectra of selected surface materials and wavelength positions of LANDSAT TM band passes.

TM bands 1 to 4 are primarily useful to detect the spectral response of vegetation and Fe minerals including hematite and goethite. TM1 (0.45–0.52 µm) and TM3 (0.63–0 69 µm) correspond to the position of absorption bands of chlorophyll pigments. TM2 (0.52–0.60 µm) lies in the "green peak" caused by lower absorption of chlorophyll and carotenoids around 550nm. TM4 (0.76–0.90 µm) is related to NIR scattering due to internal leaf structure and the amount of leaf area. The positions of TM1 to 4 also coincide with several diagnostic Fe oxide features including the charge-transfer absorption feature in TM1, a reflectance ramp in TM2, a crystal-field absorption feature in TM3, and a strong crystal-field absorption feature in TM4. Because green biomass produces a reflection peak in TM4, the responses from green vegetation and iron oxide can be uncoupled. TM5, centred at 1.65 µm, is located where most soils and rocks have their maximum reflectance. TM7, centred at 2.22 µm, covers the absorption region of Al-OH- and Mg-OH-bearing minerals. These minerals include chlorite, clay, mica, and the amphibole and carbonate groups.

Table 1. General and specific regolith spectral responses associated with Landsat TM bands (excluding band 6) (modified from Podwyzocki, et al., 1985).

	General spectral responses	Regolith spectral responses
Band 1	Ferric and ferrous iron absorption.	Fe duricrusts, ferruginous saprolite low. Haematitic Fe very low. Kaolinite high.
Band 2	Ferric iron absorption and ferrous iron reflection. Chlorophyll reflection peak	Fe duricrusts, ferruginous saprolite low. Kaolinite high.
Band 3	Short-wavelength shoulder of ferric iron reflection. Ferrous iron absorption. Chlorophyll absorption	Moderate reflection for goethitic and haematitic iron. Kaolinite high.
Band 4	Short-wavelength shoulder of ferric iron and ferrous iron absorption. Vegetation reflection peak.	Moderate reflection for goethitic and haematitic iron. Kaolinite high.
Band 5	Highest reflection for most rock types. High reflection peak for hydrothermally altered rocks. Vegetation absorption.	Highly reflective for haematitic Fe duricrusts and ferruginous saprolite and clays
Band 7	Absorption band for Al-O-H, H-O-H, Mg-O-H and $C0_3$ (clays, micas, carbonates, sulphates. Vegetation water absorption. Dry grass high.	Absorption associated with hydroxyl bearing minerals and carbonates (Bleached or pallid zone, secondary carbonate-calcrete and travertine). Highly reflective for haematitic Fe duricrusts and ferruginous saprolite.

2. METHOD

When image data, such as LANDSAT TM, are recorded using satellite and aircraft systems, they can contain errors in geometry and in the measured brightness values of the pixels (Richards, 1986). The latter are referred to as radiometric errors and can result from the instrumentation used to record the data and atmospheric effects.

Geometric processing

In order to: (1) compare and contrast the information content of each dataset; and (2) integrate datasets, it is essential for the data to be geometrically correct and registered to a common map base, a process termed geo-referencing. The most common method is to relate image pixels to ground control points either from maps, GPS or other imagery and use a polynomial process to rectify the image to a datum and map projection (Richards, 1986). Geometrically corrected imagery can be purchased from approved distributors.

Radiometric processing

Atmospheric attenuation and backscatter modulates the upwelling spectral radiance field in a wavelength-dependent manner. The amount of backscattered radiant energy recorded is greatest in the shorter wavelength bands. Thus, it is essential, before performing any image processing and enhancement techniques, to improve the radiometric quality of the data by compensating for these effects and hence increase the information content of the data.

Ideally, atmospheric corrections are made either by obtaining atmospheric measurements simultaneously with the satellite overpass or from radiometric measurements over calibrated ground targets. Generally such measurements are not available. Estimates of the additive component of atmospheric backscatter can be made using the dark pixel subtraction method. This simply takes the values for all bands of a dark pixel in the image from which there is no reflected signal, or by calculating the minimum value for each band. The latter method needs to consider any data drop-out points or bad lines in the image.

3. DATA PROCESSING

False colour composite images

Combinations of Landsat TM bands can be used to provide overviews of landscape and regolith materials. Landsat TM bands 1,4,7 displayed as BGR can highlight clays, vegetation and iron oxides in a broad context. However topographic effects, high albedo that contributes to high correlation between the bands is generally the dominant effect in colour composite images. Single band images (eg. TM5) displayed in greyscale can be used for highlighting spatial details. Both colour composites and greyscale images are useful backdrops to other thematic layers. They can be appropriately integrated further with gamma ray spectroscopy data and draped over DEM to enhance terrain visualisations.

Ratios

Ratios of Landsat TM bands are useful for separating and mapping different weathered materials. Ratios of bands remove brightness variations and highlight spectral differences between the bands. Hence ratios images are generally saturated and show no topographic information. Examples of ratio combinations include: 1) 3/1 and 5/4 for mapping ferruginous saprolite and lags; 2) 5/7 for identifying residual and transported clays; and 3) 4/2 for separating ferruginous from non-ferruginous regolith. These ratio combinations can be displayed individually or as various three band false-colour combinations.

Directed Principal Component Analysis

One of the most effective enhancements for discriminating a range of different regolith materials is a technique called Directed Principal Component Analysis (DPCA) developed by Fraser and Green (1987). The DPCA is used to separate clays in the imagery by deriving principal components from ratios of bands 4/3 and 5/7. Ratio 4/3 enhances green vegetation and ratio 5/7 enhances a mixed response of vegetation and clay. The DPCA operating on these band ratios is able to separate the vegetation from the clay response. The 'clay' band (derived from the second principal component) is then combined with a ratio of bands 5/4 and bands 7 + 1 in a colour composite image. Ratio 5/4 highlights ferruginous materials and bands 7 + 1 highlights silica-rich materials. The final image is displayed as a three-band composite image with clay in red, iron oxides in green and silica in blue.

4. DATA INTERPRETATION

An example of the application of Landsat TM data for surficial mapping is taken from regolith and landscape studies over part of the Gawler Craton near Half Moon Lake, in South Australia (Wilford, et al., 1998). The area has a semi arid with low relief and poor bedrock exposure. Regolith materials dominate the landscape consisting of aeolian sand, ferruginous lags, calcrete and silcrete. The enhanced Landsat TM image in Figure 2, once field-checked, was the main mapping surrogate for extrapolating regolith units to the surrounding region (Figure 3). The patterns derived from the image responses were used to either define regolith units or to describe the variability of surface materials within units defined by other mapping surrogates such as aerial photos and gamma-ray spectrometry imagery. Superimposed regolith polygons over the enhanced Landsat imagery enabled further assessment of the type and variability of surface materials within each regolith unit.

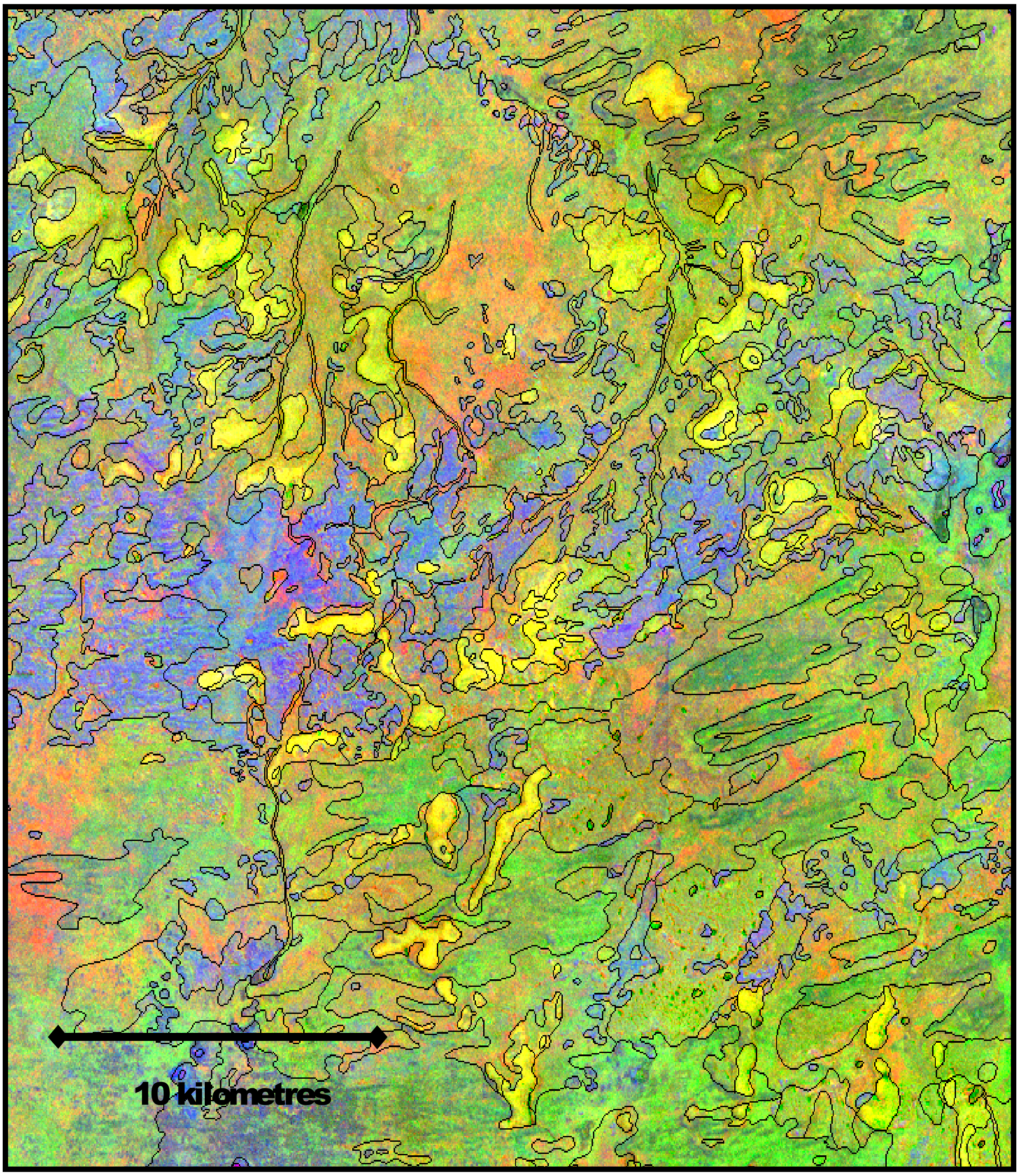

Figure 2. Three-band Landsat TM image of second principal component of ratios 4/3 and 5/7 in red, ratio 5/4 in green and the addition of bands 7 + 1 in blue, overlain with regolith and landform vectors. Ferruginous saprolite, Fe duricrust and ferruginous gravel lags appear in bright yellow hues. Silcrete, silicified saprolite appear in mottled green and yellow, ferruginous dune sands and sandplains appear in olive green to apple green hues. Orange to yellowish orange hues correspond to ferruginous sands and clays over depositional plains. Floodplain sediments and lacustrine sediments appear in red hues. Highly calcareous soils containing calcrete lags and granules appear in blue/magenta. See Figure 3 for descriptions of regolith and landform types.

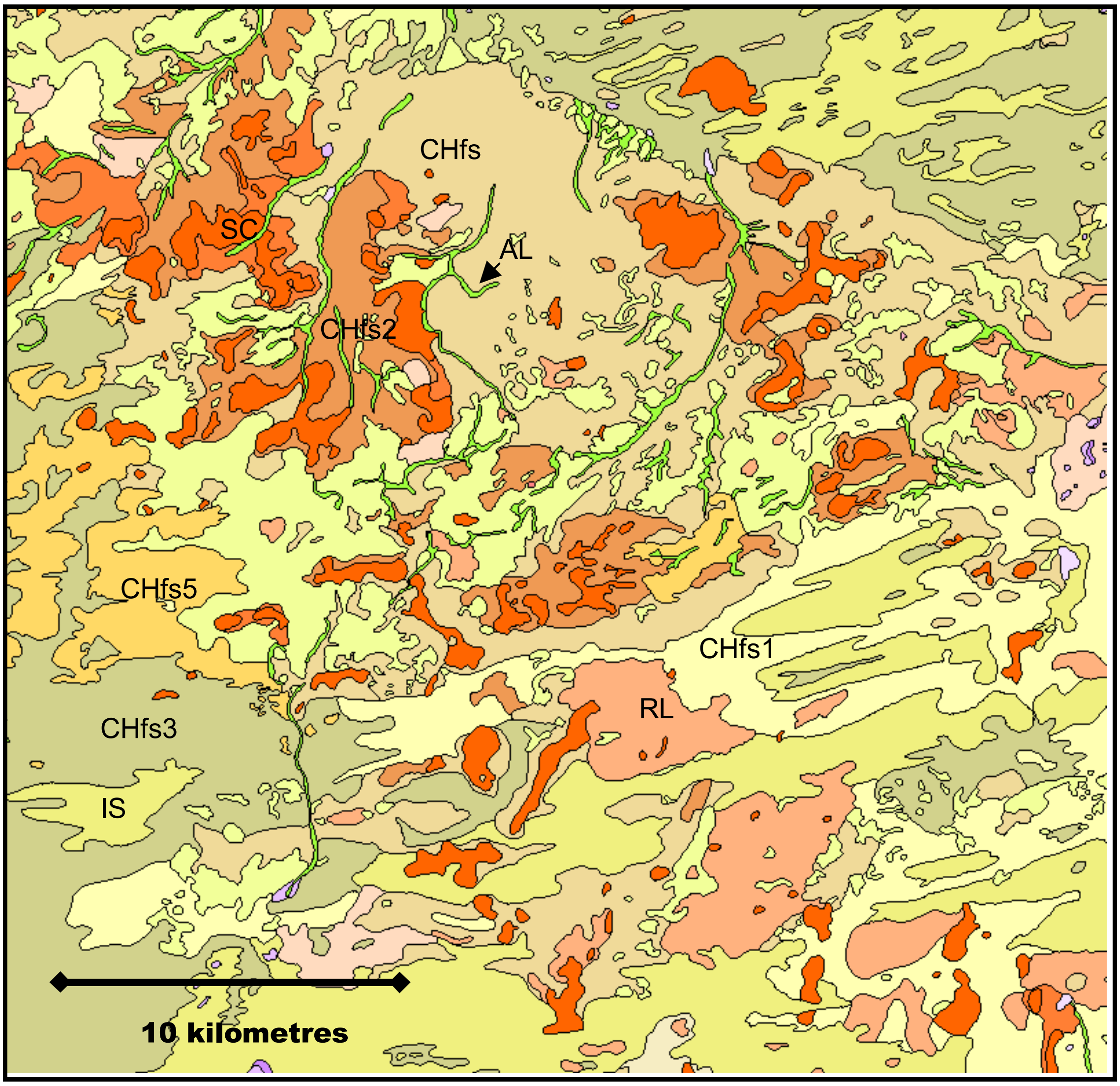

Figure 3. Regolith and landforms from part of the Jumbuck map, Half Moon Lake region, Gawler Craton, South Australia (Wilford, et al., 1998).

AL	Alluvial sediments within poorly defined drainage lines
IS	Aeolian sediments comprising undulating sandplains with occasional parabolic dunes
CHfs	Colluvium - sheet-flow sands with occasional erosional rises mantled by lag gravels
CHfs2	Colluvium - sheet-flow plains comprising lag of ferruginous saprolite and silcrete gravels and ironstone nodules over clayey sands. Occasional indurated pavements of silcrete.
CHfs3	Colluvium - sheet-flow modified sandplains and minor erosional sandplains
CHfs5	Colluvium - extensive sheet-flow sandplains and minor residual plains - calcareous nodules common
Lpp	Lacustrine sediments
SC	Erosional plain comprising abundant ferruginous buckshot gravels, ironstone granules and minor silcrete over granitic saprolite, occasional calcrete nodules
RL	Lag of ferruginous and silcrete gravels and calcrete nodules over silcrete and calcareous sands

5. PROBLEMS, LIMITATIONS

Landsat TM imagery has a scale limitation for interpretation of around 1:50,000. However the additional panchromatic 15 metre band in LANDSAT ETM7+ imagery can be used to enhance the spatial resolution of the other bands and enable larger scales to be used. Scene dependent features such as fireburns and other cultural effects such as variably-grazed paddocks can also make interpretation difficult. Field checking can resolve interpretation issues but should take into account the ground resolution of the data.

6. DATA ACQUISITION AND COST

The Australian Centre for Remote Sensing (ACRES) receives and processes data from the Landsat series of satellites. Imagery can be purchased direct from ACRES or from a network of distributors (http://www.auslig.gov.au/acres). Landsat TM digital imagery is available in a range of forms as shown in Table 2 (in $AUD as of April 2002):

Table 2. Prices for full and partial scenes for Landsat 5 and ETM7+.

LANDSAT 5 & ETM7+

	Raw	Map oriented	Orthorectified
Small scene (25x25km)		535	
Full scene (220x180km)	1400	1730	2160
Super scene (240x250km)		2590	3240

REFERENCES

Drury S.A., 1993. Image interpretation in geology. 2nd edition. Chapman and Hall, London, 283 pp.

Drury, S.A. and Hunt, G.A., 1989. Geological uses of remotely-sensed reflected and emitted data of lateritized Archaean terrain in Western Australia. International Journal of Remote Sensing 10: 475–487.

Fraser, S.J. and Green, A.A., 1987. A software defoliant for geological analysis of band ratios. International Journal of Remote Sensing 8: 525–532.

Gozzard, J.R. and Tapley, I.J., 1992. Landform and regolith mapping in the Lawlers district. Report 2: Terrain classification mapping. CSIRO Australia. Division of Exploration Geoscience, Perth. Restricted Report 240R. CSIRO/AMIRA Project P243. 223 pp. (Unpublished).

Podwysocki, M.H., Power, M.S., and Jones, O.D., 1985. Preliminary evaluation of the Landsat-4 Thematic Mapper data for mineral exploration. Advances in Space Research, Pergamon Press, 5: 13–20.

Richards, J.A., 1986. Remote Sensing Digital Image Analysis. Springer-Verlag Berlin Heidelberg, 281 pp.

Tapley, I.J. and Gozzard, J.R., 1992. Regolith-Landform Mapping in the Lawlers District. Report 1: Aerial photographic interpretation and Landsat Thematic Mapper processing for mapping regolith-landforms. CSIRO Australia. Division of Exploration Geoscience, Perth. Restricted Report 239R CSIRO/AMIRA Project P243. 119 pp. (Unpublished).

Wilford J.W., Craig M.A., Tapley I. J. and Mauger A.J., 1998. Regolith-Landform Mapping and its Implications for Exploration over the Half Moon Lake region, Gawler Craton, South Australia. CRC LEME Restricted Report 92R / E&M Report 542C. 91 pp. (Unpublished).

HYPERSPECTRAL REMOTE SENSING

Éva Papp[1] and Thomas Cudahy[2]

[1] Cooperative Research Centre for Landscape Environments and Mineral Exploration, Department of Geology, Australian National University. Canberra, ACT 0200. E-mail:eva.papp@geology.anu.edu.au

[2] CSIRO Exploration and Mining. Kensington, WA 6151. E-mail:thomas.cudahy@csiro.au

1. METHOD

Mineral exploration is becoming increasingly difficult, especially in obtaining ground access to sensitive or remote areas. Remote geophysical methods can be used to advantage in such circumstances. Spectral remote sensing has the potential to provide the detailed physicochemistry (mineralogy, chemistry and morphology) of the Earth's surface. This information is useful for mapping potential host rocks, alteration assemblages and regolith characteristics. In contrast to the older generation of low spectral resolution systems, such as the Landsat Thematic Mapper with only six "reflected" bands, the new generation of hyperspectral systems enable the identification and mapping of detailed surface mineralogy using "laboratory-grade" spectroscopic principles (Clark, et al., 1990).

For example, many tri-octahedral silicates, carbonates and other minerals generate diagnostic absorption features in the 2300 to 2400 nm region. Only hyperspectral sensors, with tens of contiguous spectral bands across this wavelength range, can provide accurate measurement of the wavelength positions and geometries of the diagnostic mineral absorption features.

With the aid of hyperspectral remote sensing, an extensive range of minerals can be remotely mapped, including: iron oxides, clays, micas, chlorites, amphiboles, talc, serpentines, carbonates, quartz, garnets, pyroxenes, feldspars and sulphates, as well as their physicochemistries such as cation composition and long and short range order.

Geological remote sensing is performed through atmospheric windows where electromagnetic radiation (EMR) is allowed to pass without significant attenuation. The five atmospheric windows available for remote mineral mapping include the visible to near infrared (VNIR), the shortwave infrared (SWIR), the mid-infrared (MIR), the thermal infrared (TIR) and the microwave wavelength regions (Figure 1). The ultraviolet (UV) and far infrared (FIR) wavelength regions are not available. Of these five atmospheric windows, the VNIR, SWIR and TIR regions are most useful for mapping surface mineralogy because these wavelengths are sensitive to a wide range of diagnostic EMR-material interactions. In particular:

1. The mineral-spectral features in the *VNIR* are largely related to the transfer of electrons between energy levels of constituent elements, especially the transition metals Fe, Mn and Cr (Hunt, et al., 1971);

2. The mineral-spectral features in the *SWIR* are largely related to the overtones and combination tones of vibrations of octahedrally coordinated cations (typically Al, Fe, Mg) bonded with OH groups (Hunt and Vincent, 1968); and,

3. The mineral-spectral features in the *TIR* are largely related to fundamental vibrations (bends and stretches) of Si-O bonds in various structural environments (Lyon, 1965).

In Papp, É. (Editor), 2002, *Geophysical and Remote Sensing Methods for Regolith Exploration*, CRCLEME Open File Report 144, pp 13-21.

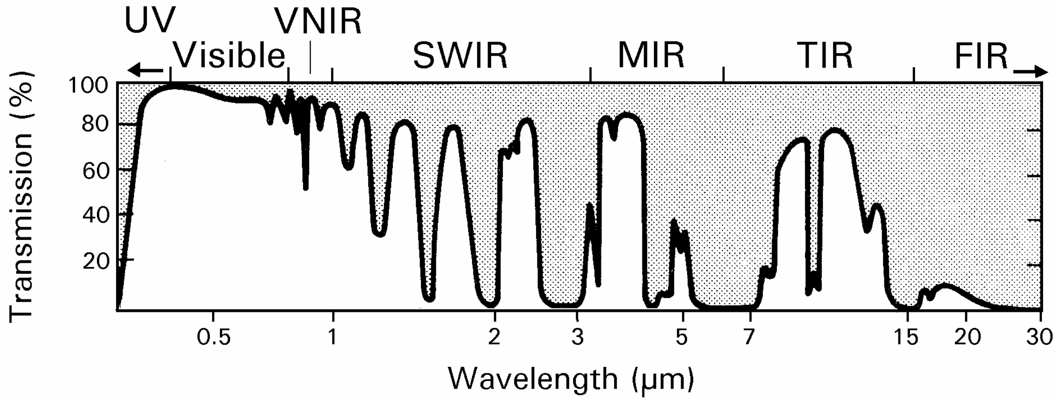

Figure 1. Atmospheric transmission spectrum (after Drury, 1987).

As a consequence, the VNIR wavelength region is useful for mapping iron oxides and oxyhydroxides (for example, hematite and goethite), the SWIR for dioctahedral and trioctahedral silicates (for example, kaolins, white micas, smectites, chlorites, amphiboles, talcs, serpentines) and the TIR for framework silicates (quartz, feldspars, garnets, pyroxenes and olivines). Carbonates and sulphates produce diagnostic spectral features at both SWIR and TIR wavelengths.

Combined use of the VNIR, SWIR and TIR atmospheric windows should therefore allow identification of a wide range of minerals necessary for most geological applications. For example:

1. The *VNIR* wavelength region is potentially useful for mapping gossans, rich in iron oxides and associated with weathered sulphide occurrences (Rowan, et al., 1977, Bladh, 1982, Buckingham and Sommer, 1983, Raines, et al., 1985, Fraser, et al., 1986, Townsend, 1987), as well as regolith characterisation (Cudahy, 1992);

2. The *SWIR* wavelength region is potentially useful for mapping alteration haloes that comprise minerals like chlorites and white micas in epithermal/porphyry styles of Cu-Au mineralisation (Marsh and McKeon, 1983, Fraser, et al., 1986, Feldman and Taranik, 1988, Kruse, 1988, Duke, 1994, Rowan, et al., 1991, Zaluski, et al., 1994) as well as regolith characterisation (Cudahy, 1992);

3. The *TIR* wavelength region is potentially useful for mapping a range of exploration targets. For example, in more weathered environments, mapping silicification associated with epithermal/porphyry alteration (Gunnesch, et al., 1994) may be useful. Similarly, Mn-rich garnets associated with Broken Hill style Pb-Zn-Ag mineralisation (Spry and Wonder, 1989) or Fe-rich garnets in Cu-Zn skarn systems (Harris and Einaudi, 1982) can be targeted. In less weathered terrains, pyroxene composition can potentially be used as an indicator for skarn deposits (Einaudi and Burt, 1982, Nakano, et al., 1994) whereas feldspars could be important in mapping granite host rocks or granite-associated mineralising fluids (Ishihara, 1981). For example, the Proterozoic Cu-Au-U mineralisation at Olympic Dam (Haynes, et al., 1995), rare earth mineralisation (Pollard, 1995) and Archaean lode Au deposits (Wyman and Kerrich, 1988) are all associated with specific types of granites.

2. HYMAP SYSTEM

The HyMap™ (Hyperspectral Mapping) system is an operational, airborne imaging VNIR-SWIR spectrometer designed and built by Integrated Spectronics Proprietary Limited (ISPL) (http://www.intspec.com). The features of the system include:

1. 450-2500 nm spectral coverage;
2. 128 spectral bands across three wavelength regions. The VNIR (visible-near infrared) region from 450-1400 nm has 64 bands, the SWIR-1 (shortwave infrared) region from 1400-1900 nm has 32 bands and the SWIR-2 from 1900 to 2500 nm has 32 bands;
3. bandwidths of 10-20 nm;
4. high signal to noise ratio for all bands (>500:1);
5. 3-10 m spatial resolution;
6. 61.3° degrees swath width;
7. on-board radiometric and spectral calibration;
8. operates in aircraft equipped with standard aerial camera ports; and,
9. 3-axis gyro-stabilised platform.

3. DATA PROCESSING

The processing of airborne hyperspectral data to derive accurate surface compositional information involves the following steps:

1. Evaluation of the HyMap instrument stability and noise;
2. Generation of radiance at the sensor data (correction for instrument gains and offsets);
3. Evaluation and correction of radiance at the sensor data for atmospheric effects (both additive and multiplicative effects as well as wavelength-dependent and wavelength independent effects);
4. Evaluation and correction for surface scattering and shadowing effects (both wavelength-dependent and wavelength independent multiplicative effects);
5. Implementation of the above corrections to yield surface radiance (or equivalent), which is directly related to surface composition;
6. Spectral compression (to reduce the large volume of spectral data, much of which is highly correlated, to a size that can be efficiently processed);
7. Evaluation and generation of specific surface compositional products for comparison with the published mapping; and,
8. Georeferencing of the information products to a standard map base for inclusion into a GIS.

This chain of processing can take one of several paths depending on the user's requirements where consideration is given to speed versus accuracy. Two possible processing strategies are most commonly applied:

1. The first strategy is very rapid and uses a technique called log residuals (Green and Craig, 1985). In fact, this method generates mineralogically interpretable products within one hour after receiving the raw data. However, log residuals suffers from scene-dependency.

2. The second strategy involves full modelling of the atmosphere to yield surface radiance. This step is itself not time-consuming (1 hour per 4000 line run), though the subsequent steps of extracting the "scene-independent" mineral information products is very time consuming mainly because of current limitations in algorithms/software.

The software which is currently available for hyperspectral processing is largely written in IDL (Interactive Display Language) and includes ENVI (developed by Analytical Imaging and Geophysics (AIG at http://www.aigllc.com/) as well as ENVI "add-ons" written by CSIRO and stand-alone IDL-based packages like HYCORR, also written by CSIRO. Much use can be made of Microsoft EXCEL©, ERMAPPER©, ARCVIEW© and other imaging, statistical and GIS packages.

4. DATA INTERPRETATION AND EXTRACTION OF MINERAL INFORMATION

Information extraction follows data reduction to surface radiance (or equivalent). The type of extraction procedure again depends on the level of accuracy, confidence and reproducibility required by the user. As with the data reduction stage, simple methods like band ratios and log residuals can be used to good effect to derive image products that pertain to a compositional parameter of interest, though these types of methods often generate non-unique products. This is especially the case if a number of different materials generate significant spectral variation at those wavelength selected for the ratio (log residual) product.

Ultimately, whether it be ratios or more sophisticated techniques like partial unmixing (Boardman, 1993), the objective is to capitalise on that spectral information unique to the material of interest. This is non-trivial and no one method can yet be considered as truly reaching this much-desired goal.

Several information extraction methods can be used, including:

1. Band ratios;
2. Log residuals;
3. Curve fitting;
4. Supervised classification; and,
5. Partial unmixing.

Other techniques, like Mahalanobis Distances and Partial Least Squares (Haaland and Thomas, 1988), can also be considered.

5. APPLICATIONS

Hyperspectral remote sensing is a powerful tool for mineralogical mapping, regolith-landform mapping, and for a range of environmental applications. The spectral signatures of land surface, derived from imagery, can be used to identify and even quantify mineralogical entities of exploration significance. The spatial analysis of imagery can lead to improved mapping by more precise identification and subdivision of regolith-landform units. Environmental processes can be identified and monitored with high spatial resolution. Examples are shown in Figures 2-4.

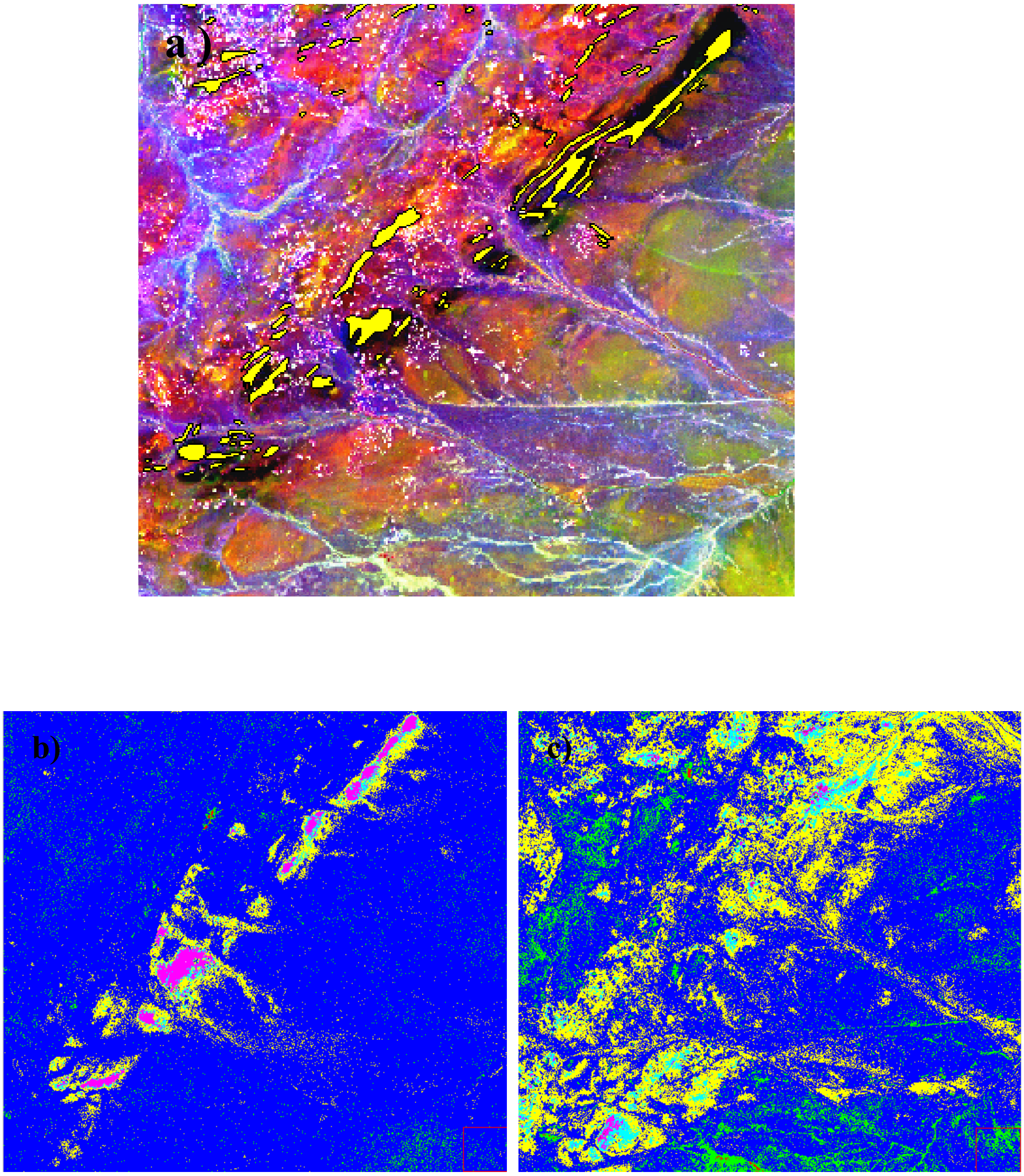

Figure 2. An example for mineralogical mapping: a) RGB image derived from HyMap, overlain by mapped amphibolite units from the published 1:25,000 geological map. b) the imaged amphibole endmember, c) the imaged goethite-illite mixture endmember. The distribution of amphibolites is well mapped, and the weathering of amphibolites and dispersion of weathering products is clearly resolved.

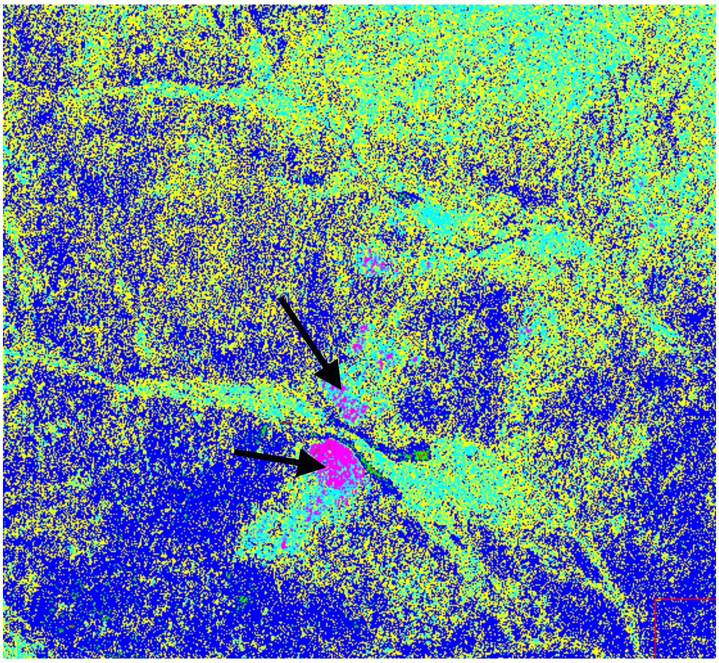

Figure 3. An example for regolith-landform mapping. Iron-oxide endmember identified from HyMap data is imaged. High iron-oxide areas appear in the landscape as ferricrete rises (red colour, indicated with black arrows) dissected by drainage.

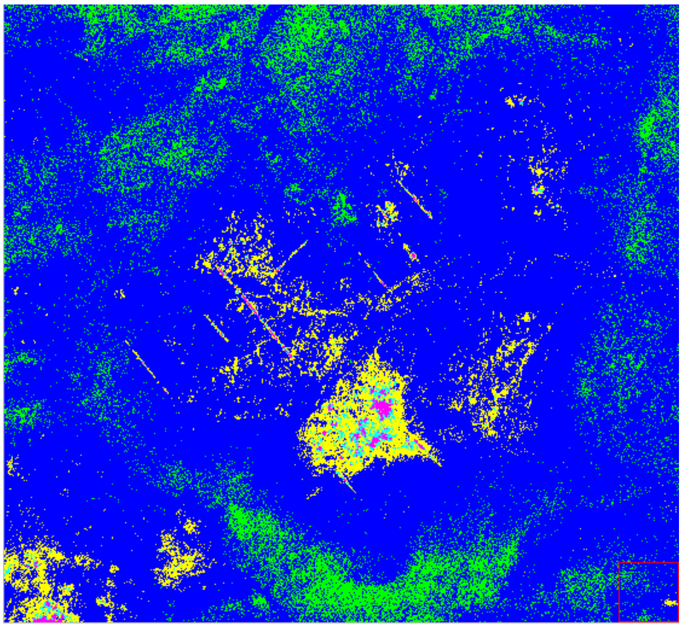

Figure 4. An example for environmental applications. The yellow lines show old drilling sites. They are invisible on aerial photography and hard to identify in the field, but are evident on HyMap imagery because of the significantly different mineralogy of drill spoil material from the natural surface materials.

6. PROBLEMS, LIMITATIONS

Because of current limitations in algorithms/software, many problems can be encountered during processing hyperspectral data. Hence, at the time of this study, no operational, scene-independent methodology is available. Hopefully the development of an accurate operational methodology in the future will provide a general solution.

What is lacking, are well-documented Australian geological case histories that demonstrate the potential of hyperspectral regolith exploration.

7. SURVEY ORGANISATIONS

A new generation of hyperspectral remote sensing systems is now becoming available for routine use by the mineral exploration community. These systems include the airborne HyMap, OARS, SWIPS, TIPS, SEBASS and AVIRIS systems and the spaceborne Hyperion, Orbview-4, ARIES-1 and NEMO systems. HyMap is operated by Integrated Spectronics Proprietary Limited (ISPL) (http://www.intspec.com).

8. COSTS

The cost of a hyperspectral survey largely depends on the volume and timing of data acquisition. Coordinating data acquisition campaigns of several projects for the same time can save as much as 50% of acquisition costs. Data for research purposes can often be obtained for much reduced price compared to commercial data. Cost of data is calculated as the sum of mobilisation costs plus price per line kilometer. The data is sold at various processing levels, which also influences the final cost. As hyperspectral techniques are in a rapid development, with constantly changing technology, it is best to contact the surveying company for details on actual costs.

9. REFERENCES

Bladh, K.W., 1982. The formation of goethite, jarosite and alunite during the weathering of sulfide-bearing felsic rocks. Economic Geology 77: 176-184.

Boardman, J.W., 1993. Automatic spectral unmixing of AVIRIS data using convex geometry concepts. Proceedings 4th Annual Airborne Geoscience Workshop, October, 25-29 1993. Jet Propulsion Laboratory Publication 93-26: 11.

Buckingham, W.F. and Sommer, S.E., 1983. Mineralogical characterisation of rock surfaces formed by hydrothermal alteration and weathering. Application to Remote Sensing. Economic Geology 78: 664-674.

Clark, R.N., King, T., Klejwa, M. and Swayze, G.A., 1990. High spectral resolution reflectance spectroscopy of minerals. Journal of Geophysical Research 95(B8): 653-680.

Cudahy, T.J., 1992. A model for the development of the regolith of the Yilgarn Craton incorporating selected spectral information. CSIRO Exploration Geoscience Restricted Report 243R. 26 pp.

Drury, S.A., 1987. Image interpretation in geology. Allen and Unwin, London, 243 pp.

Duke, E.F., 1994. Near infrared spectra of muscovite, Tschermak substitution and metamorphic reaction progress: Implications for remote sensing. Geology 22: 621-624.

Einaudi, M.T. and Burt, D.M., 1982. Introduction. Terminology, classification and composition of skarn deposits. A special issue devoted to skarn deposits. Economic Geology and Bulletin of the Society of Economic Geologist 77(4): 745-753.

Feldman, S.C. and Taranik, J.V., 1988. Comparison of techniques for discriminating hydrothermal alteration minerals with airborne imaging spectrometer data. Remote Sensing of Environment 24: 67-83.

Fraser, S.J., Gabell, A.R., Green, A.A., and Huntington, J.F., 1986. Targeting epithermal alteration and gossans in weathered and vegetated terrains using aircraft scanners: Successful Australian case histories. Proceedings of the 5th Thematic Conference on Remote Sensing for Exploration Geology. Reno Nevada. Environmental Research Institute of Michigan, Michigan: 63-84.

Green, A.A. and Craig, M.A., 1985. Analysis of aircraft spectrometer data with logarithmic residuals. Proceedings of the Airborne Imaging Spectrometer data Analysis Workshop, April 8010, JPL Publication 85-41: 111-119.

Gunnesch, K.A., Del Angel, C.,T., Castro, C.C. and Saez. J., 1994. The Cu-(Au) skarn Ag-Pb-Zn vein deposits of La Paz, northeastern Mexico: Mineralogical, paragenetic and fluid inclusion characteristics. Economic Geology 89: 1640-1650.

Haaland, D.M. and Thomas, V.T., 1988. Partial Least Squares method for spectral analysis. 1. Relation to other quantitative calibration methods and the extraction of qualitative information. Analytical Chemistry 60: 1193-1202.

Harris, N.B. and Einaudi, M.T., 1982. Skarn deposits in the Yerington District, Nevada: Metasomatic skarn evolution near Ludwig. Economic Geology 77: 877-898.

Haynes, D.W., Cross, K.C., Bills, R.T. and Reed, M., 1995. Olympic Dam ore genesis: A fluid mixing model. Economic Geology 90: 281-307.

Hunt, G.R. and Vincent, R.K., 1968. The behaviour of spectral features in the infrared emission from particulate surfaces of various grain sizes. Journal of Geophysical Research 73(18): 6039-6046.

Hunt, G.R., Salisbury, J.W. and Lehnoff, C.J., 1971. Visible and near infrared spectra of minerals and rocks: III. Oxides and Oxyhydroxides. Modern Geology 2: 195-205.

Ishihara, S., 1981. The granitoid series and mineralisation. Economic Geology. 75th Anniversary Edition: 458-484.

Kruse, F.A., 1988. Use of airborne imaging spectrometer data to map minerals associated with hydrothermal altered rocks in the Northern Grapevine Mountains, Nevada and California. Remote Sensing of Environment 24: 31-51.

Lyon, R.J.P., 1965. Analysis of rocks and minerals by reflected infrared radiation. Economic Geology 60: 715-736.

Marsh, S.E. and McKeon, J.B., 1983. Integrated analysis of high-resolution field and airborne spectroradiometer data for alteration mapping. Economic Geology 78: 618-632.

Nakano, T., Yoshino, T., Shimazaki, H. and Shimizu, M., 1994. Pyroxene composition as an indicator in the classification of skarn deposits. Economic Geology 89: 1567-1580.

Pollard, P.J., 1995. Geology of rare metal deposits: An introduction and overview. Economic Geology 90: 489-494.

Raines, G.L., McGee, L.C. and Sutley, S.J., 1985. Near infrared spectra of West Shasta gossans compared with true and false gossans from Australia and Saudi Arabia. Economic Geology 80: 2230-2239.

Rowan, L.C., Goetz, A.F.H. and Ashely, R.P., 1977. Discrimination of hydrothermally altered rocks in visible and near infrared multispectral images. Geophysics 42: 522-535.

Rowan, L. C., Salisbury, J. W., Kingston, M. J., Vergo, N.S. and Bostick, N. H., 1991. Evaluation of visible, near-infrared and thermal-infrared reflectance spectra for studying thermal alteration of Pierre shale, Wolcott, Colorado. Journal of Geophysical Research 96: 18,047-18,057.

Spry, P.G. and Wonder, D., 1989. Manganese-rich garnet rocks associated with the Broken Hill lead-zinc-silver deposit, New South Wales, Australia. Canadian Mineralogist 27: 297-327.

Townsend, T.E., 1987. Discrimination of iron alteration minerals in visible and near infrared reflectance data. Journal of Geophysical Research 92(B2): 1441-1454.

Wyman, D. and Kerrich, R., 1988. Alkaline magmatism, major structures and gold deposits: Implications for greenstone belt gold metallogeny. Economic Geology 83: 454-461.

Zaluski, G., Nesbit, B. and Muehlenbachs, K., 1994. Hydrothermal alteration and stable systematics of the Babine porphyry Cu deposits, British Columbia: Implications for fluid evolution of porphyry systems. Economic Geology 89: 1518-1541.

RADAR IMAGING

Ian J. Tapley

Cooperative Research Centre for Landscape Environments and Mineral Exploration.
CSIRO Exploration and Mining, Kensington, WA 6151. E-mail: ian.tapley@csiro.au

1. INTRODUCTION

Radar operation

Radar remote sensing (Henderson and Lewis, 1998) provides imagery that characterizes the physical properties (morphology, roughness, dielectric properties and geometric shapes) of the terrain surface, its cover and near-surface volume. Image enhancements are particularly suited to landform analysis from which geomorphological and geological inferences can be made. Because radars provide their own illumination, observations are independent of cloud cover, light rain, smoke haze and solar illumination, thus allowing all-time observation through all seasons and in all climatic regions. An important capability of radar is the ability to select the illumination geometry, that is, the incidence and azimuth angles, to highlight structure and other diagnostic properties of the terrain.

A typical radar measures the strength and round-trip time of the microwave signals that are emitted by a radar antenna and reflected off a distant surface or object. The radar antenna alternately transmits and receives pulses at particular microwave wavelengths (in the range 1 cm to 1 m, which corresponds to a frequency range of about 300 MHz to 30 GHz) and polarizations (waves polarized in a single vertical or horizontal plane). At the Earth's surface, the energy in the radar pulse is scattered in all directions, with some reflected back toward the antenna. This backscatter returns to the radar as a weaker radar echo and is received by the antenna in a specific polarization (horizontal or vertical, not necessarily the same as the transmitted pulse). These echoes are converted to digital data and passed to a data recorder for later processing and display as an image.

In radar imagery, surface roughness is the dominant factor in determining the amplitude of the return signal. Surface roughness is a measure of the irregularity of the terrain surface (both vertical and horizontal) compared with the radar wavelength. On radar images, surfaces can be classified as smooth, slightly rough, moderately rough or very rough, relative to the radar wavelength and angle of incidence. A consequence is that a surface that appears smooth at a long radar wavelength may appear rough at a short wavelength. The level of radar backscatter indicates the tone of an image - rough targets appear bright and smooth targets dark. The mean intensity of the radar backscatter from an area of interest is usually expressed in decibels (dB). Typical values (of $\sigma°$) for natural surfaces range from +5dB for very rough surfaces to -40db for very smooth surfaces.

Other factors that influence the intensity are the transmitting frequency (wavelength), polarization of the transmitted and received signals, incidence angle between the transmitted signal and terrain surface, topographic slope and dielectrical properties of the surface and sub-surface materials.

Radar polarimetry

Traditional imaging radar systems measure the radar backscatter using a single frequency, single polarization antenna. An example of such a system is the radar mounted on the Canadian RADARSAT satellite that transmits and receives C-band (5.56 MHz) signals in horizontal transmit-horizontal receive (HH) polarization mode. A radar system that measures the complete polarization response of every pixel in an image is called an imaging radar polarimeter. An example is the airborne AIRSAR (AIRborne Synthetic Aperture Radar) system developed by NASA-JPL (Jet Propulsion Laboratory). Knowledge of this entire scattering matrix permits the synthesis of the radar backscatter for any combination of transmit and receive polarizations, that is, HH, HV (horizontal transmit-vertical receive), VH (vertical transmit-horizontal receive) and VV (vertical transmit-vertical receive). Radar

In Papp, É. (Editor), 2002, *Geophysical and Remote Sensing Methods for Regolith Exploration*, CRCLEME Open File Report 144, pp 22-32.

polarimetry is, therefore, a valuable tool for identifying the dominant scattering mechanisms present in a scene and for resolving minor differences in the physical and electrical properties between surface features.

2. RADAR DATASETS

Information regarding radar datasets currently available from the Australian Centre of Remote Sensing is available on the web site http://www.auslig.gov.au/acres/prod_ser/index.htm. These include ERS-1 and ERS-2 (European Remote Sensing), JERS-1 (Japan Earth Resources Satellite) and RADARSAT datasets. The system specifications and World Wide Web Home pages for current and future spaceborne radar instruments are listed in Table 1.

Table 1. Spaceborne radar systems.

Parameter	ERS-1	EST-2	JERS-1	Radarsat-1	Radarsat-2	PALSAR	ENVISAT
Radar band	C	C	L	C	C	L	C
Polarization	VV	VV	HH	HH	HH,VV HV	HH or VV HV or VH	HH, VV HV
Incidence angle (degree)	20-26	20-26	32-38	10-60	10-60	20-55	14-45
Resolution (metres)	25	25	18	8-100	3-100	10-100	30
Swath width (Km)	100	100	76	50-500	10-527	70-250	50-400
Launch date	07/91	04/95	02/92	11/95	2002	8/2002	6/2001

The AIRSAR system mentioned earlier operates in two modes. In POLSAR (POLarimetric Synthetic Aperture Radar) mode this system is capable of simultaneously collecting HH-, VV-, VH- and HV-polarized data for three frequencies: C-band (5 cm wavelength); L-band (24 cm wavelength); and P-band (68 cm wavelength). The shorter wavelength C and L bands are more sensitive to small-scale variations in surface roughness that can be related to the extent of soil erosion, size of surface lag gravels and the extent of landscape truncation. L and P bands have a greater potential for geological studies of subsurface features and the terrain below a vegetation canopy. In TOPSAR (TOPographic Synthetic Aperture Radar) mode precision elevation data are generated from the phase information accompanying the C-band VV-polarization signal using a process called radar interferometry. L and P-band polarimetric data collected in TOPSAR mode are registered to the elevation data. Examples of TOPSAR datasets are described later in this chapter.

AIRSAR datasets were recorded during airborne missions in 1993, 1996 and 2000 over selected targets in Australia, Papua New Guinea, Southeast and East Asia. Information regarding these datasets and their availability is listed on the AIRSAR Homepage http://airsar.jpl.nasa.gov/.

ERS-1 and –2:	http://earth.esa.int/ers http://www.auslig.gov.au/acres/prod_ser/ersdata.htm
JERS1:	http://www.auslig.gov.au/acres/prod_ser/eojerdat.htm http://www.eorc.nasda.go.jp/JERS-1
RADARSAT:	http://www.auslig.gov.au/acres/prod_ser/radadata.htm http://www.ccrs.nrcan.gc.ca/ccrs/tekrd/radarsat/rsate.html
PALSAR:	http://www.nasda.go.jp/sat/alos/index_e.html http://www.eorc.nasda.go.jp/ALOS/about/overview.htm
ENVISAT:	http://envisat.esa.int

3. APPLICATIONS OF RADAR IMAGERY

Subsurface mapping

A major benefit of imaging radar is the ability of long wavelength signals (λ>60 cm) to penetrate loose overburden and map subsurface structures, provided that the volumetric soil moisture is <1% and the soils have fine to medium textures. This is a major advantage over reflectance remote sensing. In the Great Sandy Desert of Western Australia for example, where sandplains, dunefields and shrub-steppe vegetation obscure much of the subtle topography and underlying Proterozoic sedimentary rocks, enhancements of NASA-JPL AIRSAR data have demonstrated the benefits of polarimetric radar for revealing more information about the composition of the terrain than enhancements of either SPOT-PAN or Landsat TM data (Tapley and Craig, 1995). Figure 1 compares a Landsat TM image of bands 2:4:7 (left) with a composite image of the vertical polarization response for AIRSAR bands C:L:P (right). The TM scene highlights the ubiquitous nature of the dunefields and a composite history of fireburns, whereas the radar image "sees through" much of this cover and confusion to reveal significant geological detail. Some of the more significant observations in the image include:

1. The identification of the closure of a previously unmapped syncline [Location 1];

2. Regional extensions of alignments of truncated sedimentary sequences, much of which is subsurface, within the sandplains and pronounced expression of the geometric alignment of individual stratigraphic units [Location 2]; and,

3. Morphological evidence of a complex fluvial history under a former climatic regime that permits the construction of a sequence of palaeo-environmental events that produced the landforms associated with the palaeodrainage networks [Locations 3 and 4].

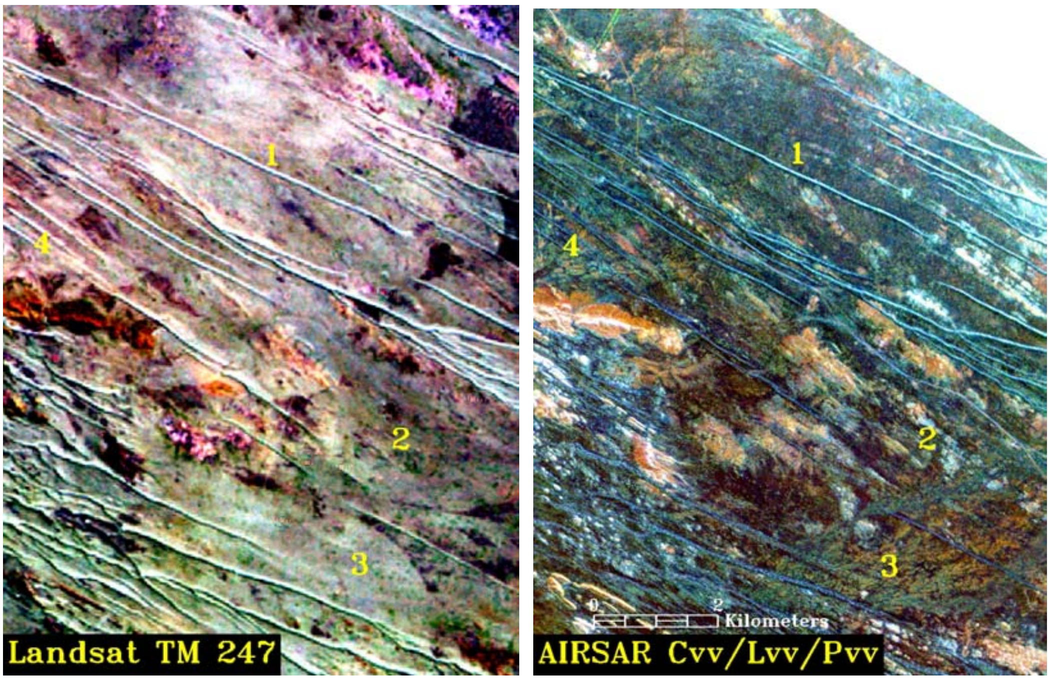

Figure 1. Images of Landsat TM and AIRSAR polarimetric data compare surface and sub-surface textural information from radar with surface mineralogy and vegetation from TM.

Regolith and landform mapping

The benefits of radar for mapping landforms and discriminating between regolith materials in deeply weathered terrains are well described by reference to an examination of AIRSAR polarimetric data in the Gawler Craton, South Australia. Findings in the Yilgarn Craton, Western Australia, were similar (Tapley, 1998). Importantly, the fundamental attributes of a deeply weathered terrain, namely erosional and depositional regimes, can be recognized. In this topographically flat, semi-arid terrain, the most distinctive radar responses occur from prominent outcrop and associated debris of Precambrian volcanics [Figure 2, Location 1] and irregular surfaces of dissected silcrete tablelands (Location 2). These contrast strongly with a blanket of alluvial, colluvial and aeolian sediments (Location 3) with a ~10% vegetative cover of chenopod-shrubland communities, which have low-to-medium backscatter. Specific observations include:

1. The mapping of regolith-landform units is primarily a function of multi-frequency rather than multi-polarization, with the greatest sensitivity to roughness being observed in the VV-polarized data for each frequency. Regolith-landform units of the erosional regime can be delineated from those in other regimes by the increased surface roughness resulting from the accumulation of coarser lag gravels and exposure of bedrock during active erosion of the landscape. Outcrops of

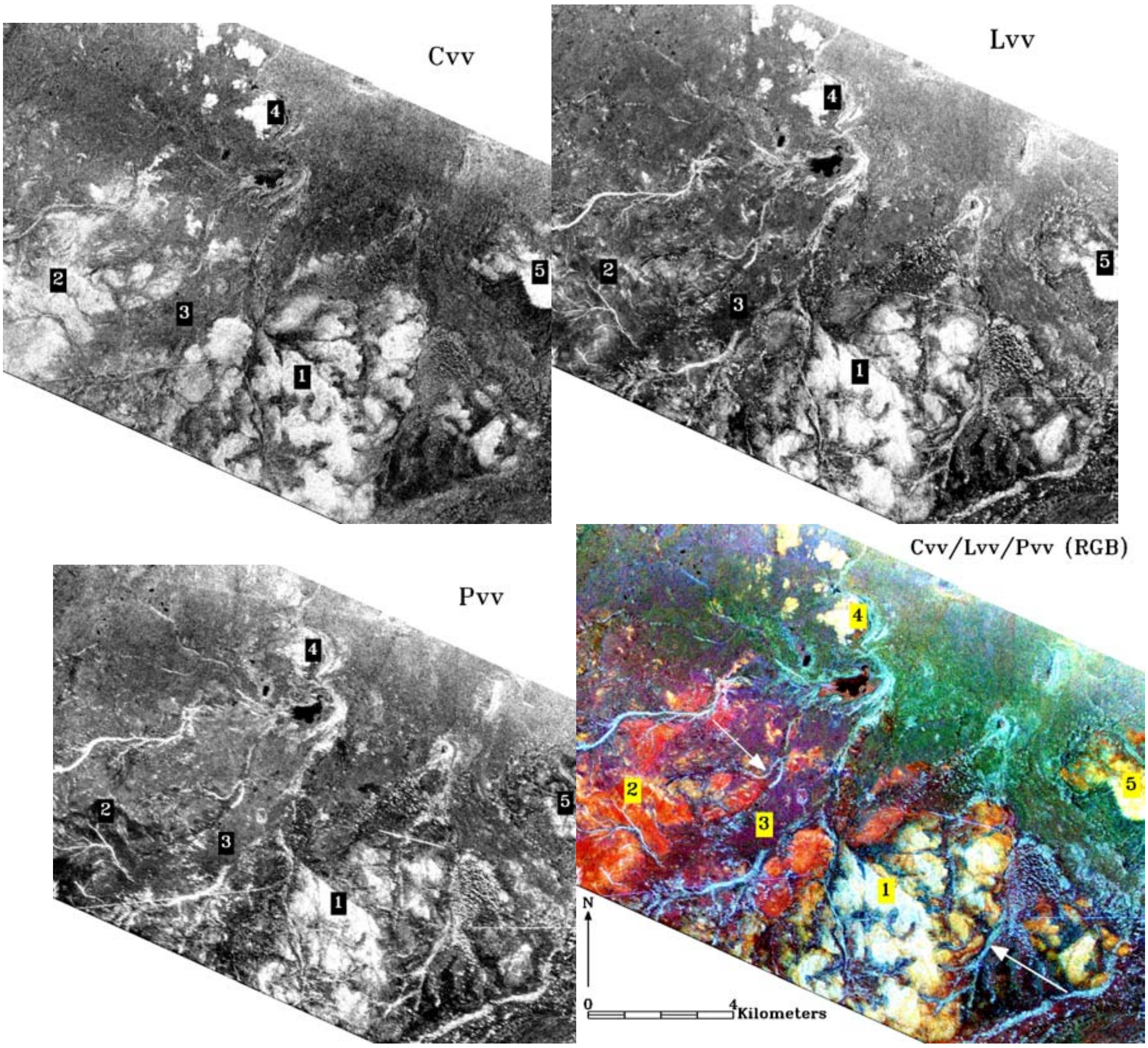

Figure 2. Variation in vertically polarized radar backscatter with changing surface roughness according to AIRSAR C, L and P band wavelengths, and a composite image of the three wavelengths. A previously unmapped NW-SE aligned linear feature [1] in the composite image is clearly evident in the Pvv band image and, to a lesser extent, in the L and C band images.

igneous rocks at Locations 1, 4 and 5 produce the strongest returns in co-polarized signals from all three frequencies and appear as white to bright yellow in the composite image.

2. Best discrimination between the landforms developed in erosional terrains is obtained from enhancements of L- and P- band data. C-band data generally do not discriminate between these landforms because their surface materials are “radar rough” at this wavelength. In Figure 2, for example, outcropping rhyodacite at Location 1 in the C-band image are confused with the medium to coarse lags of silcrete gravels and calcrete nodules developed over granite saprolite [Location 2], whereas clear distinction is made in L band. L- and, to a lesser extent, P-band signals highlight the topographic alignments of breakaway slopes that define the extent of these tablelands. Incision of the tableland by ephemeral streams has resulted in exposure and accumulations of massive to nodular calcrete and silcrete gibber that strongly backscatter the radar signals. In addition, in an area of increased dissection at Location 2, L band has clearly delineated a semi-radial pattern of isolated topographic highs of weathered granite overlain by a lag of silcrete gravels and cobbles.
3. C band provides clear discrimination between erosional and depositional terrains owing to the relative smoothness, at the scale of the L-and P-band wavelength, of regolith-landforms located in depositional terrains.

Terrain analysis

An interpretation of radar images can often permit a fuller comprehension of the morphology of the landforms and the nature of the materials that form those landforms when compared with optical datasets. This interpretation is driven by a relationship between surface morphology and composition of particular landform units. For example, in the Ophthalmia Range region of the Hamersley Basin in Western Australia, a series of landscape evolution processes can be deduced from enhancements of AIRSAR imagery (Tapley, 1996). These processes were active under former climatic regimes and led to the construction of a sequence of palaeo-environmental events to produce the landforms associated with the colluvial and alluvial units. In Figure 3 two broad morphological regimes can be recognized. Extensive bedrock outcrops of the Ophthalmia Range have been, and are still part of, an erosional regime capable of supplying large volumes of material. This material has been transported and deposited in the depositional regime by both colluvial and alluvial processes to form marginal colluvial fans [Location 1], alluvial fans [Location 2] and sheetwash plains [Location 3].

The colluvial fans form a series of interconnecting, laterally coalescing, landforms. Each displays a distinctive yellow or red hue depending on the mean grain size and/or angularity of the surface lags, and the cover ratio of lag:soil:vegetation. The “yellow” fans are considered to have formed initially in the piedmont zone at the foot of the strike ridges as debris flows of locally derived coarse materials. The “red” fans are younger debris flows of slurry material formed by landslide action following deposition of the “yellow” fans. These flowed out over the “yellow” fans. During subsequent wet climatic phases, generations of alluvial fans developed as a series of discrete and topographically prominent, alluvial fan lobes over the marginal fans. Creeks since formed have developed as well-formed flow lines.

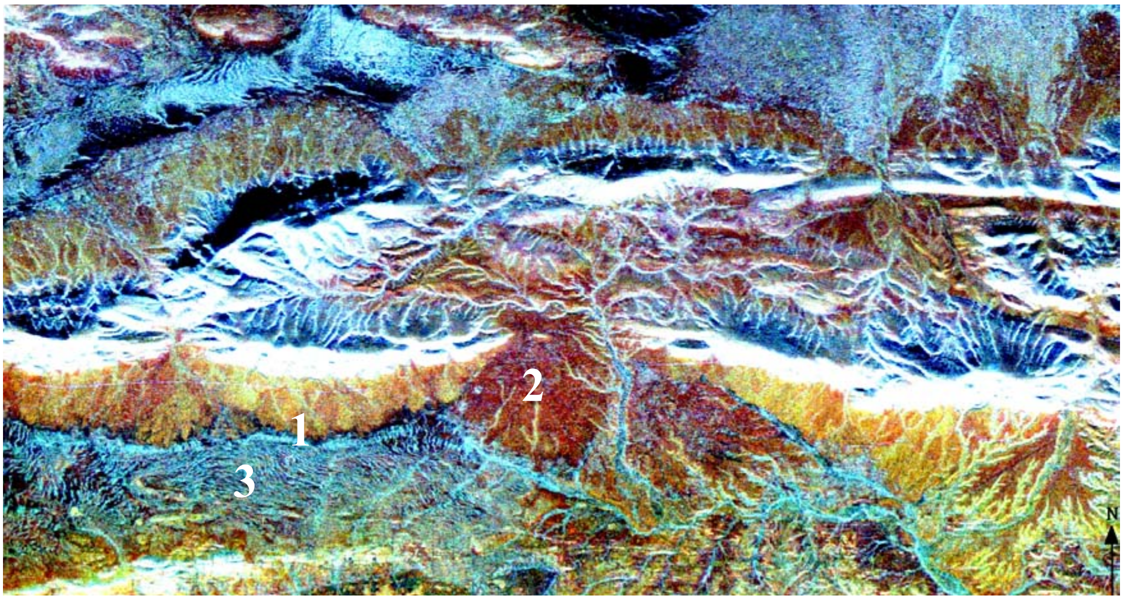

Figure 3. Landforms in vicinity of Ophthalmia Range, Hamersley Basin – a composite image of AIRSAR bands Cvv/Lvv/Pvv as RGB. Site dimensions - 16x8 km.

Geological mapping

Enhancements of multi-parameter radar data are excellent for delineating rock units based on variations in surface roughness and dielectric properties when vegetative cover is minimal. For example, rock units within the closure of Arkaroola syncline, Flinders Ranges, South Australia, have distinct roughness properties according to their lithology, weathering and erosional characteristics. A subset of three bands Cvv/Lhv/Phv displayed as an RGB image in Figure 4 provides an accurate representation of the distribution of the rock units in the accompanying geological map. The technique is more appropriate for sedimentary sequences rather than metamorphic complexes where results have shown a poor correlation between roughness and radar backscatter (Tapley, 2000).

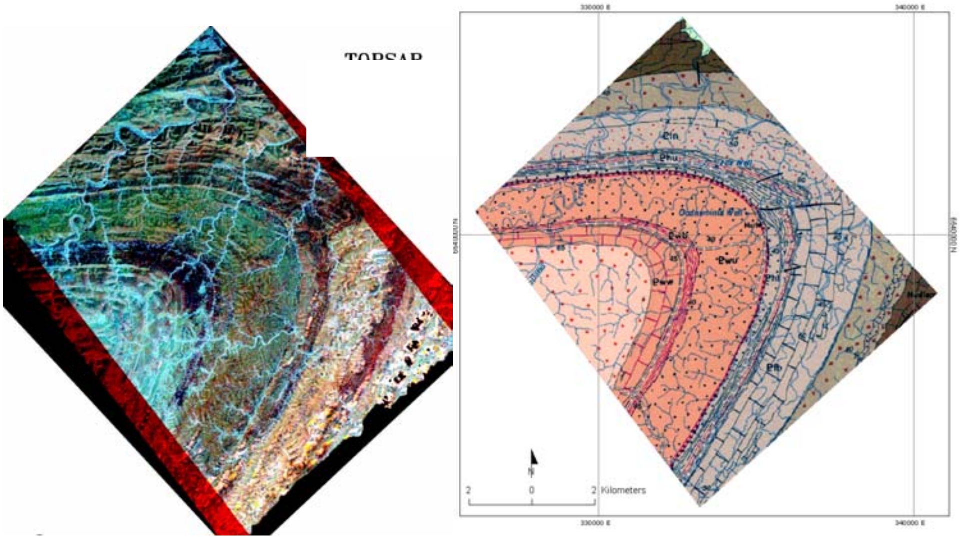

Figure 4. AIRSAR C-, L- and P-band multi-polarization composite image of stratigraphic sequence comprising Arkaroola syncline, Flinders ranges, South Australia, shows a strong relationship with the mapped geology.

Draping the radar image in Figure 4 over a precision digital elevation model would place the stratigraphic sequence in perspective with the local topography, and enhance the geological detail. Interactive viewing of 3-D perspective images on an image display screen is a simple technique for presenting the geology and landforms in a more informative way, and for understanding the relationships between landforms, geomorphic processes and terrain relief.

The highlighting and shadowing of the terrain by the side-looking illumination of radar is a distinct benefit for mapping geological structures in vegetated and non-vegetated terrains. In areas of prominent outcrop and relief, an image will commonly have a psuedo-3-dimensional perspective that highlights the position of lineaments, fault and fold structures, and morphological characteristics such as dip slopes and slope-asymmetry. For example, an enhancement of AIRSAR data in Figure 5 has provided a new insight into the geologic framework of the Ophthalmia Range region by highlighting several prominent structures within the synform, and linear extensions of these structures within the adjacent valleys (Tapley, 1996). Their appearance seems to be caused primarily by surface roughness since the alignments are mostly coincident with topographic expressions including those of stream segments, boundaries of outcrop and lithological contacts.

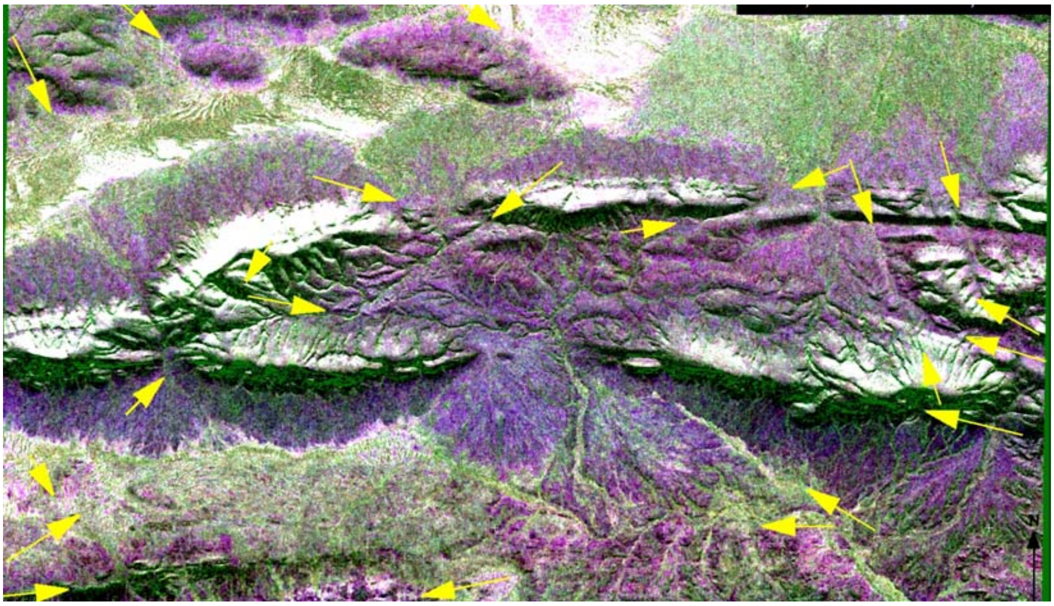

Figure 5. An interpretation of prominent linear structures from an enhancement of AIRSAR data of the Ophthalmia Range region. Site dimensions are 16x8 km, north direction to top of image.

4. RADAR INTERFEROMETRY

Topographic mapping

Radar interferometry is an innovative technique that enables very high-resolution topographic maps of the earth’s surface to be generated using spaceborne and airborne radar instruments. As with radar imagery, the technique has the advantages of automatic processing of the data, and operation in cloud, smoke and rainfall conditions, night and day. A transmit antenna mounted on a spacecraft or plane illuminates the terrain with a radar beam that is scattered by the surface. This radar echo has two components: amplitude (brightness) and phase (a measure of the distance to the target). Two receive antennas with a fixed baseline record the radar echo from slightly different positions resulting in two different radar images. The two signals received at both ends of the baseline (referred to as the interferometric baseline) show a phase shift due to differing lengths of the signal paths. The phase difference, determined by effectively subtracting the measured phase at each end of the baseline, is sensitive to both viewing geometry and the height of the terrain. If the viewing geometry is known to sufficient accuracy, then the topography can be inferred from the phase measurement to a precision of several metres.

Interferometric data can be generated from either single-pass or repeat-pass systems. Single-pass systems such as the TOPSAR (Zebker, et al., 1992) (http://airsar.jpl.nasa.gov/) and Shuttle Radar Topography Mapping Mission (SRTM) instrument http://www.jpl.nasa.gov/srtm/ use the two-antenna system to record both images simultaneously. Repeat-pass interferograms are generated from separate passes over the same target such as from the European ERS-1 and ERS-2 systems http://earth.esa.int/applications/interferometry.html.

The height accuracy of TOPSAR digital elevation models has been shown by Madsen, et al. (1995) to be 1 m RMSE in flat terrain and 3 m in mountain areas with a 2 m RMSE overall. Typical data acquisitions are for areas of 10 km across-track and up to 60 km along track. A list of TOPSAR datasets recorded over Australia and Papua New Guinea are available on the JPL web site http://airsar.jpl.nasa.gov/.

The accuracy of the data lends itself to generating precision geomorphometric and structural detail in semi-arid and humid-tropical environments. In Figure 6, shaded relief images highlight dip and strike slopes of the bedding sequence within a prominent anticline in the James Ranges, west of Alice Springs (left), and foliation trends within a metamorphic core complex masked by a canopy of tropical vegetation in Papua New Guinea (right). In the latter, it is evident that the top of the vegetation canopy conforms to the underlying topography that, in turn, is controlled by geological features and geomorphic processes. The majority of the short wavelength C-band radar backscatter is from the canopy surface thereby providing a reasonably accurate digital elevation product of the terrain.

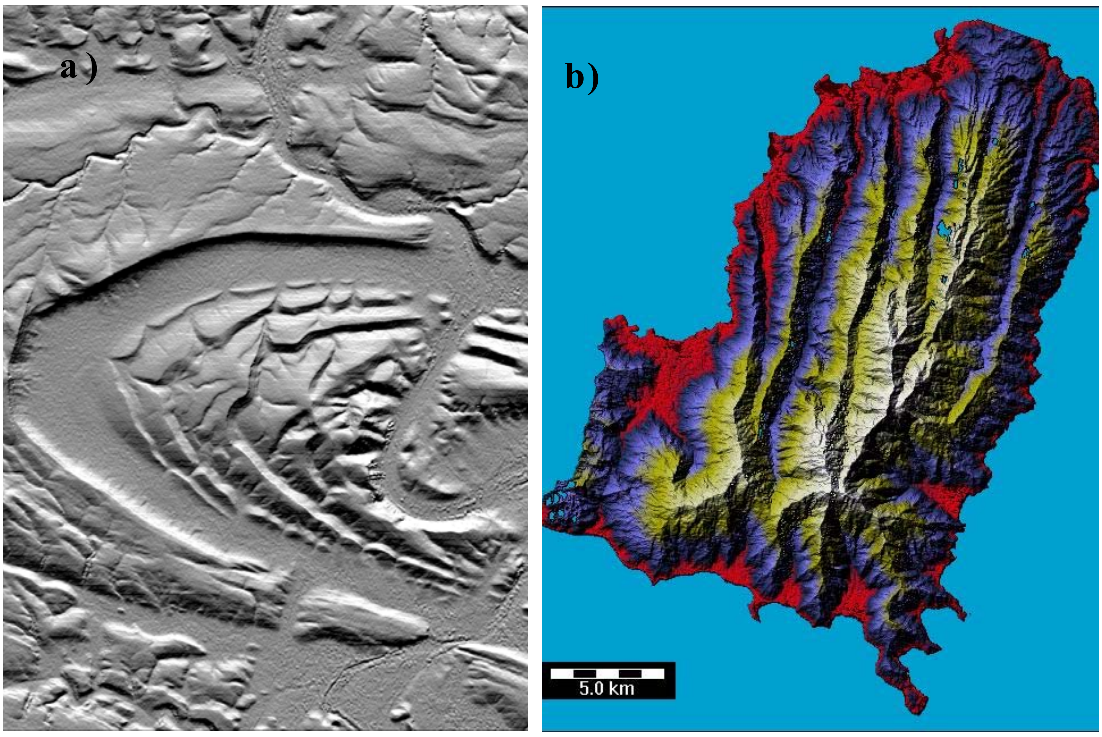

Figure 6. DEMs generated from TOPSAR radar interferometry of two contrasting terrains – semi-arid central Australia (a) and humid-tropical Papua New Guinea (b).

Shuttle Radar Topography Mapping Mission

The Shuttle Radar Topography Mapping Mission (SRTM) in February 2000 recorded images in C-band (5.56 cm) and X band (3.1 cm) frequencies during an 11-day period. Data were acquired along 225 km wide swaths imaging Earth's entire land surface between 60° north and 56° south latitude, with data points spaced every 1 arc-second of latitude and longitude (approximately 30 m). X-band coverage occurred along narrow 50 km wide swaths and cover 40% of the area mapped by the C-band data. The absolute horizontal and vertical accuracy of the C-band data will be 30 m and 16 m, respectively. Relative height accuracy will be 10 m. However, data of these specifications will not be readily available for public use. Within 2 years, data spatially degraded to 90 x 90 m horizontal resolution but retaining the initial height accuracy, will be available at the low cost of regridding the data to a 1° x 1° area. The policy for distributing the higher resolution data is currently not clear. However, it is expected that data over politically insensitive areas, such as Australia, will be accessible. X-band DEM data of the narrower 50 km wide swath have a horizontal resolution of 30 m and relative and absolute height accuracies of 6 m and 16 m, respectively. These data will be unclassified and available for public use from the German Aerospace Centre. Both C and X-band datasets will be geometrically corrected and projected to the WGS84 datum. Extensive information describing the data products and their availability is available on the SRTM and DLR Home Pages http://www.jpl.nasa.gov/srtm/ and http://www.dfd.dlr.de/SRTM/november2000/html, respectively.

5. USE OF RADAR DATA FOR EXPLORATION

The following recommendations are made on the use of operational imaging radar for providing detail about the morphologic and structural characteristics of most Australian terrains. As mentioned earlier, data availability is currently limited to ERS-1 and ERS-2 (C band, VV polarization), JERS-1 (L band HH polarization), Radarsat (C band HH polarization) and AIRSAR (multi-frequency polarimetric data from 1993 and 1996 PacRim1 missions). The SRTM and PacRim2 AIRSAR datasets will become available in 2001-02.

1. A combination of C (~5.5 cm), L (~24 cm) and P (~68 cm) bands is optimal for unmixing the signal response of the surface from that of the subsurface, and the ground-surface scattering from the canopy. C band has the highest priority for mapping outcropping lithologies and for discriminating between depositional and erosional terrains. L band is most sensitive to scales of surface change that occur through erosion of the regimes, and P band is preferred for mapping subsurface structures. However, because of distortions to low-frequency signals beyond the earth's atmosphere, P band can operate effectively only from an airborne system. Therefore L band is currently the longest wavelength possible in a spaceborne system. Increased penetration of both soil and vegetation cover can be obtained from an airborne ultra-wide-band radar system operating with wavelengths >100 cm provided that soil moisture and green biomass levels are minimal.

2. VV and HV (or VH) are the polarizations of choice for geological mapping in arid/semi-arid lands. Although VV and HH polarizations both result in useful SAR images for the majority of the terrains, VV is favoured because of its increased sharpness and ability to provide better discrimination between surfaces having similar roughness characteristics. The HV (VH) polarization for P band provides the best indication of volume scattering from the shallow subsurface. In woodland terrains, HH-polarization signals suffer less attenuation from the vertically aligned tree trunks and are more likely to provide information about the physical characteristics of the underlying ground-surface. The cross-polarized HV scattering coefficients are less dependent on incidence angle than the co-polarized (HH and VV) scattering coefficients. They are also less sensitive to variations in terrain slope. If geobotanical relationships exist or are being sought, VV-polarization data are preferred since they have increased interaction with the tree trunks.

3. A spatial resolution of approximately 10 m is necessary to resolve many of the narrow alignments of subcrop and lithic fragments found in sandy arid terrains. For general synoptic mapping and morphologic characterization, a footprint of 20 m will probably suffice.

4. Incidence angles of between 30° and 50° are recommended for mapping surficial bedrock units and regolith materials based on variations in their surface roughness. Angles <30° can reduce the ability of the radar signals to discriminate between surfaces of different RMS roughness levels, although in sandy terrains, the steep 23 degree angle of incidence of ERS data is a distinct advantage since the majority of outcrop is low profile and intermittent.
5. For maximum geological information, the flight direction should parallel the regional strike, or be within 45° of strike if there are several suites of geological structures present. In sand-ridge terrain, if there is no preferred direction, the flight lines are best positioned orthogonal to the dune direction. The current spaceborne radar sensors including those on the Radarsat, ERS-1 and JERS satellites collect data from ascending and descending passes meaning that both east-looking and west-looking azimuth directions are available.

6. PROCESSING AND LIMITATIONS OF RADAR DATASETS

Such is the high level of radiometric quality of AIRSAR data that enhancements derived from these data can be used in their original form for valid interpretations. Nevertheless, it is widely recognized that radar datasets collected from airborne platforms do regularly contain an unwanted signal component, commonly referred to as "noise" introduced by system and aircraft electronics. In addition, all radar datasets contain an inherent random and multiplicative "noise" component called "speckle" that has the capability to reduce the visual information content of the data, especially in the shorter wavelength bands. Much of this is due to the coherent nature of the return signals.

A technique used regularly to reduce speckle in spaceborne and airborne datasets has been that of spatial filters. A common finding from examinations of speckle filters is the superiority of adaptive filters, such as Lee and Frost filters, over the standard digital noise filters such as low pass and median filters. Ideally, a filter should reduce speckle while preserving the radiometric information (the radar backscatter value), and the spatial sharpness in the data. Adaptive filters essentially retain important high-frequency detail in the form of point of small targets whereas the standard convolutions filter, for example the median filter, smoothes the data obliterating narrow linear features. However, experience with processing ERS and JERS datasets of sandplain regions has demonstrated the benefit of a 3 x 3 median filter for suppressing much of the scene speckle. Speckle and "noise" reduction can also be achieved in the ENVI image processing software http://www.rsinc.com/envi/ by implementing the Minimum Noise Fraction (MNF) Rotation option. Advice on its proper use should be sought from the author.

Enhancements of ERS-1, JERS-1 or RADARSAT datasets cannot resolve the detailed information about the land-surface observed in images of equivalent AIRSAR wavelength-polarization band combinations. Maximum value for each can be gained from the synoptic view afforded by small-scale images and image mosaics of large areas. This is especially applicable to JERS data, where the degrading effects of speckle and reduced radiometric integrity are visually concealed by the scale of the data.

Designed for ocean observations, the ERS radar instruments are not ideally configured for geological applications. Over hilly terrains, the steep incidence angle will promote topographic distortion in the data. However, in low-relief terrains, the steep incidence angle has the potential to provide maximum discrimination between outcrop and non-outcrop, and to differentiate between lithologies featuring surfaces with different and near-similar erosional characteristics. In sand-ridge terrains, where the radar signal responds strictly to the physical characteristics of the surface elements, the synoptic view can "piece-together" scattered outcrop into sensible alignments and patterns to allow an improved synthesis of the regional, geological picture.

Unfortunately the authors experience of RADARSAT data has been limited to two scenes of Fine-1 Near Beam mode data – one in prominent sedimentary outcrop with minimal vegetation, another in low relief, degraded terrain with a regular cover of chenopod shrubs. Both scenes were severely contaminated by speckle that required vigorous spatial filtering to suppress. Once filtered, the resultant images contained less information than are available from optical datasets, including aerial photographs.

Experience with AIRSAR data of degraded landscapes has shown that colour-composite images of AIRSAR data, processed to remove geometric and radiometric errors, will generally permit the recognition of the principal and subtle attributes of the terrain when the multi-frequency bands are ideally assigned to the colour components of an RGB display. However, felsic erosional landforms such as stripped convex hills, are seldom discernible from equivalent units in mafic terrain owing to similar radar responses from the surficial regolith materials of these landforms. Their separation can be best achieved from mineralogical differences observed on enhancements of Landsat TM data. In sub-tropical woodlands, images of AIRSAR data are very useful for recognizing the structural fabric of a region, but they cannot resolve landforms with the same definition as 1:25 000-scale aerial photographs.

The processing of polarimetric radar data requires the use of specialized tools included in commercial image-processing software packages such as ENVI (http://www.rsinc.com/envi/) and RADARSOFT (http://www.pcigeomatics.com/product_ind/easipace.html). Most packages have the adaptive filters necessary to process the single-band datasets.

REFERENCES

Henderson, F.M. and Lewis, A.J., 1998. Principles and applications of imaging radar. Manual of Remote Sensing. 3rd Edition, Volume 2. American Society for Photogrammetry and Remote Sensing. John Wiley & Sons Inc, Canada 866 pp.

Madsen, S. N., Martin, J.M. and Zebker, H.A., 1995. Analysis and evaluation of the NASA/JPL Across-Track Interferometric SAR System. Institute of Electrical and Electronic Engineers (IEEE) Transactions on Geoscience and Remote Sensing 33(2): 383-391.

Tapley, I.J. and Craig, M.D., 1995. An evaluation of AIRborne Synthetic Aperture Radar (AIRSAR) for mapping surface and sub-surface structures in the Telfer region, Paterson Province, Western Australia (Volumes 1 and 2). CSIRO/AMIRA Project 392. CSIRO Exploration and Mining Report 146R, pp. 110.

Tapley, I.J. 1996. An assessment of airborne synthetic radar (AIRSAR) as an aid to iron exploration in the Hamersley Basin, Western Australia. Executive summary report. CRC LEME Restricted Report 12R. CSIRO Exploration and Mining Report 282R. pp. 15.

Tapley, I.J., 1998. Landform, regolith and geological mapping in Australia using polarimetric and interferometric radar datasets – Executive Summary Report. CRC LEME/AMIRA Project 392. CRC LEME Report 90R. CSIRO Exploration and Mining Report 529R. pp. 38.

Tapley, I.J., 2000. Geological mapping and terrain analysis in Australia using multifrequency, polarimetric radar data. The recognition of geological units within the Flinders and Olary Ranges, South Australia (Volumes 1 and 2). Prepared for Sumitomo Metal Mining Co. Ltd. CRC LEME Restricted Report 154. pp. 93.

Zebker, H.A., Madsen, S.N., Martin, J., Wheeler, K.B., Miller, T., Lou, Y., Alberti, G., Vetrella, S. and Cucci, A., 1992. The TOPSAR interferometric radar topographic mapping instrument. Institute of Electrical and Electronic Engineers (IEEE) Transactions on Geoscience and Remote Sensing 30(5): 933-940.

AIRBORNE AND GROUND MAGNETICS

Ross C. Brodie

Geoscience Australia. PO Box 378, Canberra, ACT 2601. E-mail: ross.c.brodie@ga.gov.au

1. OVERVIEW

Magnetics is a geophysical survey technique that exploits the considerable differences in the magnetic properties of minerals with the ultimate objective of characterising the Earth's sub-surface.

The technique requires the **acquisition** (Horsfall, 1997) of measurements of the amplitude of the **magnetic field** at discrete points along survey lines distributed regularly throughout the area of interest.

The magnetic field, whose amplitude is measured, is the vector sum of;

1. the Earth's **main field** which originates from dynamo action of conductive fluids in the Earth's deep interior (Merrill, et al., 1996);

2. an **induced field** caused by magnetic induction in magnetically susceptible earth materials polarised by the main field (Doell and Cox, 1967);

3. a field caused by **remanent magnetism** of earth materials (Doell and Cox, 1967); and,

4. other (usually) less significant fields caused by solar, atmospheric (Telford, et al., 1976) and cultural influences.

It is the induced and remanent fields that are of particular interest to the regolith geoscientist because the magnitudes of these fields are directly related to the **magnetic susceptibility,** spatial distribution and concentration of the local crustal materials. Fortunately only a few minerals occur abundantly enough in nature to make a significant contribution to the induced and remanent fields. The most important of these is magnetite and to a lesser extent ilmenite and pyrrhotite (Clarke, 1997, Telford, et al., 1976).

Once the main field and the minor source effects are removed from the observed magnetic field data via various **data reduction and processing** methods (Luyendyk, 1997), the processed data serve as an indicator of the spatial distribution and concentration of the magnetically significant minerals. At this point the data are **enhanced and presented** (Milligan and Gunn, 1997) in readiness for their analysis. Most importantly the analysis ultimately leads to an **interpretation** (Gunn, et al., 1997a, Mackey, et al., 2000) of structure, lithology, alteration, regolith and sedimentary processes, amongst many other factors.

The geological ingredients that can be interpreted from magnetic surveys are those that influence the spatial distribution, volume and concentration of the magnetically significant minerals. It is important to realise that the magnetic data serve only as an indicator because it is generally not possible to ascertain a definitive, unambiguous and direct lithological or structural interpretation.

In Papp, É. (Editor), 2002, *Geophysical and Remote Sensing Methods for Regolith Exploration*, CRCLEME Open File Report 144, pp 33-45

2. DATA ACQUISITION

General

The magnetic field is usually measured with a total field magnetometer. The most common instrument in use today is the caesium vapour magnetometer. Observations are made at regular intervals (generally between 1 to 7 metres) along a series of **traverse lines** of constant azimuth and spacing. Observations are similarly made along **tie lines** oriented perpendicular to the traverse lines. Tie lines are necessary to assist in the removal of temporal variations in the main field. Tie lines are usually spaced ten times further apart than traverse lines.

Data may be acquired close to ground level (ground magnetics) either via a person carrying a magnetometer or with a magnetometer mounted on a motor vehicle such as a quad motorcycle or four-wheel drive. Alternatively airborne magnetics (aeromagnetics) can be acquired via mounting the magnetometer on a fixed wing aircraft or a helicopter. Fixed wing acquisition is preferred due to the lower cost, however helicopters are necessary where the terrain is rugged.

While data are being collected along the survey lines a **base station magnetometer** also measures the magnetic field at a stationary point. These data serve as an estimate of the temporal variation of the main field, which is subtracted from the survey data. The base station magnetometer is also used to identify **magnetic storm** events (where the magnetic field is varying rapidly due to disturbances in the ionosphere/magnetosphere). On such occasions data acquisition is suspended (or data re-acquired) because the estimate of the temporal variation is less accurate at a distance from the base station.

2.2 Survey design

Survey specifications are normally determined by consideration of several factors. Some specifications are discussed below.

1. A trade off between cost and the required detail determines the traverse line spacing – smaller line spacing equates to higher cost but also higher resolution. The distribution and shape of the magnetic sources to be mapped is important. Since narrow features have narrow anomalies they may not be resolved if the line spacing is too coarse. Conversely, deeper sources have broader anomalies (though more subtle), accordingly it is not always necessary to use a fine line spacing if the sources are deep. Common airborne traverse line spacings in use today range from 400m in regional mapping programs through to 200 m, 100 m and down to 50 m for detailed mapping projects at prospect scale. Finer lines spacing (down to 20 m) are sometimes employed in special circumstances. Ground magnetic surveys usually have traverse line spacings from 25 to 50 metres. Finer spacings are also possible if necessary.

2. Maximum information is extracted when survey lines are oriented perpendicular to the geological strike (or at least to the structures of most interest).

3. Flying height is always ultimately determined on the basis of safety. The main factors affecting the safety of a particular flying height is the ruggedness of the terrain and the climbing capability of the aircraft. Other than the safety factor it is generally best to carry out surveys at a constant, and lowest possible, terrain clearance. However, due to the difficulty of processing, and interpreting data acquired at highly variable clearances, it is better to choose a flying height that the aircraft can comfortably maintain rather than a height that is difficult to maintain and results in significant variation in flying height. Flying height and line spacing are often considered linked to the extent that it is desirable to have lower flying heights with finer line spacings. This is to maintain better spatial resolution of anomalies along flight lines to reflect the better resolution between flight lines. Standard combinations of line spacing and flying height are 400 m/80 m, 200 m/60 m, 100 m/60 m and 50 m/40 m.

3. DATA REDUCTION AND PROCESSING

Data reduction and processing is the series of steps taken to remove both signal and spurious noise from the data that are not related to the geology of Earth's crust. This process thereby prepares the dataset for interpretation by reducing the data to only contain signal relevant to the task. These steps are summarised below.

1. **Magnetic compensation** removes the influence of the magnetic signature (remanent, induced and electrical) of the aircraft on the recorded data. This is often done in real time on-board the aircraft.

2. **Data checking and editing** involves the removal of spurious noise and spikes from the data. Such noise can be caused by cultural influences such as powerlines, metallic structures, radio transmissions, fences and various other factors. This step will ideally include systematic and detailed viewing of all data in graphical profile form to ensure instrumental and compensation noise is within tolerance.

3. **Diurnal removal** corrects for the temporal variation of the earth's main field. This is achieved by subtracting the time-synchronised signal, recorded at a stationary base magnetometer, from the survey data. This procedure relies on the assumption that the temporal variation of the main field is the same at the base station and in the survey area. Best results are obtained if the base station is close to the survey area, the diurnal variation is small and smooth and electromagnetic induction effects are minimal (Lilley, 1982, Milligan, 1995).
4. **Geomagnetic reference field removal** removes the strong influence of the earth's main field on the survey data. This is done because the main field is dominantly influenced by dynamo action in the core and not related to the geology of the (upper) crust. This is achieved by subtracting a model of the main field from the survey data. The Australian or International Geomagnetic Reference Field (AGRF or IGRF) is generally used for this purpose. This model accounts for both the spatial and long period (>3 year) temporal variation (secular variation) of the main field (Lewis, 2000).
5. **Tie line levelling** utilises the additional data recorded on tie lines to further adjust the data by consideration of the observation that, after the above reductions are made, data recorded at intersections (crossover points) of traverse and tie lines should be equal. Several techniques exist for making these adjustments. Luyendyk (1997) gives a detailed account of the commonly used techniques. The most significant cause of these errors is usually inadequate diurnal removal because of the assumptions stated above.
6. **Micro-levelling** is used to remove any errors remaining after the above adjustments are applied. These are usually very subtle errors caused by variations in terrain clearance or elevated diurnal activity. Such errors manifest themselves in the data as anomalies elongate in the traverse line direction. Accordingly they can usually be successfully removed with directional spatial filtering techniques (eg. Minty, 1991).

4. GRIDDING

Data are recorded along traverse lines that are never perfectly straight or equally spaced and the sampling rate along the lines is much denser than across the lines. It is usually desirable to interpolate these data (profile data) onto a regular lattice or grid. This procedure is known as gridding and permits further algorithms and image processing techniques to be applied to the processed data. Several gridding techniques are commonly used (eg. Briggs, 1974, Fitzgerald, et al., 1997).

In most cases the data are interpolated onto a grid with a cell size of one fifth or one quarter of the line spacing. It is important to note that in the vast majority of cases, gridded data do not contain the full information content that is contained in the original profile data because it is under sampled in the flight line direction during gridding. Hence it may be necessary to use profile-based presentations of the data as well as grid-based presentations in order to retrieve maximum information.

5. PRESENTATION

Although post processing and enhancement are the next logical steps in the sequence, it is convenient first to address presentation techniques. There are several methods of presenting magnetic data (both pre and post enhancement), some of which are summarised below.

1. **Stacked profiles** are line-based maps in which all lines of data are plotted as XY graph style profiles. Each profile is geographically located beside each other. The X axis of each profile is along the line of best fit through the survey line and the Y axis is at right angles to that. This is the oldest form of presentation but still has the advantage of being able to show detail that cannot be shown in grid-based presentations due to loss of information (in the gridding process) in the flight line direction. One disadvantage of this type of presentation is that it is usually difficult to choose a single vertical scale and base level that is appropriate (optimised) for all of the displayed data. However there are pre-processing methods such as high pass and automatic gain control filtering that can be applied to alleviate this problem. Stacked profile plots are likely to be a useful form of presentation for regolith studies because the high sampling rate along lines is not compromised by the necessity for gridding as in contouring and imaging.

2. **Contour** maps have traditionally been a popular way of presenting gridded data. These maps have largely been replaced by images in recent years. Like stacked profiles it can be difficult to choose a single contour interval suitable for all the data. Where recognition of absolute amplitudes of anomalies is important these presentations are important. Many interpreters continue to use contours because they are superior to images when gradients of anomalies are to be used in determining dips of structures.

3. **Images** are the most common style of presentation today. Images are essentially a presentation in which individual pixels in the image are colour (or greylevel) coded according to some attribute of the gridded data being imaged. The advantage of images is that they are capable of showing extremely subtle features not apparent in other forms of presentations. They are also quickly manipulated in digital form, thereby providing an ideal basis for GIS based on screen interpretation. Milligan, et al. (1992) and Milligan and Gunn (1997) provide useful descriptions of these techniques as applied to magnetic data.

4. **Bipole plots** are a further form of presentation that have particularly relevant application in regolith studies due to their ability to resolve subtle detail (Gyngell, 1997). Similarly to stacked profiles, this method is applied to profile data but employs colour coded bar graphs where the colour represents polarity and length represents amplitude of an enhanced attribute of the data (Mudge, 1991).

6. POST PROCESSING AND ENHANCEMENT

Enhancement and post processing includes a range of transformations of the processed data that assist in its interpretation. These transformations usually either simplify the anomalies, make features of particular interest more prominent at the expense of others or make an attempt to relate the measured field to rock properties.

Post-processing techniques are based on the well-known theory of magnetic fields. The most important of these are summarised below and the reader should refer to Milligan and Gunn (1997) for an excellent overview of their application.

1. **Reduction to the pole** simplifies the interpretation of anomalies by removing the asymmetry introduced due to its induction by the inclined main field. The main field is only vertical (and induced anomalies symmetric) at the north and south magnetic poles. As the name suggests reduction to the pole transforms the data to that which would be measured at the magnetic poles. This simplifies the anomalies by centring anomalies over the causative magnetic body rather than being skewed and offset to one side.

2. **Vertical and horizontal derivatives** quantify the spatial rate of change of the magnetic field in vertical or horizontal directions. Derivatives essentially enhance high frequency anomalies relative to low frequencies.

3. **Upward and downward continuation** of magnetic data transforms the data to that which would be observed on different surfaces either above or below the actual observation surface. Upward continuation thus tends to attenuate the effect of near surface sources relative to deeper sources. Downward continuation has the opposite effect.

4. **Analytic signal** transformations combine derivative calculations to produce an attribute that is independent of the main field inclination and direction of magnetisation as well as having peaks over the edges of wide bodies. Thus a simple relationship between the geometry of the causative bodies and the transformed data are observed.

These transformations need to be applied and interpreted with careful consideration of their in-built assumptions. For instance downward continuation to a surface below the magnetic sources is not valid and reduction to the pole assumes there is no remanent magnetisation. Additionally there are some practical limitations to their application, for example high order derivatives and downward continuation tend to amplify noise and other errors in the data.

Other types of transformations known as enhancements, which are not necessarily based on the fundamental theory of magnetic fields, can be applied. Some typical examples follow.

1. **Artificial illumination** is a method of visually enhancing image data so that if the magnetic data were a surface, it is illuminated as if the sun was shining on it from a certain azimuth and elevation (Pelton, 1987). Otherwise know as sun angle or hill shade enhancement this method is excellent for making high frequency subtle features easily identifiable. Figure 1 is an example of an artificial illumination enhancement.

2. **Frequency selective filtering** is used to selectively remove, attenuate or amplify the effect of a certain band of frequencies. Such filters include high pass, lowpass and bandpass filters. They are important to the extent that, given a particular geometry, shallow sources have a higher frequency content than deep sources. Thus it is an important method of differentially enhancing the effects of sources at different depths.

3. **Directional filtering** enhances anomalies trending in particular directions. Such a technique is useful where subtle yet important trends need to be mapped but are complicated or even obscured by trends in other directions. To an extent artificial illumination acts as a directional filter because anomalies trending perpendicular to the sun angle are preferentially enhanced.

4. **Regolith filters** have been designed (Dauth, 1997, Gunn, et al., 1997b) which aim to specifically separate the effect of regolith materials from basement material.

5. **Automatic gain control** (Rajagopalan and Milligan, 1995) is an amplitude filtering method that has great application in the identification of subtle anomalies. It works on the principle of equalising the power of the signal in a moving window passed over the dataset; thus it attenuates strong anomalies and amplifies weak anomalies. This filter can be particularly useful in regolith studies because regolith materials often have a low magnetic susceptibility.

6. **Statistical filters** such as averaging and median filters can also be used to remove spurious noise or to smooth anomalies to make them more interpretable.

7. **Textural filtering** is a method that responds to the shape, size and continuity of adjacent anomalies (Dentith, et al., 2000). Because assemblages of regolith material usually have a characteristic textural appearance, textural filtering has application in regolith studies.

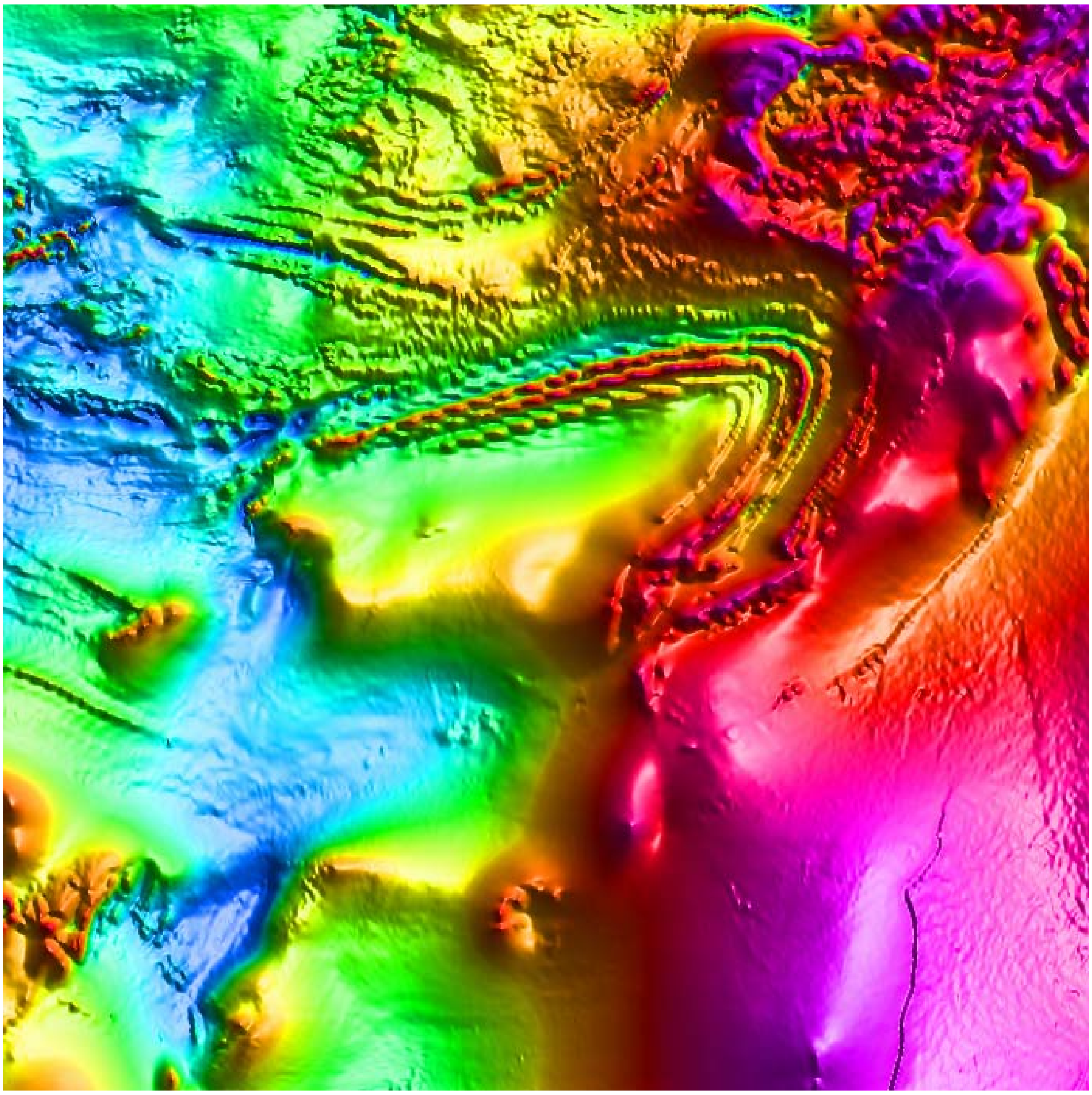

Figure 1. Colour image of magnetic data reduced to the pole with artificial illumination from the northeast. The data are from a portion of regional airborne survey in the Flinders Ranges of South Australia, flown with 400-metre line spacing and 80 metre terrain clearance. The image covers an area of 70 x 70 km. The data allow direct mapping of structures (folding and faulting).

7. APPLICATIONS

Analysis of the magnetic data and their various enhancements via a suite of qualitative and quantitative methods results in an interpretation of the sub-surface geology. Most interpretation schemes utilise a broad qualitative interpretation of the complete dataset with detailed quantitative methods applied on certain anomalies to test the validity the interpreted source.

Qualitative interpretation relies on the spatial patterns that an interpreter can recognise in the data. Faults, dykes, lineaments and folds are usually easily identified (eg. Figure 1). Intrusive bodies are often recognised by virtue of the shape and amplitude of their anomalies. Palaeolandscape features such as buried volcanic flows and palaeochannels usually show distinct dendritic pattens. Figure 2 shows the delineation of maghemite filled palaeochannels in the West Wyalong district of New South Wales. Magnetic units or assemblages with anomalous susceptibilities can often be directly mapped by recognition of domains with a characteristic magnetic signature. After correlation with additional information direct lithological inferences can sometimes be drawn. Weathering and alteration can also be interpreted where these processes have either depleted or enriched the magnetite content (Gunn and Dentith, 1997). Recognition of reversely polarised anomalies due to remanently magnetised rocks can be useful in differentiating volcanic flows of various ages. Dauth (1997) demonstrates how magnetic data gives insights into regolith processes through an example of the identification of maghemite-rich lateritic weathering products. Gunn, et al. (1997a) give a detailed overview of qualitative interpretation techniques and the types of geological entities that can be mapped by magnetic data.

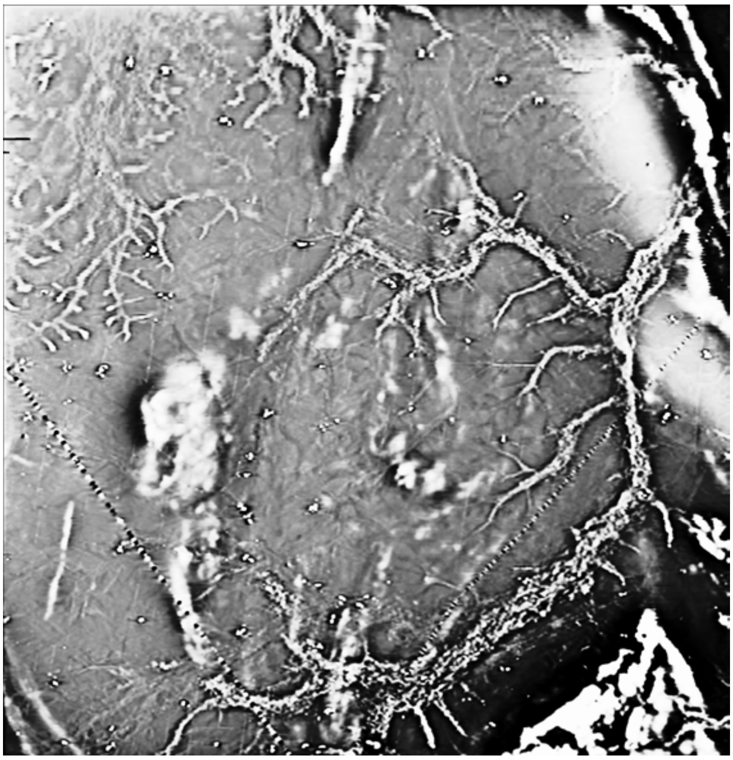

Figure 2. Greyscale image of the first vertical derivative of magnetic data reduced to the pole. The data are from a portion of detailed survey flown near West Wyalong in New South Wales, with 50-metre line spacing and 50 metre terrain clearance. The image covers an area of 17 x 22 km. The obvious dendritic patterns are characteristic of palaeochannel and volcanic flows. In this case they relate to maghemite filled palaeochannels (Mackey, et al., 2000). Several cultural anomalies relating to buildings, fences and powerlines are also evident in the image.

Qualitative interpretation may be complemented with several forms of quantitative interpretation that seek to provide useful estimates of the geometry, depth and magnetisation of the magnetic sources. Broadly categorised as curve matching, forward modelling or inversion, quantitative techniques rely on the notion that simple geometric bodies, whose magnetic anomaly can be theoretically calculated, can adequately approximate magnetic more complex bodies. Gunn (1997) provides a subjective review of the more important techniques.

The simplest of these are the so-called "rules of thumb" and curve matching methods. Rules of thumb are simple approximate empirical rules that relate a magnetic body's depth, shape and magnetisation to certain parameters measured manually from profile plots of its anomaly (Blakely, 1996). Curve matching is slightly more sophisticated because in this case the interpreter matches parameters measured from plots to "type" curves (eg. Naudy, 1970, Parker Gay, 1963) that have been published for various types of simple geometric bodies. Although these methods are conceptually simple they are tedious to apply and have generally fallen from favour.

Forward modelling is a trial and error process whereby;

1. A geometric body (model) is chosen to approximate the real geological body to be modelled.

2. The theoretical magnetic anomaly of the model is calculated and compared to the measured anomaly.

3. Adjustments are made to the parameters that define the model and the anomaly is recalculated until the calculated and observed anomalies match or "fit" to the interpreter's satisfaction.

Geometric bodies such as ellipsoids, plates, rectangular prisms, polygonal prisms and thin sheets can all be calculated. For example faults are often modelled using a thin sheet model. In this case the parameters that describe the model are the depth to the top, dip, strike and magnetisation contrast thickness product. Complex bodies can be built by superposing the effects of several simple bodies. Assumptions about the strike length, azimuth and depth extent are used in formulating the forward modelling algorithms; accordingly interpreters need to be cautious and use the appropriate model for each situation otherwise erroneous results will occur. Figure 3 is a quantitative model from Mackey, et al. (2000) in which a near surface palaeochannel deposit and deeper volcanic units are modelled.

Like most other geophysical methods, magnetics is ambiguous to the extent that there are an infinite (although not all geologically plausible) number of models that have the same magnetic anomaly. Hence if a model is forward modelled and it fits the observed anomaly, it is not proof that the model is correct. Irrespective of this, forward modelling is a method that has stood the test of time and is probably the single most useful quantitative technique in use.

Inversion is a procedure in which a geological model, whose theoretical magnetic anomaly matches (within some tolerance) the observed magnetic field, is determined by an automated process. There are two ways this can be achieved, known as linear inversion and iterative or non-linear inversion.

Linear inversion is possible only where the theoretical magnetic anomaly of the model can be formulated in terms of a system of linear equations where the model parameters are the unknowns. In this case the model parameters are determined by solving the system via standard linear algebra methods. Linear inversion is restrictive since it can only be applied to relatively simplistic models. Linear inversion has been applied in several useful schemes for susceptibility mapping (eg. Bott, 1967).

Iterative or non-linear inversion is more widely applicable because it can be used with models that are more geologically realistic. The technique is essentially the same as forward modelling except that an automated routine is used to determine the adjustments to be made to the model parameters. Also a calculated measurement of fit, such as RMS or chi-squared error is used in place of an interpreters visual inspection. Several different schemes exist for determining the adjustments, some of which use random search methods and others that use downhill minimisation methods. Both linear and iterative inversions suffer from the effects of ambiguity in the solution. This is recognised where geologically implausible models are produced while the fit is very good. Constraints can be placed on the model parameters using *a priori* information in these cases.

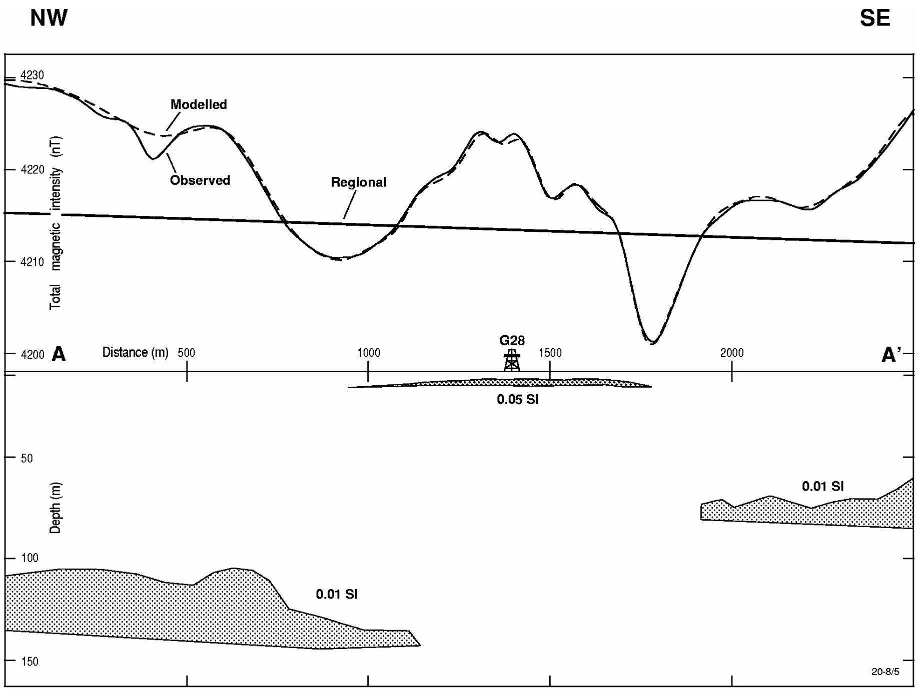

Figure 3. Forward modelling from Mackey, et al. (2000) in which a near surface palaeochannel deposit and deeper volcanic units are modelled. In this case, polygonal shapes approximate each body. The theoretically calculated (modelled) anomaly fits the observed anomaly well, indicating that this model is a possible cause of the observed anomaly.

Many automated routines exist for estimating the depth to basement. These routines cannot distinguish between magnetic sources in the basement and magnetic sources in the regolith and are more correctly termed depth to magnetic source routines. Gunn (1997) gives a detailed description of several of these. Popularly used techniques include Naudy curve matching, Phillips' autocorrelation method, Werner deconvolution, Euler deconvolution and spectral depth estimates. Although these are automated methods, careful consideration of the results is required, because many assumptions are made about the shapes of the causative bodies.

8. PROBLEMS AND LIMITATIONS

The greatest limitation of the magnetic method is the fact that it only responds to variations in the magnetic properties of the earth. Accordingly, many characteristics of the sub-surface that a regolith geologist wishes to delineate are not resolvable by the magnetic method because there is no associated change in the distribution of magnetite.

While novice interpreters may be able to easily identify some geological units, structures and characteristics from magnetic datasets, highly experienced interpreters are usually required to extract the subtle information contained in the data.

The inherent ambiguity in magnetic interpretation is problematic where several geologically plausible models can be attained from the data. Interpreters must be aware of this limitation and be prepared to use any available ground truth information or other datasets to decrease the ambiguity.

Cost

Airborne surveys are almost always priced on a dollar per line kilometre basis. In recent years fixed wing survey prices have generally been between $4.50 to $6.00 per kilometre for medium to larger size surveys (7,000 km or larger). Small surveys usually attract a price premium and may cost up to $8 or $12 per kilometre. Helicopter surveys are usually three to five times more expensive than fixed wing surveys and will cost up to $35 per kilometre. Airborne acquisition prices will usually include gamma-ray spectrometric data.

Ground surveys are more time consuming and more expensive. Because ground conditions and access play a major part in production rates, prices are often quoted on a per day basis. A reasonable guide is $1,500 per day per two-person crew. Such a crew may acquire 40 km per day ($37.50 per km) in easily traversed country, whilst they might only achieve 20 km per day ($75 per km) in heavily vegetated country with numerous physical obstructions.

Non-production charges are also incurred as part of the data acquisition cost to account for production delays that are not in the control of the contracting company (stand-by charges). These are usually due to bad weather or magnetic storms. These charges are around $1,000 to $2,000 per airborne crew per day. Most companies will include a mobilisation/demobilisation fee as a one off charge to cover the overhead of setting up a new field base.

Apart from the dollars per kilometre rate the major influence on the cost of a survey is the traverse line spacing. As a general rule of thumb the number of line kilometres can be calculated as follows;

$$line\ kilometres = \frac{1000 \times (1 + \frac{traverse\ line\ spacing\ in\ metres}{tie\ line\ spacing\ in\ metres}) \times area\ in\ square\ kilometres}{traverse\ line\ spacing\ in\ metres}$$

For example for a 300 square kilometre (20 x 15 km) survey area with a traverse line spacing of 200 metres and tie line spacing of 2,000 metres, the total line kilometres will be;

$$line\ kilometres = \frac{1000 \times (1 + \frac{200}{2000}) \times 300}{200} = 1650 km\ .$$

Service Providers

Several companies in Australia offer magnetic data acquisition and processing services. The major companies are listed below.

1. Fugro Airborne Surveys - aeromagnetics
2. Universal Tracking Systems - aeromagnetics
3. Geophysical Technology Limited - ground magnetics and aeromagnetics)
4. Ultra Mag - ground magnetics
5. Baigent Geosciences - magnetic data processing, presentation
6. Pitt Research - magnetic data processing, presentation
7. Geoimage - presentation
8. Quadrant Geophysics - ground acquisition, some processing
9. Solo Geophysics - ground acquisition, some processing
10. Elliott geophysics - ground acquisition, some processing

11. Southern Geoscience Consultants - some processing, presentation
12. GPX Airborne Surveys - airborne acquisition, processing
13. GPX - ground acquisition, some processing.

Choosing between ground magnetics and aeromagnetics

Some comparative pros and cons of ground magnetics and aeromagnetics are summarised below.

1. Aeromagnetics has lower costs per line kilometre ($5-9/km compared to $50-80/km).

2. Aeromagnetic data are acquired more rapidly (eg. 1800 km/crew/day compared to 30 km/crew/day).

3. There are few access difficulties in aeromagnetics unless the survey area is in a built-up area where flying restrictions apply or in rugged terrain where a helicopter is necessary, thereby increasing the per line kilometre cost by three to five times. Ground magnetic surveys can suffer where access to private property is difficult or ground conditions are unfavourable, such as where there is dense vegetation, fences or watercourses.

4. Higher spatial resolution can be achieved and more subtle anomalies can be detected with ground magnetics because line spacings and sample distances are usually smaller and the measurements are made nearer to the magnetic sources.

5. Near surface magnetic sources are more readily resolved with ground magnetic surveys (Gyngell, 1997). Hence where the objective of the survey is the very detailed delineation of narrow magnetic sources in the top 20 metres, ground magnetics will probably be the method of choice. Conversely, strong magnetic sources at or near the surface, commonly caused by ferruginous pisoliths, may mask more subtle deeper sources – although delineation of the pisoliths may be of equal importance to the regolith geoscientist.

9. CONCLUSION

The magnetic method is a powerful tool that can be successfully applied in regolith studies. Since magnetics provide a relatively direct mapping of the abundance of magnetic minerals, it also serves as a useful indicator of lithology, structure, weathering and alteration processes. The method is mature and inexpensive technology. Australia has several experienced contracting companies and a competitive industry.

Airborne and ground magnetics have various advantages and disadvantages but airborne magnetics will be the method of choice unless subtle near surface anomalies are crucial. Routine data reduction and processing methods exist but need to be applied with rigour. There are several variations on enhancement and presentation methods that need to be selectively applied depending on both the data and the aim of the project. Specialised enhancements have been developed for dealing with regolith materials.

Qualitative interpretation is based on recognition of spatial patterns within the data. Many geological entities such as faults, folds and intrusions can often be easily identified whilst more skilled interpreters may be required to distinguish the probably more subtle effects of weathering. Direct lithological interpretation is usually not possible without additional information. Several quantitative methods exist that can estimate the depth, geometry and magnetisation of simple geometric bodies that could produce the observed anomaly. Ambiguity is an inherent property of magnetic data, accordingly all quantitative interpretations need to be reviewed with caution.

REFERENCES

Blakely, R.J., 1996. Potential theory in gravity and magnetic applications. Cambridge University Press, Cambridge, 441 pp.

Bott, M.H.P., 1967. Solution to the linear inverse problem in magnetic interpretation with application to oceanic magnetic anomalies. Geophysical Journal of the Royal Astronomical Society 13: 313-323.

Briggs, I.C., 1974. Machine contouring using minimum curvature. Geophysics 39: 39-48.

Clarke, D.A., 1997. Magnetic petrophysics and magnetic petrology: aids to geological interpretation of magnetic surveys. AGSO Journal of Geology and Geophysics 17: 83-103.

Dauth, C., 1997. Airborne magnetic, radiometric and satellite imagery for regolith mapping in the Yilgarn Craton of Western Australia. Exploration Geophysics 28: 199-203.

Dentith, M., Cowan, D.R. and Tompkins, L.A., 2000. Enhancement of subtle features in aeromagnetic data. Exploration Geophysics 31: 104-108.

Doell, R. and Cox, A., 1967. Magnetization of Rocks. In: SEG Mining Geophysics Volume Editorial Committee (Editors), Mining Geophysics, Volume 2: Theory. Society of Exploration Geophysicists, Tulsa pp. 446-453.

Fitzgerald, D., Yassi, N. and Dart, P., 1997. A case study on geophysical gridding techniques: INTREPID perspective. Exploration Geophysics 28: 204-208.

Gunn, P.J., 1997. Quantitative methods for interpreting aeromagnetic anomalies: a subjective review. AGSO Journal of Geology and Geophysics 17: 105-113.

Gunn, P.J., Maidment, D. and Milligan, P.R., 1997a. Interpreting magnetic data in areas of limited outcrop. AGSO Journal of Geology and Geophysics 17: 175-185.

Gunn, P.J., Fitzgerald, D., Yassi, N. and Dart, P., 1997b. New algorithms for visually enhancing airborne geophysical data. Exploration Geophysics 28: 220-224.

Gunn, P.J. and Dentith, M.C., 1997. Magnetic responses associated with mineral deposits. AGSO Journal of Geology and Geophysics 17: 145-155.

Gyngell, N.R., 1997. Second horizontal derivatives of ground magnetic data applied to gold exploration in the Yilgarn Craton of Western Australia. Exploration Geophysics 28: 232-234.

Horsfall, K.R., 1997. Airborne magnetic and gamma-ray data acquisition. AGSO Journal of Geology and Geophysics 17: 23-30.

Lewis, A., 2000. Australian geomagnetic reference field, 2000 revision. Preview 85: 24.

Lilley, F.E.M., 1982. Geomagnetic field fluctuations over Australia in relation to magnetic surveys. Bulletin of the Australian Society of Exploration Geophysics 13: 68-78.

Luyendyk, A.P.J., 1997. Processing of airborne magnetic data. AGSO Journal of Geology and Geophysics 17: 31-38.

Mackey, T., Lawrie, K., Wilkes, P., Munday, T., de Souza Kovacs, N., Chan, R., Gibson, D., Chartres, C. and Evans, R., 2000. Paleochannels near West Wyalong, New South Wales: A case study in delineation and modelling using aeromegnetics. Exploration Geophysics 31: 1-7.

Merrill, R.T., McEthinny, M.W. and McFadden, P.L., 1996. The magnetic field of the earth: paleomagnetism, the core and the deep mantle. Academic Press, San Diego, 531 pp.

Milligan, P.R. and Gunn, P.J., 1997. Enhancement and presentation of airborne geophysical data. AGSO Journal of Geology and Geophysics 17: 63-75.

Milligan, P.R.M., 1995. Short-period geomagnetic variations recorded concurrently with an aeromagnetic survey across the Bendigo area, Victoria. Exploration Geophysics 26: 527-534.

Milligan, P.R.M., Morse, M.P. and Rajagopalan, S., 1992. Pixel map preparation using the HSV colour model. Exploration Geophysics 23: 219-224.

Minty, B.R.S., 1991. Simple micro-levelling for aeromagnetic data. Exploration Geophysics 22: 591-592.

Mudge, S.T., 1991. New developments in resolving detail in aeromagnetic data. Exploration Geophysics 22: 277-284.

Naudy, H., 1970. Une methode d'analyse sur profiles aeromagnetiques. Geophysical Prospecting 18: 56-63.

Parker Gay, S., 1963. Standard curves for interpreting magnetic anomalies over long tabular bodies. Geophysics 28: 161-200.

Pelton, C., 1987. A computer program for hill-shading digital topographic data sets. Computers and Geosciences 13: 545-548.

Rajagopalan, S. and Milligan, P., 1995. Image Enhancement of aeromagnetic data using automatic gain control. Exploration Geophysics 25: 173-178.

Telford, W.M., Geldart, L.P., Sheriff, R.E. and Keys, D.A., 1976. Applied Geophysics. Cambridge University Press, Cambridge, 860 pp.

AIRBORNE GAMMA-RAY SPECTROMETRY

John Wilford

Cooperative Research Centre for Landscape Environments and Mineral Exploration,
Geoscience Australia. PO Box 378, Canberra, ACT 2601. E-mail: john.wilford@ga.gov.au

1. METHOD

Airborne gamma-ray spectrometry (AGRS) measures the abundance of Potassium (K), Thorium (eTh) and Uranium (eU) in rocks and weathered materials by detecting gamma-rays emitted due to the natural radioelement decay of these elements.

Potassium abundance is measured directly as gamma-rays are emitted when ^{40}K decays to Argon. Uranium and Thorium cannot be measured directly. Daughter nuclides generated during the decay of parent elements are measured, and the abundance of parent elements is inferred. Distinct emission peaks associated with ^{208}Tl and ^{214}Bi are used to calculate the concentration of Th and U (Figure 1). Therefore, U and Th are expressed in equivalent parts per million (eU and eTh).

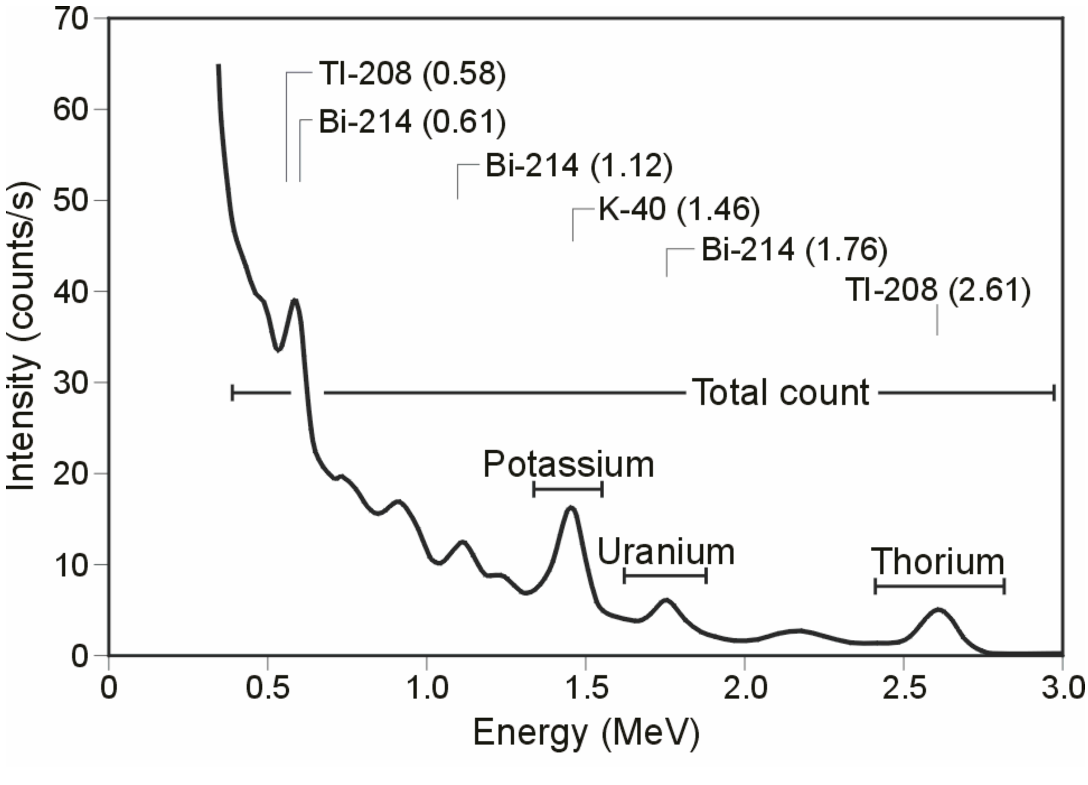

Figure 1. Gamma-ray spectrum showing the position of the K, Th, U and total count windows.

2. DATA COLLECTION AND SOURCE

Airborne gamma-ray data is collected by either helicopter or aeroplane, typically between 60 to 100 metres flying height above the surface. Sodium-iodide scintillation crystals on the aircraft measure gamma-rays emanating from the surface. Photomultiplier tubes attached to the scintillation crystals record and amplify the gamma-ray induced signal (Minty, 1997). The spatial resolution of gamma-ray data largely depends on the line spacing of the airborne survey. Flight line spacing is usually a compromise between data resolution and acquisition costs. Regional airborne geophysical surveys are

In Papp, É. (Editor), 2002, *Geophysical and Remote Sensing Methods for Regolith Exploration*, CRCLEME Open File Report 144, pp 46-52.

typically flown at 400 or 200 metre line spacing, whereas detailed surveys are usually between 50 to 100 metres.

Gamma rays emanate from the top 30 cm of dry rock and soil (Minty, 1997). Potassium has a crustal abundance of 2.3 % and occurs in many rock-forming minerals such as K-feldspars, micas and as clays like illite. Uranium and Th are much less common compared with K, with an estimated crustal average of 3 ppm and 12 ppm, respectively. Uranium is associated with pegmatites, syenites, radioactive granites, some black shales and many accessory minerals. Thorium is most common in accessory and resistate minerals such as zircon, sphene, apatite, xenotime, monazite and epidote. Typical concentration of radioelements in Australian rocks and soils are given in Table 1. Vegetation, unless thick, generally has little effect on the gamma-ray response. Spectrometric surveys therefore have an advantage over other remotely sensed data such as Landsat and SPOT which can be difficult to interpret due to fire scarring and vegetation masking of soil and regolith materials (Wilford, 1992).

3. PROCESSING AND INTEPRETATION

Airborne gamma-ray survey datasets are typically displayed as images. Individual radioelements are displayed as pseudocoloured images or combined as false colour composites with K in red, eTh in green and eU in blue. White and black hues in the image correspond to high and low abundances, respectively, of all three of the radioelements. Mixtures of K, eU and eTh appear as magenta and yellow hues, respectively. Gamma-ray images are usually expressed as percent K and parts per million for eTh and eU. Images can be contrast stretched or ratioed (eg. K/eTh) to highlight subtle variations in the data. Before images are generated from the flightline profiles, several corrections are applied to the data (eg. to remove noise). These corrections are not discussed here but are described at length by Minty (1997).

Gamma-ray images can be readily integrated and manipulated with other datasets using geographic information systems and image processing systems. Combining gamma-ray images with SPOT or Landsat TM using additive or HIS colour space transforms (Wilford, et al., 1997) is particularly useful for adding terrain attributes and locational information for image interpretation. Digital elevation models can be combined with gamma-ray data as shaded relief images or as 2.5D perspective. Supervised and unsupervised classification techniques can be used to cluster radioelement responses into similar spectral groups for separating major lithological units.

4. APPLICATIONS FOR REGOLITH AND SOIL MAPPING

Gamma-rays emitted from the surface will relate to the mineralogy and geochemistry of the bedrock and weathered materials (eg. soils, saprolite, alluvial and colluvial sediments). Weathering modifies the distribution and concentration of radioelements compared to the original bedrock. Understanding the bedrock and regolith responses has proven invaluable for not only mapping regolith materials but also understanding geomorphic processes (Wilford, et al., 1997). Fortunately, from a regolith perspective K, Th and U behave quite differently from one another during bedrock weathering and pedogenesis. As a general rule, K concentration decreases with increasing weathering. This is because K is highly soluble under most weathering environments and is rapidly leached from a regolith profile. An exception to this is where K is incorporated into potassic clays such as illite. In contrast U and Th are associated with resistate minerals and are scavenged by iron oxides in the weathering profile. Therefore U and Th concentration tends to either stay the same or are preferentially increased in regolith materials as other more soluble minerals are lost in solution. These relationships are summarised in Figure 2.

Table 1. Radioelement content of Australian rocks and soils. Measured K, Th and U values (averaged value in brackets) for various rock types (modified from Dickson and Scott, 1997).

Rock type	Rock			Soil		
	K %	U ppm	Th ppm	K %	U ppm	Th ppm
Intrusives						
granitoids	0.3 - 4.5 (2.4)	0.4 - 7.8 (3.3)	2.3 - 45 (16)	0.4 - 3.9 (2.1)	0.5 - 7.8 (2.7)	2 - 37 (13)
gneissic rock	2.4 - 3.8 (2.4)	2.1 - 3.6 (2.5)	18 - 55 (15)	0.7 - 1.9 (1.3)	1.6 - 3.8 (2.2)	6 - 19 (12)
pegmatite	2.6 - 5.5 (3.7)	0.3 - 1 (0.7)	0.3 - 9.6 (2)			
aplites	0.6 - 4 (2.4)	1 - 8 (3.3)	3 - 20 (7)			
quartz-feldspar porphyry	1 - 5 (2.9)	1.3 - 2.9 (1.7)	6 - 14 (13)			
intermediate intrusives	0.7 - 5.6 (2.7)	0.1 - 1.2 (0.8)	0.8 - 6.1 (2.4)	0.7 - 3.4 (1.6)	1.5 - 2.3 (1.9)	2.9 - 8.4 (5.6)
mafic intrusives	0.1 - 0.8 (0.4)	0.0 - 1.1 (0.3)	0.0 - 3.1 (1.2)			
Extrusives						
felsic volcanics	2.0 - 4.4 (3.7)	1.4 - 13 (2.4)	13 - 28 (17)	1.8 - 3.2 (2.4)	1.3 - 2.4 (2.1)	10 - 18 (13)
intermediate volcanics	1.8 - 4.1 (2.7)	0.9 - 5.6 (2.3)	1.5 - 15 (9)	1.0 - 2.7 (1.9)	1.2 - 3.6 (2.1)	4 - 17 (10)
low-K andesites	0.7 - 0.9 (0.8)	1.0 - 2.5 (1.6)	3 - 8 (5)	0.8 - 1.5 (1.1)	1.2 - 1.5 (1.3)	4 - 6 (5)
mafic volcanics	0.3 - 1.3 (0.9)	0.3 - 1.3 (0.7)	2.0 - 5.0 (3.0)	0.2 - 1.4 (0.7)	0.6 - 2.5 (1.6)	3.3 - 13 (7.9)
ultramafic volcanics	0.2 - 0.9 (0.4)	0.3 - 0.9 (0.6)	0.0 - 4.0 (1.2)	0.6	2.0	6
Sedimentary rocks						
Archaean shales	0.4 - 1.6 (0.9)	0.3 - 1.3 (0.9)	1 - 5 (2.7)	0.8	1.2	3
other shales	0.1 - 4.0 (2.6)	1.6 - 3.8 (2.6)	10 - 55 (19)	0.7 - 3.0 (1.5)	1.2 - 5 (2.3)	6 - 19 (13)
arenites	0.0 - 5.5 (1.8)	0.7 - 5.1 (2.3)	4 - 22 (12)	0.1 - 2.4 (1.3)	1.2 - 4.4 (2.1)	7 - 18 (11)
carbonates	0.0 - 0.5 (0.2)	0.4 - 2.9 (1.6)	0 - 2.9 (1.4)			

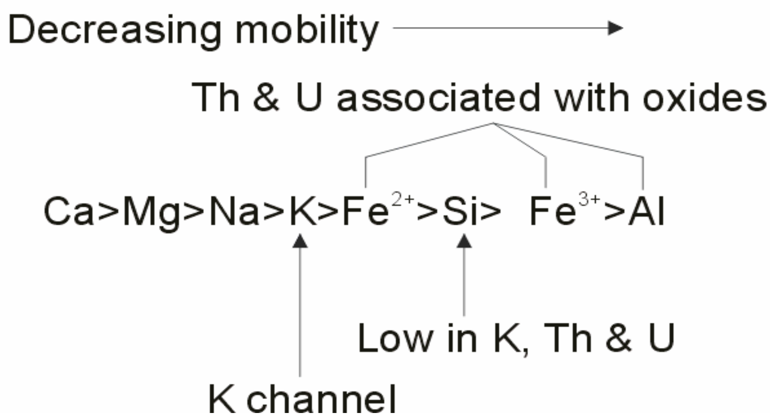

Figure 2. Element weathering and gamma-ray response (Wilford, et al., 1997).

Highly weathered landscapes in parts of Cape York Peninsula have either low abundance of K, eTh and eU (eg. quartzose sands) or low K and high eTh and eU associated with the accumulation of oxides and resistate minerals at or near the surface (Wilford, 1992). For example, highly leached aluminous and ferruginous bauxitic soils around the Weipa region are identified on the gamma-ray imagery by their low K and elevated eTh and eU values. This is reflecting soils with very low exchangeable cations and high content of iron and aluminium oxides and resistate minerals (eg. Zircons).

Gamma-ray spectrometry imagery can be used to separate areas of high geomorphic activity with shallow regolith from stable surfaces that are less geomorphically active and that have deeper and more highly weathered regolith (Wilford, 1992). Gamma-ray response over an actively eroding landscape is likely to reflect the mineralogy and geochemistry of the bedrock, whereas that over stable landforms is likely to reflect soil/regolith materials (Figure 3).

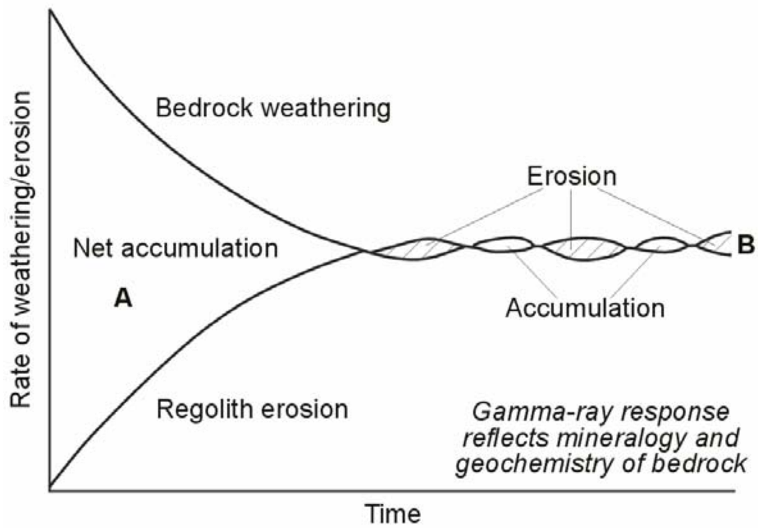

Figure 3. Relationship between gamma-ray response and denudation balance in landscapes. A - areas of active erosion (eg. where erosion rates are higher than rates of weathering) the gamma-ray response will reflect bedrock geochemistry. B – area where the rates of weathering are higher than the erosion rates the gamma-ray response will reflect regolith and soil geochemistry.

Draping the gamma-ray image over a digital elevation model as a perspective view is an excellent way of understanding geomorphic relationships and separating bedrock and regolith gamma-ray responses (Figure 4). An integrated approach using gamma-ray spectrometrics and digital elevation models was used to identify large-scale erosional and depositional processes within river catchments (Pickup and Marks, 1999).

Mapping catenas using airborne gamma-ray imagery is a good illustration of the relationship between geomorphic process and gamma-ray response. Catenas are recognised on gamma-ray imagery over granitic landforms in Cape York (Wilford, et al., 1997) and on shaly lithologies in the Wagga Wagga area in NSW (Bierwirth, 1996). In both cases the upper slopes have thin soils, with deeper soils and regolith on the lower slopes. The gamma-ray response of the upper slopes is dominated by bedrock chemistry whereas the gamma-ray response over the lower slopes has reduced K concentration due to weathering.

Gamma-ray images can be used to separate depositional regolith materials derived from different sources, or of different ages. In some landforms, potassium concentration can be used as a gauge of the degree of surface weathering, where depleted Potassium (K) is associated which leaching (eg. the development of podzolic soils where soluble cation are leached from the upper part of the soil profile). Bierwirth (1996) demonstrated the use of gamma-ray images for mapping soil properties in the Wagga region NSW in southeastern Australia. Interpreted images over the Wagga Wagga region provided information about soil nutrients, texture and chemistry. Ratios of K and Th have been used to separate different regolith materials from bedrock signatures in the Yilgarn Craton of Western Australia (Dauth, 1997), demonstrating that low K/Th ratio values generally related to highly weathered and ferruginous saprolite.

Gamma-ray imagery forms one of several datasets used for mapping regolith materials. Combining radioelement (K, eTh, eU and Total count) bands with ratio bands from Landsat TM (eg. clay and Fe) will improve the separability of regolith materials, based on their radioelement and reflective signatures.

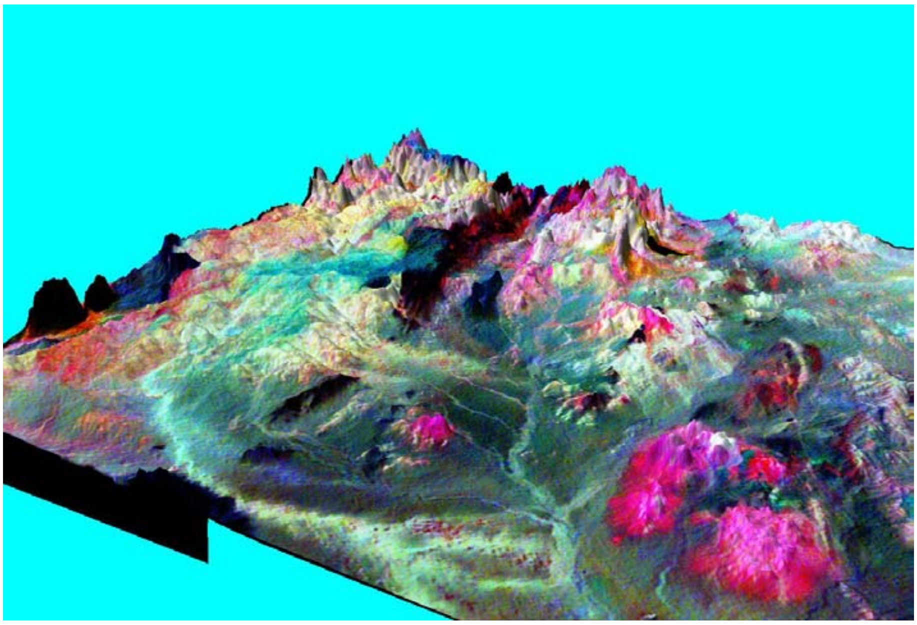

Figure 4. 3D landscape perspective and gamma-ray image over part of the Cootamundra 1:250 000 map sheet. Combined gamma-ray spectrometic images with DEM as 3D perspective views enable the visualisation of complex relationships between the gamma-ray response and terrain morphology attributes.

5. APPLICATION FOR MINERAL EXPLORATION

In addition to mapping the regolith, airborne gamma-ray spectrometric surveys show increasing potential to detect alteration associated with mineralisation (Dickson and Scott, 1997). Mineralising processes can change the abundance of one or several of the radioelements (eg. potassic alteration) compared to the surrounding host bedrock. Changes in radioelement concentration can either relate to primary mineralisation event(s) or to secondary processes. For example hydrothermal alteration may result in the rock being more susceptible to weathering. The higher degree of weathering may produce a distinctive gamma-ray response compared with the surrounding bedrock.

Residual analysis techniques can be used to identify subtle variation in radioelement abundance that may relate to localised mineralisation processes. Residual analysis involves calculating background K, eTh and eU values and then subtracting these values from the original image. For example regolith and geological units can be used to determine mean or average radioelement values for each unit. These average values are then subtracted from the original radioelement images to highlight values either higher or lower than the predicted regolith/bedrock response. This approach was used to identify elevated potassic values associated with quartz-illite-kaolinite-pyrite alteration in the Temora-Barmedman area, NSW (Lawrie, et al., 1998). Dickson, et al. (1996) has used a more sophisticated technique to develop predictive models of K, eTh and eU distribution in prospective rock units. Predictive abundance maps (generated using correlations with Landsat TM and DEM derived attributes) are compared with the original radioelement images to highlight subtle changes that may relate to mineralisation.

6. COSTS AND LIMITATIONS

Costs for acquiring airborne gamma-ray data is approximately $8.00 per line km. The cost to fly a 1:250 000 map sheet at 400 m line spacing would therefore be about $400,000. This includes all processing and also magnetic data. Not all regolith materials have a unique gamma-ray signature, therefore gamma-ray data for regolith mapping is best used together with other datasets including Landsat TM, airphotographs and digital elevation models. Gamma rays emanate from the top 20-30 cm and are therefore recording the radioelement characteristics of the ‘A’ or upper ‘B’ horizon of soils or bedrock. Relating gamma-ray responses to regolith properties at depth may be misleading.

Estimating U and Th using their daughter isotopes assumes equilibrium in the decay chain. However disequilibrium can occur and should be considered when interpreting their abundances. For example, U anomalies can be caused by the accumulation of radium (^{226}Ra) in ground waters (Giblin and Dickson, 1984).

The behaviour of radioelements during weathering will depend on the initial bedrock composition or chemistry. For example, weathered felsic rocks usually show a loss of K whereas weathered basic or ultramafic rocks are barren in all three radioelements, and as a consequence will be a poor surrogate for mapping the degree of surface weathering. The same radioelement response can relate to different materials depending largely on the bedrock chemistry and mineralogy. For example highly weathered residual quartz sands developed on granitic saprolite can have the same radioelement signature as exposed fresh ultramafic bedrock. For this reason it is best to interpret the gamma-ray response within major lithological-geochemical groups (eg. sandstones, granite, basalt).

REFERENCES

Bierwirth, P., 1996. Investigation of airborne gamma-ray images as a rapid mapping tool for soil and land degradation – Wagga Wagga, NSW. AGSO Record 1996/22: 69 pp.

Dauth, C., 1997. Airborne magnetic, radiometric and satellite imagery for regolith mapping in the Yilgarn Craton of Western Australia. Exploration Geophysics 28: 199-203.

Dickson, B. L. and Scott, K.M., 1997. Interpretation of aerial gamma-ray surveys – adding the geochemical factors. AGSO Journal of Australian Geology and Geophysics 17(2): 187-200.

Dickson, B.L., Fraser, S.J. and Kinsey-Henderson, A., 1996. Interpreting aerial gamma-ray surveys utilising geomorphological and weathering models. Journal of Geochemical Exploration 57: 75-88.

Giblin, A.M. and Dickson, B. L., 1984. Hydrogeochemical interpretations of apparent anomalies in base metals and radium in groundwater near Lake Maurice in the Great Victoria Desert. Journal of Geochemical Exploration 22: 361-362.

Lawrie, K.C., Chan, R.A., Gibson, D.L., Wilford, J., Mackey, T. and Murray, A., 1998. Au-Cu mineral associations in the Temora Region, NSW. Professional Opinion, Report No. 1998/04. 56 pp., 110 maps and 8CD GIS in MapInfo.

Minty, B.R.S., 1997. The fundamentals of airborne gamma-ray spectrometry. AGSO Journal of Australian Geology and Geophysics 17(2): 39-50.

Wilford, J.R., Bierwirth, P.N and Craig, M.A., 1997. Application of airborne gamma-ray spectrometry in soil/regolith mapping and applied geomorphology. AGSO Journal of Australian Geology and Geophysics 17(2): 201-216.

Wilford, J. R., 1992. Regolith mapping using integrated Landsat TM imagery and high resolution gamma-ray spectrometric imagery – Cape York Peninsula. Bureau of Mineral Resources Record 1992/78: 35 pp.

GROUND AND AIRBORNE ELECTROMAGNETIC METHODS

Richard Lane

Geoscience Australia. PO Box 378, Canberra, ACT 2601. E-mail: richard.lane@ga.gov.au

1. SUMMARY

Electromagnetic (EM) methods are used to map variations in electrical properties. The main physical property involved in these methods is inductive electrical conductivity, which is a measure of how easily electrical current can pass through a material. Conductivity is a complex function of several variables including the conductivity of solid materials, conductivity of pore fluids, porosity, arrangement of pores and degree of saturation. Case studies are continuing to improve our understanding of the relationship between the conductivity of geological units and the processes such as weathering and groundwater movement that influence the principal controls on bulk conductivity.

For many years, variations in the conductivity of regolith were seen as a source of geological noise for EM surveys that were focussed on conductive base metal mineralisation. Applications that call for mapping regolith conductivity variations as an adjunct to discrete conductor detection or as an end in themselves are now well established.

A range of simple-to-operate, compact instruments are available to map average conductivity to depths of less than a metre to several metres. These instruments are used extensively in salinity and shallow groundwater applications. The addition of data logging and satellite navigation functionality to the EM system permits large volumes of well located data to be acquired relatively quickly.

The most significant advances have been to EM systems that image conductivity as a function depth. Improvements in acquisition systems and data processing (eg. bandwidth of recorded information, signal to noise ratio and methods to convert recorded information into subsurface conductivity) have combined to enhance the quality of the information about the subsurface and to simplify interpretation.

2. DESCRIPTION

Introduction

Subsurface materials exhibit a very large range of electrical conductivity values (Figure 1). Fresh rock is generally a poor conductor of electricity, but layers of graphite and certain metallic minerals containing iron, copper or nickel are very good conductors. These latter substances conduct electricity by allowing the migration of electrons and are hence termed “electronic conductors”.

Highly conductive minerals are quite rare in the majority of geological settings. The electrical properties of most rocks are governed to a large degree by the amount of water filling the gaps between the mineral grains and amount of dissolved salt in this water. Pure water has a very low electrical conductivity while seawater contains high levels of dissolved salts (approximately 35ppt), mostly NaCl, and is a relatively good conductor of electrical current. Groundwater can vary in salt content from fresh through brackish (slightly salty) to saline (similar in salt content to seawater) through to hyper-saline (more salty than seawater). These materials conduct electricity through the migration of ions through the pore fluid and hence are termed “ionic conductors”.

In Papp, É. (Editor), 2002, *Geophysical and Remote Sensing Methods for Regolith Exploration*, CRCLEME Open File Report 144, pp 53-79.

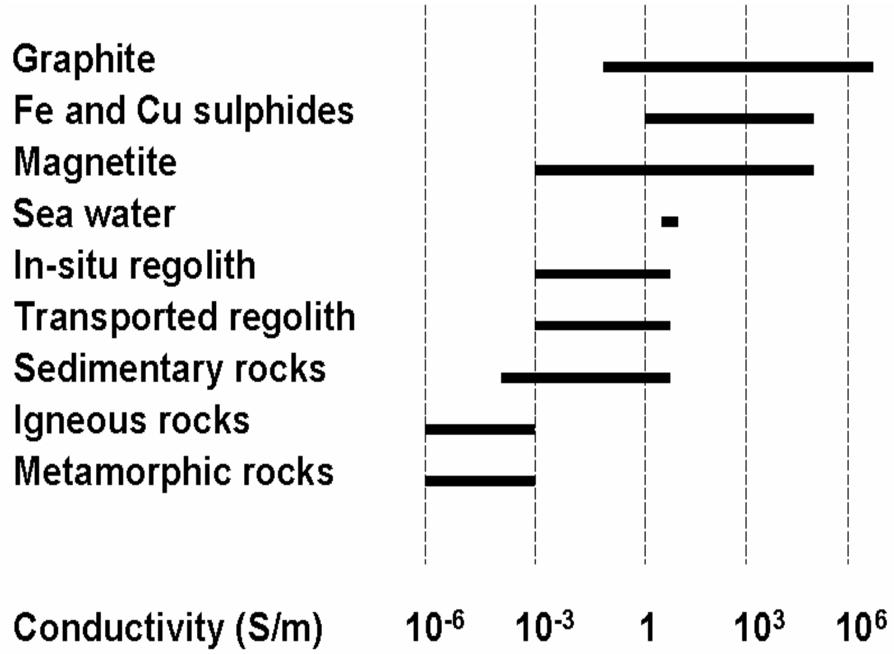

Figure 1. The range of conductivity values for various rocks and minerals.

EM subsurface investigation involves the transmission of electromagnetic energy, interaction of this energy with the ground, and reception of secondary, induced energy at a receiver (Figure 2). EM systems come in all shapes and sizes, but there will always be a source of electromagnetic energy (transmitter) and a receiver to detect the response of the ground. Currents induced in the ground are a function of conductivity. By processing and interpreting the received signals, it is possible to make deductions about the distribution of conductivity in the subsurface.

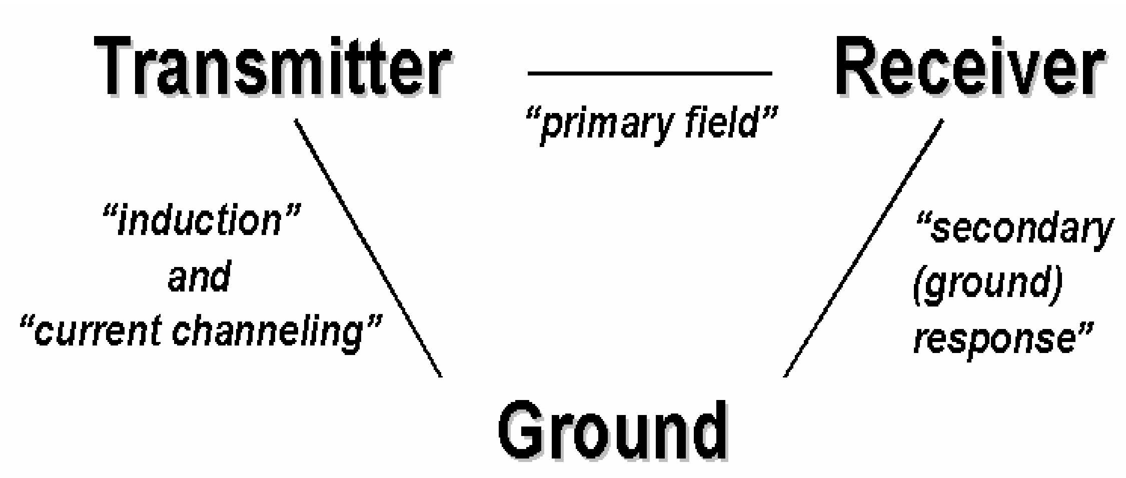

Figure 2. Interactions for an EM system.

Some electromagnetic methods take advantage of currents induced in the ground by natural electromagnetic waves. Lightning on a global scale is one of the strongest natural sources of electromagnetic energy used in this fashion. However, in the majority of cases, a man-made transmitter of electromagnetic waves is used, and the systems are described as "active" or "controlled source". A simple example of an electromagnetic instrument is a metal detector. This instrument is able to detect highly conductive metal objects buried at shallow depths. The same principles are used in EM mapping applications at vertical scales ranging from less than a metre to tens, hundreds or even thousands of metres.

The "active" nature of EM systems is in strong contrast to passive magnetic, gravity or gamma-ray spectrometric methods. Hardware limitations on signal to noise and bandwidth lead to proprietary configurations and added complexity in the processing and interpretation of EM data.

EM systems are classified in various ways by different authors according to the instrumentation, geometry of the transmitter-ground-receiver elements and the nature of the transmitted and recorded signal. A pure frequency domain (FD) EM system transmits a magnetic field signal at a single frequency with sinusoidal variation in amplitude. The recorded response can either be described by its total amplitude and phase with respect to the transmitter signal or by the amplitudes of components in-phase ("in-phase") and 90° out of phase ("quadrature") with respect to the transmitter signal. A pure time domain (TD) EM system transmits a magnetic field signal with a sharp step. The time decay of currents induced in the subsurface is sampled at a number of delay times ("windows") following the step change in magnetic field. "Early" and "late" are qualifiers applied to windows in reference to the elapsed time following the change in the magnetic field. The window measurements contain information equivalent to that which would be obtained with a number of FD systems covering a range of frequencies. The equivalent range of frequencies is referred to as the "bandwidth" of the system. In practice, EM systems are often a combination of these two end members, and it is important to note both the bandwidth and signal to noise characteristics of the system being employed at each of these equivalent frequencies.

A single or multi-turn loop is generally used as the transmitter element of EM systems. A time varying current passing through the loop is used to create a time varying magnetic field. Wire coils are most commonly used as the receiver element of EM systems, but superconducting SQUID magnetometers have also been used. A voltage is induced in the receiver coils proportional to the time rate of change of the magnetic field directed along the axis of the coil. Two or three coils may be used to measure the response along perpendicular axes. The horizontal component of the response along the survey line is referred to as the X component. The horizontal component of the response perpendicular to the survey line is referred to as the Y component. The vertical component of the response is referred to as the Z component. An X component transmitter loop teamed with a trailing X component receiver coil is referred to as a horizontal "coaxial" configuration. A Z component transmitter loop teamed with a trailing Z component receiver coil is referred to as a vertical axis "coplanar" configuration.

The "scale" of an EM system is an indication of the largest dimension of the transmitter-ground-receiver geometry. For different systems, it may be the size of the transmitter loop, or the separation of the transmitter and receiver, or the terrain clearance of the transmitter or receiver. The "footprint" of an EM system is the area (but more strictly the volume) of the ground beneath the system that contributes the majority of the response (Liu and Becker, 1990). This is a complex function of the "scale" of the system, the transmitted power and frequency range, receiver sensitivity, and ground conductivity distribution. As a guide, the footprint is approximately a disk with a diameter which is a small multiple (eg. 2 to 3 times) the scale of the system.

The "skin depth" is the depth at which signal is reduced to 1/e (~37%) of the original amplitude. For a FD EM system:

$$\text{skindepth} = \sqrt{\frac{2}{\mu_0}} \cdot \sqrt{\frac{1}{\sigma \cdot 2 \cdot \pi \cdot f}} \approx 500 \cdot \sqrt{\frac{1}{\sigma \cdot f}}$$

where $\mu_0 = 4 \cdot \pi \cdot 1 \cdot e^{-7}$ H/m, σ is the conductivity of the subsurface in S/m and f is the frequency of the system in Hz. The equivalent concept for a TD EM system is the "diffusion depth" which is the depth at which the local electric field reaches a maximum,

$$\text{diffusion depth} = \sqrt{\frac{2}{\mu_0}} \cdot \sqrt{\frac{t}{\sigma}} \approx 1260 \cdot \sqrt{\frac{t}{\sigma}}$$

where $\mu_0 = 4 \cdot \pi \cdot 1 \cdot e^{-7}$ H/m, σ is the conductivity of the subsurface in S/m and t is the delay time in seconds of the measurement after a step change in the transmitted magnetic field. The concept of skin depth or diffusion depth is a convenient way to represent the relative penetration of electromagnetic energy at different frequencies or times (ie. signal) (Figure 3), but does not include allowance for noise (ie. signal to noise). “Depth of investigation” or “depth of detection” are more complex quantities which are derived by factoring in noise levels into “depth of penetration” calculations.

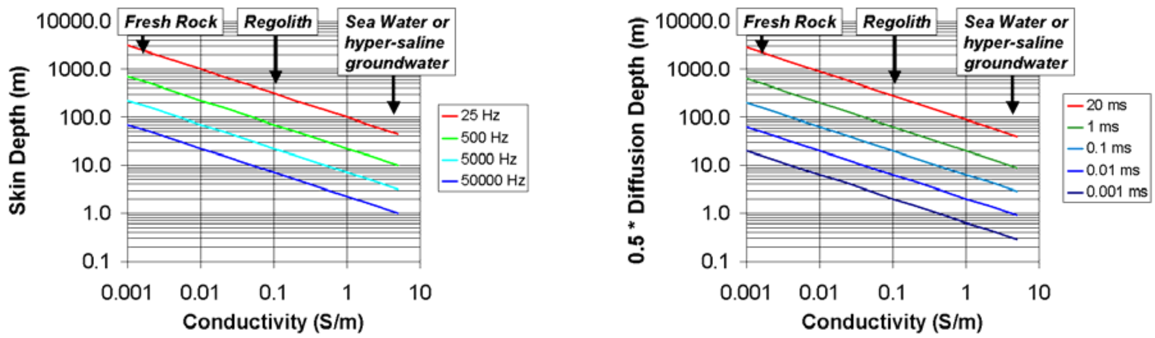

Figure 3. Skin depth and diffusion depth charts.

Since the depth of penetration is a function of frequency or delay time, measurements made at a number of frequencies or delay times can be used to determine the variation in conductivity with depth. The process of determining conductivity is akin to taking the difference between measurements at successive frequencies or delay times. An unfortunate consequence of this differencing procedure is that sensitivity to noise increases. Shallow vertical resolution is determined by high frequency / early time performance. The depth of penetration is determined by performance at low frequency / late time. Intermediate frequencies / times provide the detail between these extremes. Factors in the success of transformation of recorded response to conductivity include bandwidth, the distribution of intermediate measurement frequencies or times, noise levels, the system geometry (due to its effect on the sampling volume), knowledge of variations in system geometry at different measurement points, spatial sampling and spatial processing functions.

Transformation of measured response to conductivity can help to overcome the complexity present in the measured response due to the system’s hardware, software and geometry characteristics. Ideally, the final output of a detailed EM survey would be a 3-D conductivity distribution of the subsurface. This would be the optimum output for data integration and follow-up work.

Due to difficulties in computing the response for 3D conductivity distributions, practical conductivity transformations are restricted to those employing a “1D” approximation for each recorded location. Measurements taken at each location are treated in isolation from those acquired at other locations. The ground is assumed to show conductivity variations in only one direction (ie. along a vertical axis), and hence all conductivity layers are infinite in horizontal extent. A special case used with single frequency or single time delay measurements is a “halfspace” where the subsurface is considered to have uniform conductivity both vertically and horizontally. In reality, the 1D criteria will never be exactly satisfied, but the results can be useful provided the ground has a reasonable degree of horizontal uniformity over the footprint of the measurement. This is often the case in regolith and flat to shallow dipping sedimentary environments. Hence, conductivity is the primary form of output for some applications (eg. regolith mapping and mapping for salinity and groundwater). Tabular, steeply dipping targets do not satisfy a 1D assumption, and hence are misrepresented on conductivity sections that employ this assumption. This is one of the reasons why conductivity is a secondary form of output for discrete conductor applications.

3. FIELD PROCEDURES

Electromagnetic measurements can be made using ground-based instruments, but also using instruments mounted in specially adapted aircraft. The latter enables rapid systematic coverage over large areas for relatively low cost, without causing ground disturbance. In doing so, however, there is usually some trade-off in spatial resolution, near surface vertical resolution, and depth of penetration against the best possible ground-based data (see Smith, et al. (2001) for an example of a comparison of ground and airborne EM methods over the same target). Given knowledge of the likely conductivity variations in the survey area, simplifying assumptions can sometimes allow flexibility in the choice of EM method, allowing cheaper, less sophisticated options to be used to produce an adequate outcome.

Airborne EM

Typical airborne EM (AEM) systems include:

1. Time domain (TD) fixed wing airborne EM (AEM) systems, such as TEMPEST (Lane, et al., 2000) (Figure 4) and GEOTEM (Smith, et al., 1996);

2. Time domain (TD) helicopter systems, such as Hoistem (Boyd, 2001);

3. Frequency domain (FD) helicopter systems, such as DIGHEM (Huang and Fraser, 2001) (Figure 5) and Hummingbird (Valleau, 2000); and,

4. Frequency domain (FD) fixed wing EM systems, such as that operated by the Geological Survey of Finland (GTK) (Poikonene, at al., 1998).

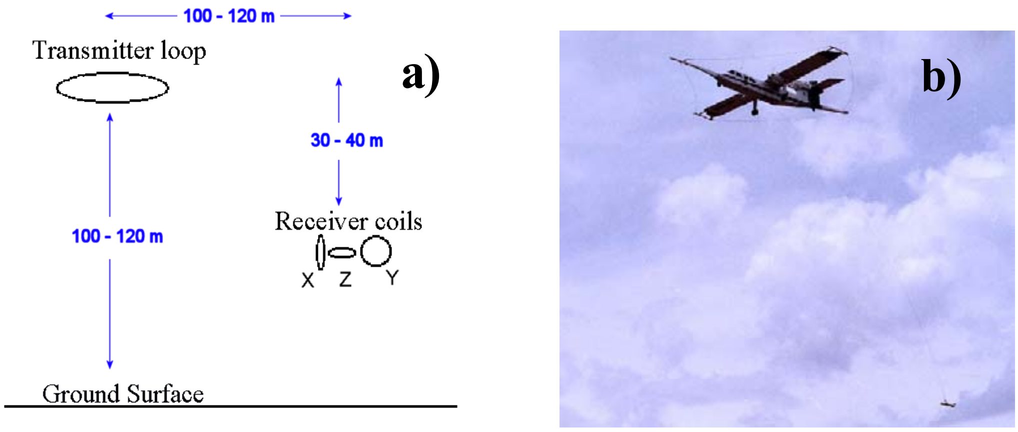

Figure 4. a) Transmitter loop and receiver coil configuration for the TEMPEST AEM system. b) TEMPEST AEM system on a Trislander aircraft in 1999. The transmitter loop is draped around the nose, tail and wingtips of the aircraft. The receiver coils are housed in a bird trailed behind the aircraft on a tow cable. The bird is visible in the lower right corner of the photograph. The tow cable is only partially extended in this photograph. Processed data typically consist of measurements at 15 delay times ranging in time from 0.013 to 20 milliseconds after a step change in the transmitted current.

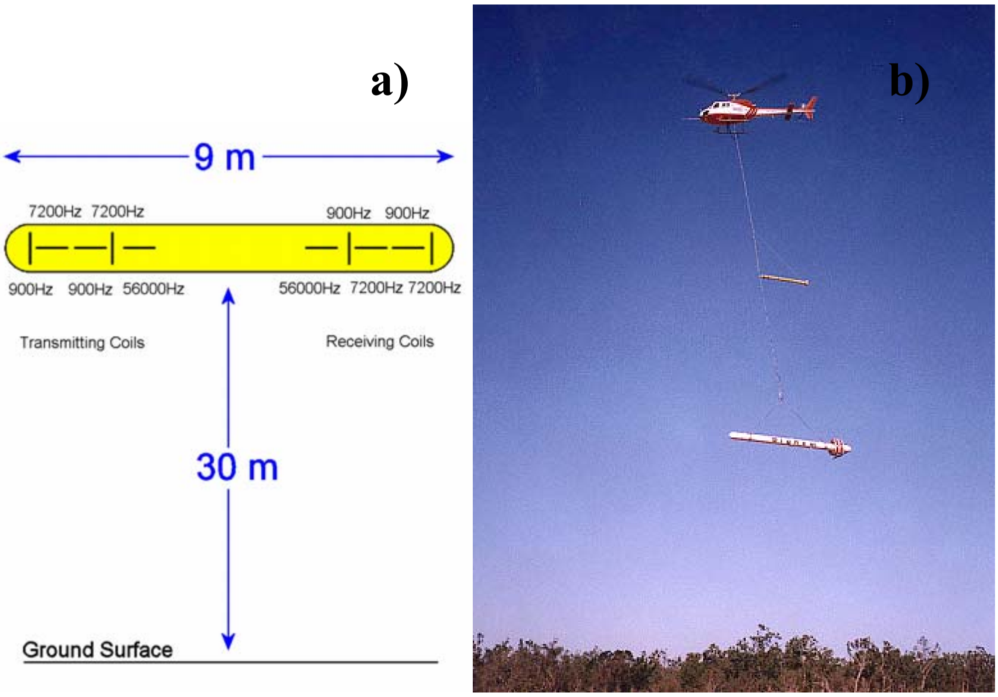

Figure 5. a) Arrangement of the 5 separate transmitter and receiver coil pairs for one of several possible configurations of the DIGHEM system. Each coil is shown as a black bar inside the bird shell. There are two horizontal dipole ("coaxial") coil pairs and three vertical dipole ("coplanar") coil pairs in this example. b) DIGHEM system preparing for operations. The small yellow bird halfway down the tow cable is a magnetometer bird. The EM bird is the larger bird at the end of the tow cable, 30 m below the helicopter.

Data are acquired at relatively close spacing along flight lines (3 to 15 m). The use of along line processing functions reduces the independence of the individual measurements. The selection of the spacing between lines is one of the major decisions to be made when planning a survey as it is a major influence on survey cost for a given system. The expected spatial variability of the subsurface conductivity needs to be considered. A rule of thumb is that the maximum line spacing should be approximately 0.5 times the across-line horizontal dimension of the smallest feature to be detected (after noting the effect of the system footprint). This ensures that features of this size will be sampled on at least 2 adjacent lines. For example, a line spacing of 200 m or less would be desirable for detecting the response of a nickel sulphide orebody with a strike length of 400 m. It is also worth bearing in mind that the grid cell size of plan view images will generally be about 0.25 to 0.2 times the line spacing.

Typical production rates are between 50 and 120 line km per hour of operation. Weather conditions and operational procedural requirements can restrict production to 20 to 30 hours per week.

AEM methods are generally combined with other geophysical methods, for example magnetics, acquisition of a digital elevation model (DEM) and/or gamma ray spectrometrics. The operation of the EM system, the type of magnetics system utilised, the terrain clearance of the magnetic sensor and the choice of line spacing can degrade the quality of the output of the magnetic system from that which could be obtained with a dedicated airborne magnetic system. However, the differences are not always significant. Similarly, weight restrictions, the terrain clearance of the gamma ray detector and the line spacing can degrade the quality of the output of the gamma ray spectrometric system from that which could be obtained with a dedicated airborne gamma ray spectrometric system.

The overall accuracy of a DEM derived from airborne geophysical measurements (Figure 6) depends on the altimeter and satellite navigation instruments used. A standard differential GPS receiver and radar altimeter would result in elevation values with a standard deviation of around 2 m in flat terrain. A carrier phase GPS receiver and scanning laser altimeter are capable of sub-decimeter accuracy in flat terrain (Stone and Simsky, 2001, Carter, et al., 2001).

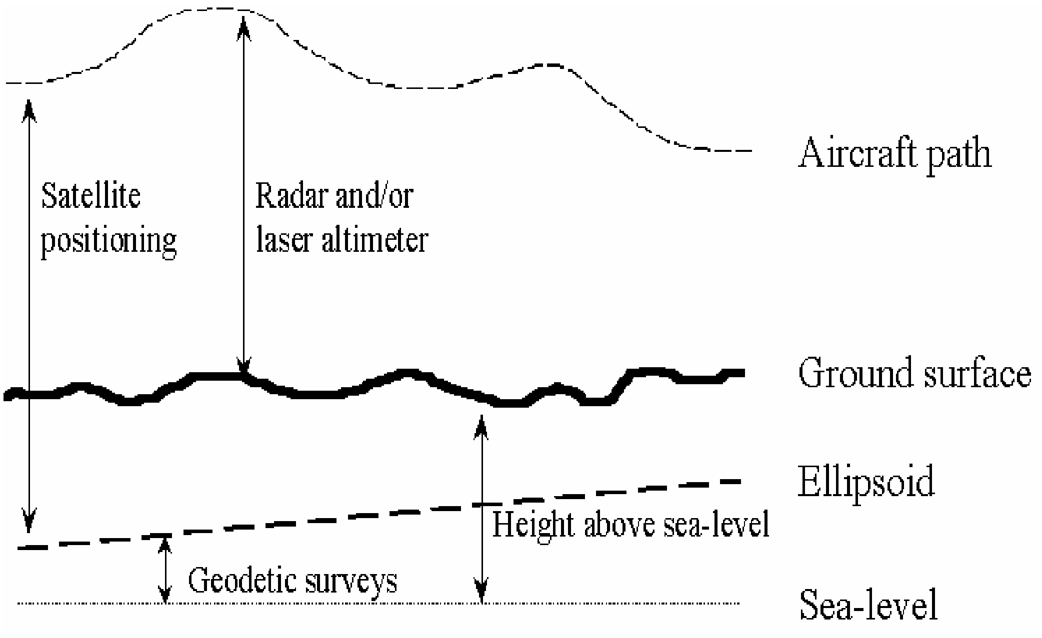

Figure 6. Method for deriving elevation (ie. the height above sea level) from airborne measurements. A GPS system on the aircraft measures the height of the aircraft above the ellipsoid. An altimeter measures the height of the aircraft above the ground ("terrain clearance"). The separation between the ellipsoid and sea level is known from geodetic surveys. Height above sea level is calculated as height above the ellipsoid plus the ellipsoid – sea level separation minus the terrain clearance.

Ground EM

Ground EM measurements are acquired at points along line traverses or at individual spot locations using either FD or TD instruments.

The most popular FD ground EM instruments are the Geonics suite of instruments (eg. EM31 (Figure 7), EM34 and EM38). These instruments take measurements using a single transmitter frequency and apply an approximate transformation to convert the output to apparent conductivity (ie. the halfspace conductivity that would produce the observed response). For further information on the theory of these instruments see McNeill (1980). Production with the smaller instruments that have the transmitter and receiver coils in a fixed assembly carried by an operator (eg. EM31 and EM38) can be several line km per hour of operation. Production with the larger EM34 system can be up to 1 km per hour depending on the transmitter and receiver coil separation and station spacing. Depth of penetration depends on the separation and orientation of the transmitter and receiver coils, ranging from 0.75 to 1.5 m for the EM38, 3 to 6 m for the EM31 and 10 to 60 m for the EM34. The addition of a data logger and GPS satellite navigation can substantially improve survey productivity and accuracy.

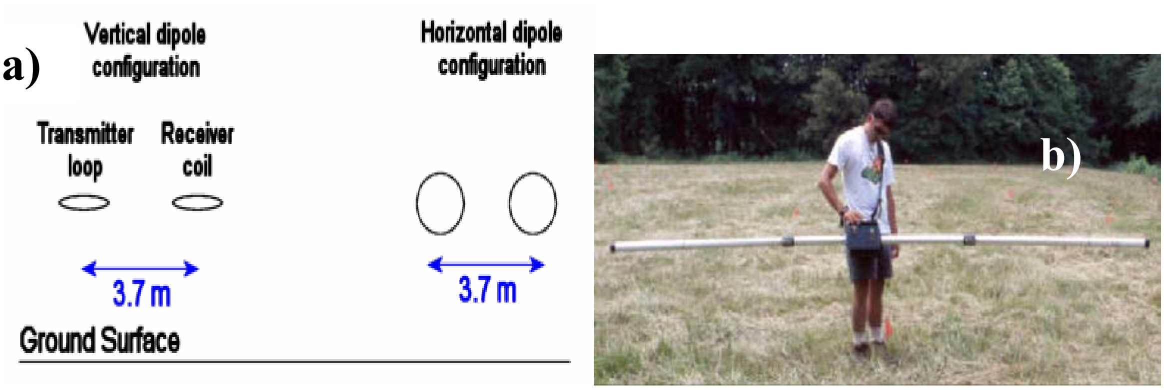

Figure 7. a) Transmitter loop and receiver coil configuration for the EM31 frequency domain ground EM instrument showing both vertical and horizontal dipole configurations. b) EM31 instrument in operation.

Time domain ground EM instruments use a square loop for the transmitter and either a small loop or a specifically designed coil for the receiver (Figure 8). A team of 2 or more people is generally required to lay out the wires for the transmitter loop at each station. Instruments are marketed under various trade names by several companies (eg. Zonge GDP, Zonge NanoTEM, PROTEM, SMARTem, SIROTEM). Output consists of the response amplitude for a range of delay times after the current in the transmitter loop is turned off. A repetitive waveform is utilised, and the response is averaged over a period of time to improve the signal to noise. This process can last from just a few seconds to several minutes. As a guide for ground TEM survey design, the loop side length needs to be between 0.25 and 1.00 times the required depth of investigation. Production depends on the nature of the terrain, vegetation cover, station spacing and size of the transmitter loops. Typically, production of 1 to 3 line km per day is achieved.

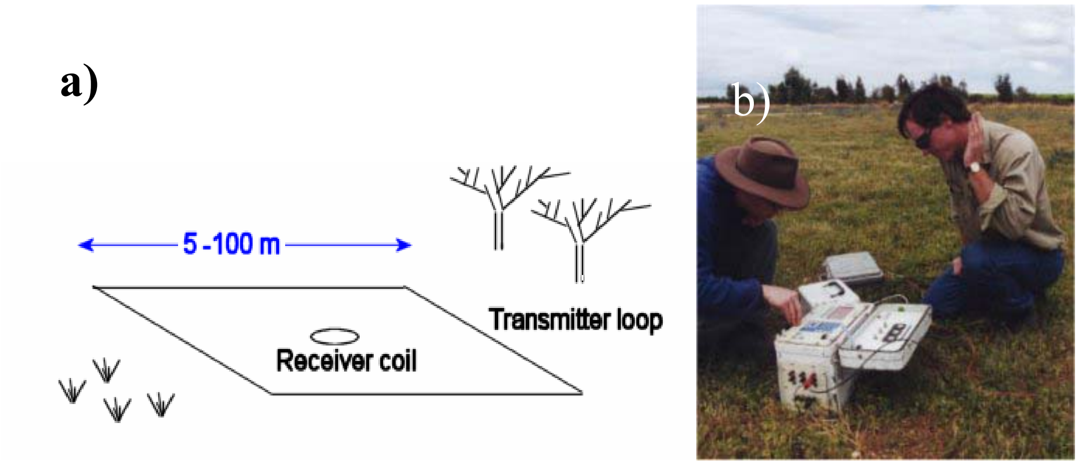

Figure 8. a). Transmitter loop and receiver coil configuration for typical in-loop time domain ground EM. b). Time-domain ground EM instruments (NanoTEM transmitter and GDP data recorder). (Photo courtesy: Mike Wall, University of Adelaide).

EM instruments are also used in borehole surveys to measure the conductivity of material within a short distance of the borehole wall. An example of a borehole conductivity logging tool is the Geonics EM39 instrument. Further information on the theory and practice of borehole conductivity logging can be found in McNeill (1986).

4. DATA PROCESSING AND PRESENTATION

Traditionally, data from EM surveys were viewed as line profiles of the measured response. This is still the principal mode of presentation when searching for the response of a discrete conductor. Contour maps and images are the basic presentation forms for displaying the spatial patterns in EM data. Increasing use of this style of presentation spurred an interest in AEM as a regolith and geological mapping tool, since an association between systematic variations in the conductivity and thickness of *in situ* regolith materials and bedrock type became apparent in many areas (Palacky, 1989).

Data Processing

Single frequency ground instruments (eg. EM31) produce output (eg. apparent conductivity) that can be readily viewed as along line profiles or images of the single parameter. Data reduction and processing for FD airborne EM surveys and TD ground and airborne EM systems is quite involved. The outputs for FD systems are levelled and filtered in-phase and quadrature amplitude together with levelled and filtered apparent conductivity for each measurement frequency. See Valleau (2000) and Huang and Fraser (1999) for further information on the processing of FD AEM data. The outputs for TD systems are levelled and filtered window response amplitudes for a series of delay times ("windows") (eg. the profiles at the top of Figure 9). See Duncan, et al. (1998), Strack (1992) and Lane, et al. (2000) for further information on the processing of TD ground and airborne EM data.

Simple Image Presentations

Data from frequency domain AEM surveys are typically presented as images of the apparent conductivity at different transmitter frequencies. The depth of penetration is greater at lower frequencies, but the actual depth of penetration at a particular frequency is a function of the subsurface conductivity. The more conductive the ground, the shallower the penetration (Figure 3). Images of apparent conductivity for a single frequency will thus represent some form of average conductivity from surface to different depths across the survey area depending on conductivity.

TD EM systems can have complex transmitter waveforms and response functions. Although generally true, later windows do not necessarily correspond with greater depth of penetration. Greater amplitude does not necessarily correspond with higher conductivity. Images of response amplitude or apparent conductivity represent time slices of response rather than slices at constant depth across the survey area. It is important to keep this in mind when working with images of window data.

For any airborne EM system, the geometry of the transmitter loop, receiver coil and ground elements are continually varying along each line. These variations have a significant effect on the measured ground response. Approximate corrections can be applied to the measured response for these geometry variations (Green, 1998a) provided the variations are known with sufficient accuracy. Application of these corrections reduces the number of variables affecting the response, thus simplifying interpretation and enhancing the effectiveness of subsequent processing should this processing not account for these geometry variations separately.

Methods of processing and displaying multi-spectral remote sensing data such as principal component analysis can be applied to multi-frequency or multi-time delay EM data (Green, 1998b). Computational demands are generally low, and large AEM surveys can be processed quite quickly. These methods are often applied to AEM data to obtain a quick overview of the spatial and "spectral" (time or frequency dimensions) patterns in the data. The disadvantage of these methods is that it remains difficult to relate the output to conductivity and depth, and hence difficult to integrate the products with other subsurface information.

Transformation to Con*d*uctivity

Through a combination of circumstances (eg. discrete high conductance base metal targets, resistive terrain, narrow bandwidth, poor signal to noise ratio), the early airborne and large ground EM systems were used solely for the detection of discrete conductors associated with base metal mineralisation. These were essentially binary systems where there was either an anomalous response or background response. As a result of improvements to EM systems, it has become possible to map more subtle contrasts in electrical properties, and it is increasingly worthwhile to pursue methods to convert the measured response to conductivity.

The measured response needs to be converted to conductivity to determine how conductivity is changing with depth and position. As previously discussed, all of the practical methods to convert response to conductivity assume that the subsurface conductivity is horizontally layered (ie. a 1D approximation). Iterative inversions determine a model of the subsurface conductivity structure that has a response that matches the observed response. These procedures are computationally intensive, particularly if a large number layers are used. Two classes of inversion are commonly used. "Smooth model" or "Occam" inversions (Farquharson and Oldenburg, 1993, Zhang and Oldenburg, 1999) use many layers but link the conductivity of each layer to that of adjacent layers and to a reference model through a model objective function. The layer thickness values are generally fixed, with only the layer conductivities being free to vary during the inversion process. In the other class, the layer thickness and conductivity parameters are independent of each other and both the layer thickness and conductivity values are generally allowed to vary (Sattel, 1998). The number of layers is far more restricted than is the case in "smooth model" inversions. Approximate transformation methods such as those used by "EMFlow" (Macnae, et al., 1998) employ various approximations and only a single iteration. This reduces the time taken to convert response to conductivity in comparison with inversion methods.

Presentation of Conductivity Data

Conductivity data can be displayed in a variety of ways. Although the 1D assumption means that each observation is treated in isolation and that the subsurface is perfectly horizontally layered, conductivity-depth values calculated for each observation can be stitched together into sections to provide a representation of the 2D variation of conductivity. This is sometimes referred to as a "parasection". Further, the conductivity depth profiles can be combined into a 3D gridded volume from which arbitrary sections, horizontal depth slices and isosurfaces can be derived (Lane and Pracilio, 2000).

Distillation of essentially continuous and gradational conductivity distributions into discrete conductive "units" or layers can be useful for summarising information from large surveys. This is particularly so when the application calls for mapping the conductivity, depth to top and thickness of a semi-continuous layer of transported or *in situ* regolith. Several (semi-)automated schemes exist for picking the layer boundaries, for example layered inversion (Sattel, 1998), conductive unit parameters (Lane, 2000) and inflection point analysis (Hunter and Macnae, 2001). Lawrie, et al. (2000) and Worrall, et al. (2001) contain examples comparing calculated layer boundaries with boundaries interpreted from lithological mapping.

5. INTERPRETATION

Interpretation of EM data can be thought of as a four-step process. First, the data are assessed in terms of quality. Next, the data are related to subsurface conductivity. Then the conductivity distribution is related to units of more direct significance to the application (eg. discrete massive sulphide bodies in base metal exploration applications, pore fluid salt concentration in soil salinity applications). Finally, the mapped EM response is fully integrated with all other information in the project area and recommendations for further action are determined.

The assessment during the first step establishes limits for how far the data can be pushed before noise features or other artifacts become significant. During the second step, the measured data are converted to a meaningful physical property distribution. The limitations of the data, model and the conversion algorithm are noted at this time so that a suitable appreciation of the fidelity of the output in relation to the true conductivity distribution can be established. The third step involves an analysis of the controls on conductivity so that conductivity can be related to something of more direct relevance to the application. The final integration step generally involves a broad range of inputs from the project team. On some occasions, the data integration exercise prompts another iteration through earlier steps with a different focus or different set of constraints.

An understanding of the controls on bulk electrical conductivity is required for interpretation. Sauer, et al. (1955) present a model of conduction for porous aggregates immersed in a conductive fluid that can in turn be related to conduction along three separate pathways - conduction through the solid material, conduction through the pore fluid and conduction across the interface between solid material and the pore fluid. Bulk conductivity is then a function of the conductivity of the solid material, conductivity of the pore fluid, the electrical properties of the solid/fluid boundary, porosity, arrangement of the pores and saturation.

Various empirical relationships have been developed between some or all of the components of this model and conductivity. In the context of sedimentary units within a petroleum exploration setting, Archie (1942) used the expression

$$\sigma_e = \frac{1}{a}\varphi^m s^n \sigma_w$$

where σ_e is the bulk effective conductivity, σ_w is the pore fluid conductivity, φ is the porosity, s is the saturation, and a, m and n are derived factors ($0.4<a<2$, $1.3<m<2.5$, $n\approx2$). The "formation factor" is defined as a/φ^m. This expression assumes that contributions related to conduction through the solid material and conduction across the solid/fluid boundary are not significant. These assumptions hold true when the pore fluid is moderately to highly conductive and clay minerals are low in abundance.

Expressions that describe the bulk conductivity of partially saturated materials containing clays and low salinity pore fluid are far more complex. When considering the bulk conductivity of fresh rock and low salinity groundwaters, a term related to the conductivity of the solid materials (σ_s) needs to be considered. Conduction can be electronic, in the case of sulphide minerals, or related to cation exchange for many clay minerals. This term dominates when considering many graphitic or metal sulphide lithologies.

Regolith materials are variably conductive, by virtue of differing physical and chemical properties. Bodies of regolith materials with the same parent material and subject to the same weathering processes can produce spatially coherent responses in electromagnetic data. Unfortunately, regolith materials do not have unique conductivity values. This is perhaps obvious since regolith conductivity is strongly influenced by saturation and pore fluid conductivity and these vary from one area to the next. Thus, it is not possible to consult a reference table of conductivity values for different regolith materials and use this information to unambiguously separate different classes of regolith material (eg. separate transported regolith from *in situ* regolith, *in situ* regolith derived from parent material A from that derived from parent material B, or regolith unit 1 from regolith unit 2). Some educated guesses based on previous experience in similar environments can be made when relating conductivity variations with geological units. However, strategic drillhole lithological logging, conductivity logging and detailed surface mapping are required to verify and quantify relationships.

6. APPLICATIONS WITH SELECTED EXAMPLES

Discrete Conductors

Massive sulphide deposits are localised bodies that generally have substantially elevated solid material conductivity. When conductive regolith is present, an understanding of the regolith is required to correctly interpret the EM response of a discrete conductor as the regolith response may mask or modify the response of the discrete conductor. The converse is also true in that the presence of a discrete conductor or basement conductor will influence the interpretation of regolith response. An appreciation of the response of discrete conductors can be obtained from examples in Dentith, et al. (1994). McIntosh, et al. (1999) present a case history of gravity, IP and TD ground EM for the Las Cruces massive sulphide deposit located beneath 120 m of conductive transported Tertiary sediments. Leggatt, et al. (2000) present examples of the airborne EM response of base metal deposits in Canada. Wolfgram and Golden (2001) present examples of the airborne EM response of several nickel sulphide deposits. Further examples are provided by Peters (1996, 2001).

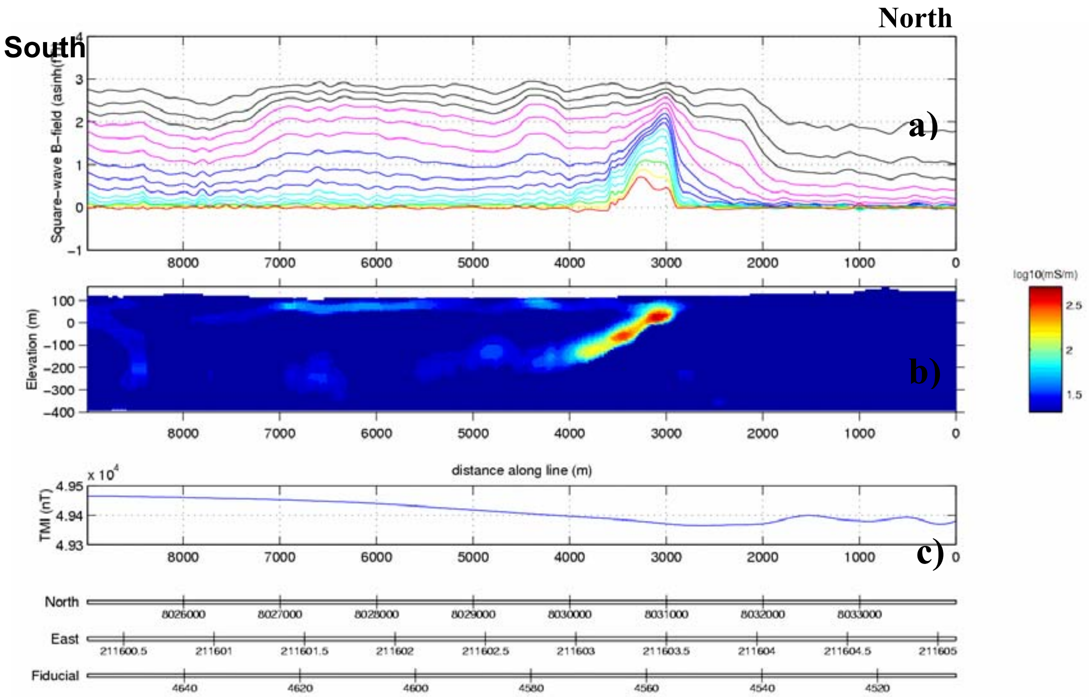

Figure 9. a). TEMPEST AEM Z-component square-wave B-field response profiles. b). conductivity section; and, c). total magnetic intensity profile for line 10281 (211600 mE) over the Walford East base metal prospect, Queensland (Lane, et al., 2000).

The example in Figure 9 illustrates the usefulness of applying a conductivity transformation in a situation where the input data are sufficiently broadband and accurate and where the 1D assumption in the transformation is reasonable (ie. dips are shallow or flat such that conductivity variations within the system footprint can be approximated by horizontal layers). The presence of a strong dipping conductor, corresponding to semi-massive to massive pyrite, is obvious in the profiles of response between 2900 and 4000 m distance along the line. The characteristics of a variably conductive regolith layer and extensions to basement conductors further to the south are not immediately obvious in the profiles yet are well imaged in the conductivity section. The sedimentary sequence in this location is essentially non-magnetic, enhancing the value of mapping regolith and basement conductors with AEM methods.

Kimberlites

Macnae (1995a, 1995b) discusses the application of geophysics to exploration for kimberlites and lamproites. In general, these diatremes are associated with discrete geophysical anomalies related to a physical property contrast between the intrusion and the host rock. Jenke and Cowan (1994) present examples of ground and airborne EM response for pipes in the Ellendale region of Western Australia. The majority of the pipes with a recognisable EM response show a localised enhancement in near-surface conductivity. This may be due to a combination of factors such as the increased depth of weathering of the kimberlitic material relative to the host, the presence of clays with elevated solid material conductivity or increased conductive pore fluid levels in the weathered kimberlite. Smith, et al. (1996) present examples of the airborne EM response of pipes in the Lac de Gras region of Canada. In this environment, the weathered kimberlitic material is more deeply scoured during glaciation leading to an association between kimberlites and small freshwater lakes containing conductive lake-bottom clays. An increase in near surface conductivity is thought to result from a combination of the conductive lake bottom sediments and saturated weathered kimberlite.

Groundwater

Potts (1990) presents examples from the Murray Basin in southeast Australia of the use of an EM34 instrument to define low conductivity zones associated with buried shoestring sands. These sands, in the depth range 0 to 20 m, have lower solid material conductivity and lower pore fluid conductivity relative to the surrounding clays. Bores are used to pump low salinity groundwater from the sands.

Gettings, et al. (1999) and Wynn, et al. (2000) describe the use of TD airborne EM to map aquifer features in the San Pedro Basin, USA. There was generally a good correlation between the uppermost conductor recognised in conductivity sections and water table depth. The increase in conductivity below the water table possibly reflects an increase in saturation by conductive groundwater (20-100 mS/m) below the water table. Paine, et al. (2000) and Rodriguez, et al. (2001) used TD airborne EM and conductivity logs for groundwater investigations in the Middle and Lower Rio Grande, USA. The conductivity of sediments in the Middle Rio Grande was found to be inversely proportional to grainsize, with implications for hydraulic permeability.

Fitterman and Deszcz-Pan (2001) used FD airborne EM, TD ground EM soundings and conductivity logs, to map characteristics of a shallow aquifer in the Everglades region of the USA. The extent of seawater intrusion was mapped by noting the transition when moving inland from high conductivity to low conductivity at shallow depth. The depth to the base of this shallow aquifer was mapped by picking the depth associated with a change in conductivity.

Salinity

Slavich and Petterson (1990) present examples of the use of an EM38 instrument to estimate soil pore fluid salinity in the 0 to 0.6 m depth range. Cook, et al. (1992) and Cook and Kilty (1992) present examples from Borrika (approximately 50 km east of Murray Bridge in South Australia) of ground and FD airborne EM methods used to map recharge. Shallow conductivity was inversely proportional to recharge rate. Areas of low recharge had higher saturation, higher pore fluid conductivity and hence higher conductivity than areas of high recharge.

Bennett, et al. (2000) provide a summary of the use of EM38, EM31, EM34 and EM39 instruments in southwestern Australia and conclude that most of the observed variation in conductivity can be correlated with various measures of salinity (electrical conductivity of the soil saturation extract, EC1:5, percentage by weight of chloride ions). Variations in saturation, porosity, arrangement of pores, conductivity of solid material (clay content) and temperature were minor contributors to the observed variations in conductivity.

Street (1992), George, et al. (1998), Lane and Pracilio (2000), Lawrie, et al. (2000), and Lane, et al. (2001) present examples of the application of airborne EM to hydrological investigations in areas of dryland salinity in Australia.

Paine, et al. (1997) present an example of using FD airborne EM for mapping near-surface conductivity plumes associated with leakage of brines from petroleum wells in Texas, USA.

Mapping

Palacky (1989) was instrumental in recognising the potential for mapping geological units in weathered terrains via the response of conductive *in situ* regolith. Attention was drawn to the local-scale influence of parent lithology, together with structure and alteration, over the *in situ* regolith clay mineralogy, clay content, porosity and in some instances, even groundwater conductivity. The local-scale consistency of these factors, and their impact on conductivity, enables units with the same parent lithology to be identified and mapped. Based on a number of studies, it was found that saprolite was generally the most conductive regolith horizon, and that saprolites developed over mafic and ultramafic parent lithologies were generally thicker and more conductive than those developed over felsic lithologies.

Two well documented examples of regolith mapping applications in the Yilgarn Province of Western Australia are the Lawlers study area (Emerson, et al., 2000, Bishop, et al., 2001, Emerson and Macnae, 2001, Macnae and Bishop, 2001, Munday, et al., 2001) and the Balgarri or Grant's Patch study area (Lane, 2000, Worrall, et al., 2001, Bell, et al., 2001, Meyers, et al., 2001). A comparison of the regolith section and conductivity sections derived from TD ground and airborne EM measurements for Grant's Patch is shown in Figure 10. The conductive interval correlates well with *in situ* saprolite. This result was confirmed with downhole conductivity measurements. The spatial patterns in near-surface conductivity, thickness and conductance were used in a complementary manner with information from aeromagnetic and gravity data to map bedrock geology as part of a gold exploration project (Meyers, et al., 2001).

Rutherford, et al. (2001) examined the regolith material from a number of drill holes at the Cawse lateritic Ni deposit, Western Australia. The regional watertable is located near the base of the regolith profile at a depth of 50 m or more. Hence, the degree of saturation is an important control on conductivity in the unsaturated zone at depths of less than 50 m. Soluble salt content is also an important control on the electrical conductivity. A coincidence of elevated conductivity and Ni enrichment was noted at hydromorphic barriers, but the relationship between conductivity and Ni grade was quite variable. Subdivision of the regolith into hydrostratigraphic units and identification of hydromorphic barriers enabled a better understanding of the spatial patterns in electrical conductivity to be obtained. Armed with this knowledge, airborne EM data could be used to locate impermeable barriers and faults that are the important controls on the development of Ni laterite mineralisation.

An airborne EM survey was flown over an area surrounding the Challenger gold deposit, central South Australia, for Geoscience Australia, Primary Industries and Resources South Australia and the Cooperative Research Centre for Landscape Evolution and Mineral Exploration. The deposit is hosted by granulite-facies granite gneiss (Bonwick, 1997). Topographic relief is subdued and the presence of a variable thickness (generally less than 50 m) of weathered and transported material makes it difficult to map subsurface features using surface mapping techniques. The patterns in an image of conductance of near-surface material (Figure 11) reflect very deep channels (200 m +) filled with conductive material (red), areas of thinner conductive transported cover generally less than 30 m thick (yellow and green areas with dendritic outline), areas of *in situ* conductive regolith (green and yellow linear and curvi-linear zones) and areas without conductive regolith (blue). The pair of N/S trending channels were interpreted to be up to 200 m deep (Figure 12) and filled with sediments carrying saline groundwater. A drill hole (Figure 11) into the eastern channel encountered 210 m of sediments and lignite before passing into gneissic basement material. The water resource encountered in basal sands of the channel is being evaluated for use in the proposed mine. The host gneissic material is not easily differentiated either visually or using magnetics. In areas where the conductivity of basement material is not obscured by transported material, basement is separated using EM data into ovoid and elongated resistive areas and surrounding mantles where conductive *in situ* regolith is developed over fresh rock. The sub-crop of the Challenger deposit is located in a zone of conductive regolith (Figure 11). The source of the variability in the nature of *in situ* regolith materials is unknown. The bedrock is uniformly resistive, however it is probable that weathering may have picked out subtle variations in bedrock composition and/or structure.

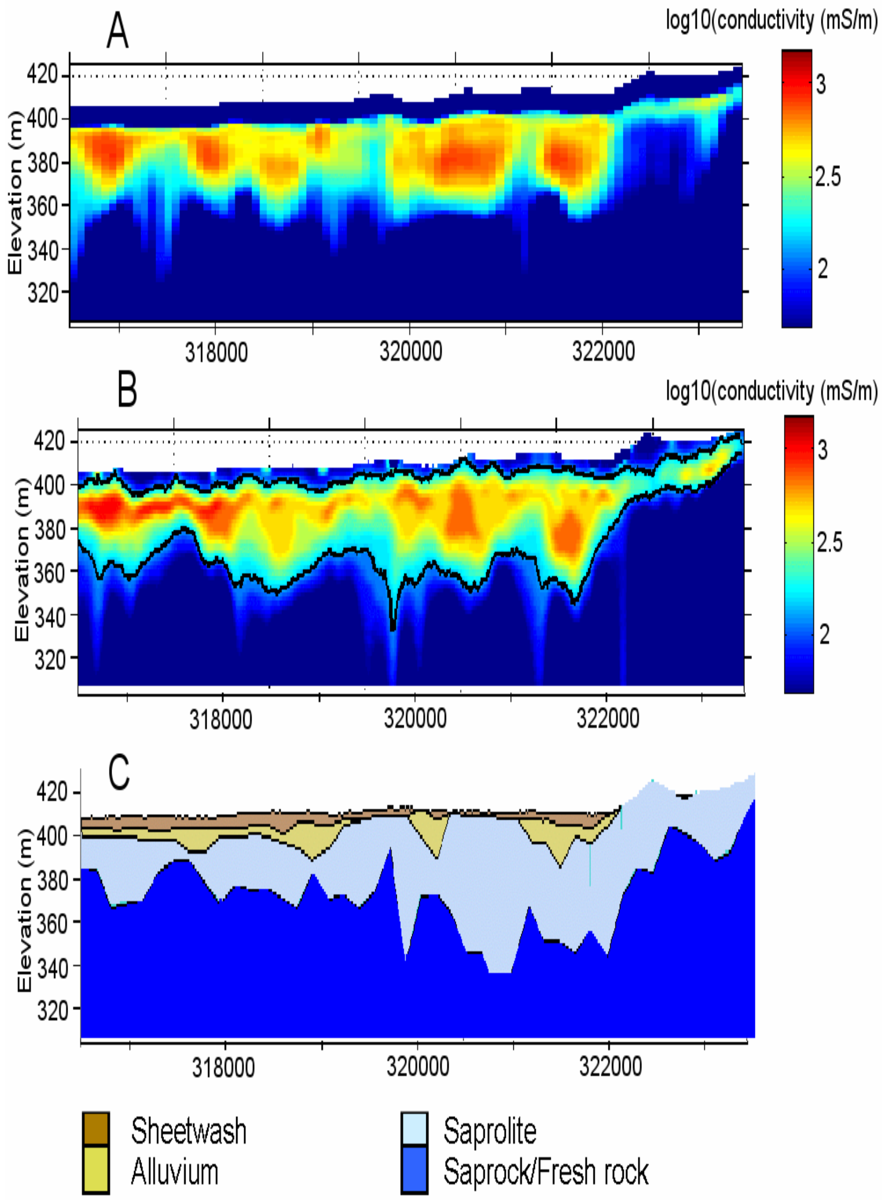

Figure 10. Conductivity sections for a) PROTEM ground EM and b) TEMPEST airborne EM data along line 6626720 mN at Grant's Patch, Western Australia. The upper and lower bounds of a 'conductive unit' with a minimum threshold of 100 mS/m are shown over the TEMPEST section. The regolith profile derived from drilling c) is also shown (Worrall, et al., 2001).

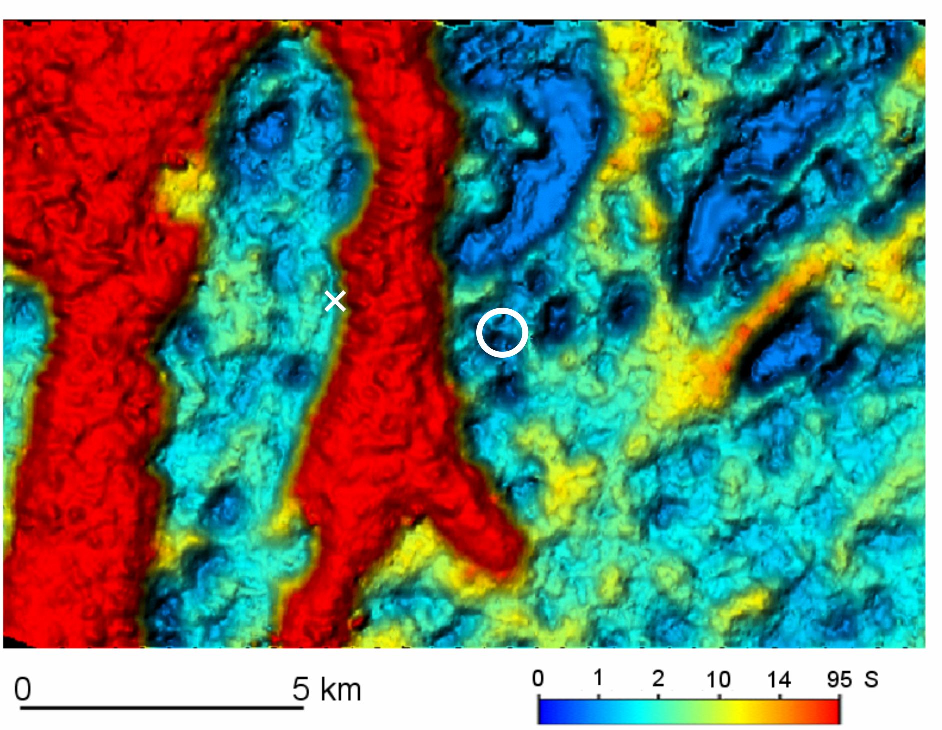

Figure 11. Image of conductance of the conductive unit defined by a variable conductivity with a minimum threshold of 30 mS/m, calculated from TEMPEST AEM data for the Challenger area, South Australia. The location of the Challenger deposit is shown with a white circle. The location of a borehole into one of the deep channels is shown with a white cross.

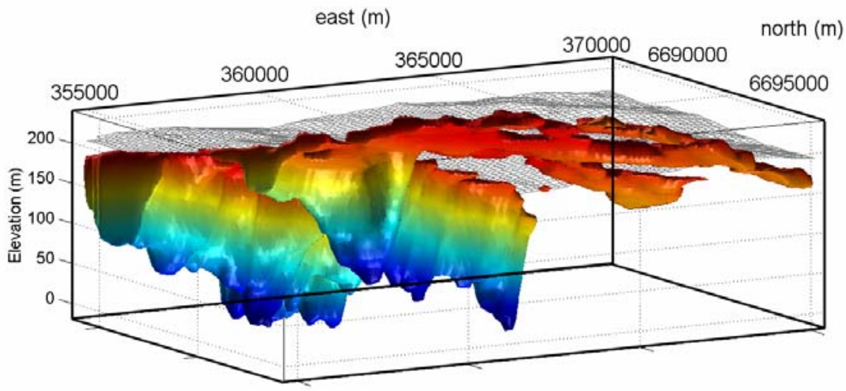

Figure 12. A conductivity isosurface from the Challenger area, South Australia, derived from TEMPEST AEM data. Elevation is in metres above sea level. The grey mesh representing the surface elevation shows very subdued topography. The isosurface, enclosing all material with conductivity greater than 200 mS/m, is coloured by elevation above sea level from blue (sea level) to red (200 m above sea level). The conductive material includes two deep channels of transported material in the west and thinner transported material and in situ regolith in the east. The viewpoint has an azimuth of 150° and an elevation of 10° below the horizontal (Skirrow, 2001).

Regolith stripping for gravity interpretation

In situ and transported regolith materials most commonly have a negative density contrast with underlying fresh bedrock. In areas where the thickness of regolith varies laterally, the gravity response of the regolith layer can substantially contribute to the local-scale gravity response. This will produce many false anomalies and mask the true anomaly of an underlying target (Braine and Macnae, 1999; Bell, et al., 2001) unless the regolith contribution to the gravity response can be independently determined and subtracted from the local gravity response.

EM methods can be used to map the depth to the base of the near-surface conductive layer (Figure 13). Under suitable conditions, this interface will relate to the transition from regolith to fresh rock. After selecting a representative density for the regolith material, the gravity response of the regolith layer is calculated and subtracted from the gravity data. The residual reflects the gravity variations due to fresh bedrock materials, departures from the assumption of lateral and vertical uniformity in regolith density and local differences between the interpreted base of the conductive layer and the actual regolith / fresh rock interface.

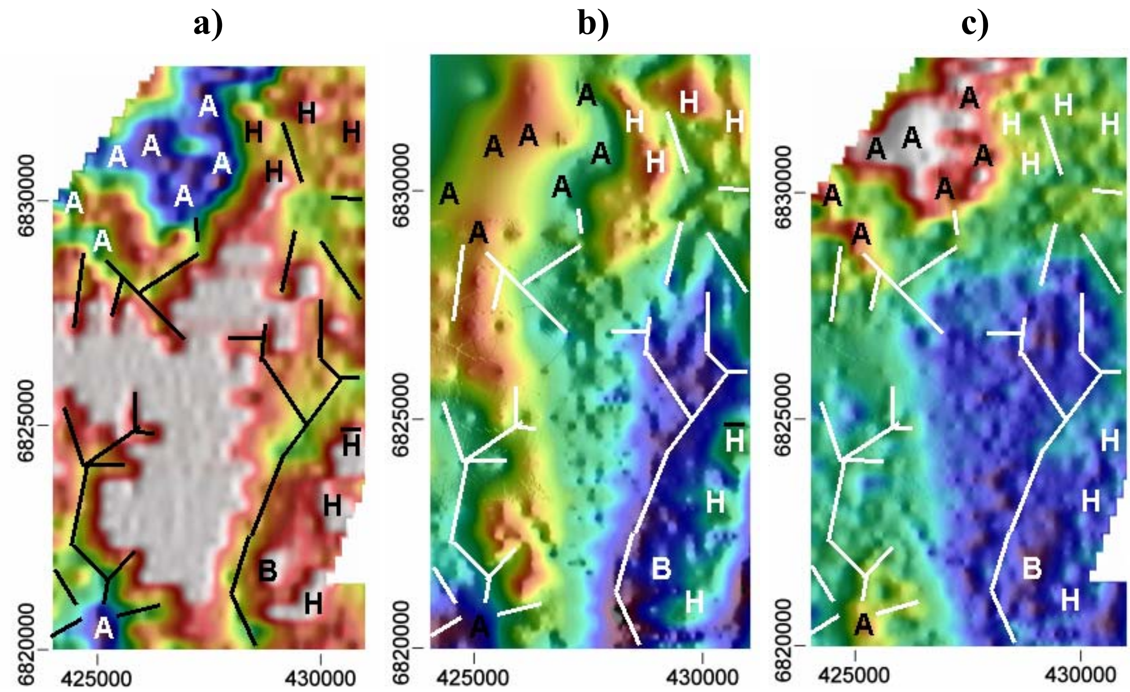

Figure 13. a) Depth to base of conductive regolith, based on manual interpretation of conductivity sections derived from TEMPEST AEM data. The linear colour scale ranges from less than 25 m (white-red) to 100 m (blue-purple). Locations labelled with “H” are local bedrock topographic highs with associated residual gravity highs. “B” is a local bedrock topographic high without an associated residual gravity high. Locations labelled with “A” are areas with thick regolith. Lines mark the axes of regolith troughs. b) Residual Bouguer gravity after removing a regional trend from the data. The linear colour scale ranges from –2 mgal (blue-purple) to 2 mgal (white-red). c) Residual Bouguer gravity adjusted for response of the regolith layer using a density contrast of –0.6 g/cm^3. The linear colour scale ranges from –1 mgal (blue-purple) to 6 mgal (white-red). Data provided by Metex Resources NL. Processing and interpretation by Southern Geoscience Consultants.

An example from the Laverton area in Western Australia is shown in Figure 13. Troughs in the interpreted regolith unit, the axes of which are marked with lines, correspond to local gravity lows in the Bouguer gravity. The absence of a correlation between these axes and bedrock gravity (Figure 13c) suggests that an appropriate density contrast has been used to remove the response of these regolith features. A series of local highs in the observed gravity in the NE and SE corners of the survey area (marked with “H” symbols) are interpreted to be directly attributed to bedrock topographic highs.

They do not appear to have any bedrock density contrast (Figure 13c). The interpreted bedrock topographic high, labelled as “B”, appears to be different in that it is not associated with a local gravity high. This could be a low-density bedrock feature or a patch of resistive regolith misinterpreted as a bedrock topographic high (eg. an area of silica-alteration). Areas of interpreted thick regolith (marked with “A” symbols) appear to be associated with high density bedrock units (eg. mafic volcanics or intrusions). An alternate possibility is that the Bouguer gravity has been overcompensated for the regolith gravity response in these areas (ie. the interpreted regolith thickness is too large and/or the magnitude of the assigned density contrast is too large).

7. PROBLEMS AND LIMITATIONS

Acquisition

Selection of the most appropriate acquisition system and parameters is a common problem with EM methods. A clear understanding of the survey objectives will certainly help guide the selection process. Some of the factors to consider in planning an EM survey are:

1. Survey objectives;
    - expected 3D conductivity variations
    - target size
    - required depth of investigation
    - resolution
    - area to be covered
    - coupling of the EM field with the target

2. Ground conditions;
    - results of previous electrical or EM surveys (these provide indications of the conductivity variations)
    - presence of substantial grounded metal objects (eg. pipelines, railway lines)
    - presence of interfering EM sources (eg. powerlines, electric fences)
    - topographic variations
    - altitude (AEM surveys)
    - vegetation (ground surveys)
    - location and access

3. Output requirements;
    - basic products, advanced products or complete planning, monitoring and interpretation service

4. Available technologies;
    - developments occur quite rapidly in the field of EM methods

5. Selection of contractor;
    - safety systems
    - experience
    - availability
    - support

6. Temporal conditions;
    - required time frame for the survey
    - weather conditions (dry, stable conditions preferable)
    - EM noise levels (ambient EM noise levels are lower in winter than in summer)

7. Financial constraints.

Broad advantages and disadvantages of different acquisition systems can be established but detailed comparison is difficult because it is not always possible to establish an appropriate common point of reference between the systems. For example, if systems have different measured quantities, how do you compare noise levels? How do you weight performance in diverse categories such as bandwidth, footprint, signal to noise, and cost? Improvements to methods of converting from measured response to 3D conductivity will greatly assist in providing a more logical common point of reference.

When embarking on a major survey, a small trial survey can assist to sort out teething problems and to confirm that appropriate survey parameters have been chosen. Factors to consider include:

1. Timing of the trial with respect to the main survey;

    - immediately beforehand (Are all relevant parties on site and empowered to make decisions on the spot?); or,
    - well in advance (more time to analyse and interpret the results, but increased mobilisation costs)?

2. Isolated traverses or a grid?

3. Ensuring coverage of representative ground conditions, noting the variability of the ground conditions in the project area and the nature of the target;

    - it is very frustrating to undertake a trial that is too small to indicate whether the chosen configuration will be effective over a larger survey area.

4. Survey an area with ground truth;

    - but be prepared to discover that not everything about the area was known or "true".

5. System tests to establish signal to noise levels;

    - repeat lines,
    - acquisition of data at high altitude (free of ground response).

Processing and Presentation

Simple presentations of measured response for a particular frequency or delay time are often difficult to interpret. These presentations reflect the contribution from the conductivity distribution to varying depths across a survey. Additionally, the measured response is strongly influenced by complex system characteristics. This results in a highly non-linear relationship between conductivity and response.

The most significant impediments to simplifying the interpretation of EM data are the restrictions placed on the conversion from measured response to 3D conductivity. A 1D assumption leaves significant residual artifacts near strong lateral contrasts in conductivity (Figures 14 and 15). Even in areas where a 1D assumption is a valid simplification, artifacts in predicted vertical conductivity distribution need to be considered in detailed quantitative applications (Hunter and Macnae, 2001) (Figure 16). Non-uniqueness in predicted vertical conductivity variation could also be a significant issue in some applications.

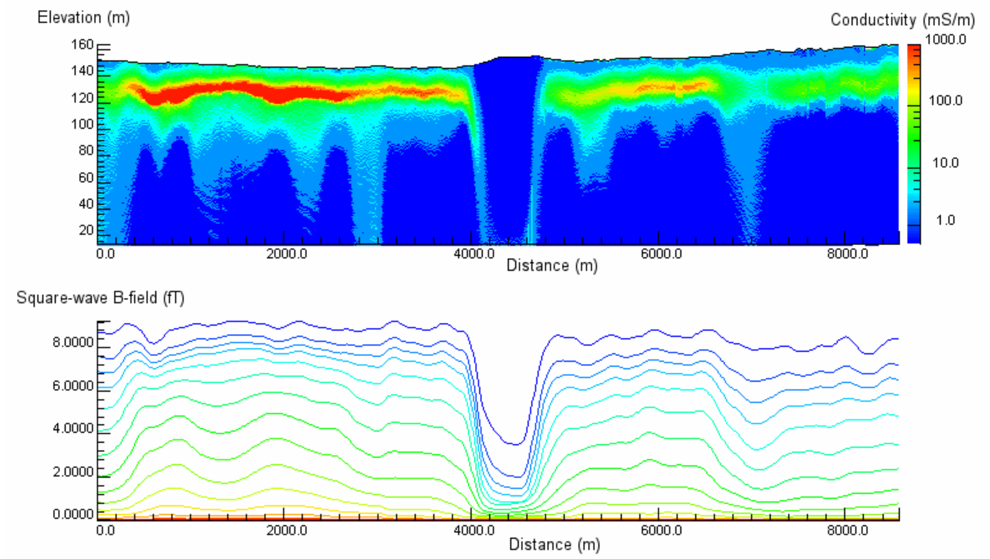

Figure 14. CDI conductivity section and TEMPEST Z component window response amplitudes for line 10390, Lake Harris, South Australia. The 1D assumption in CDI calculation results in "drooping moustache" edge artifacts at strong lateral contrasts in conductivity. Examples are evident at distances of 4000 and 4650 m along this line. Weakly elevated conductivity values extending from the conductive near-surface layer to depth at 0-200 m, 2700-3000 m and 7000 m are more subtle edge effects.

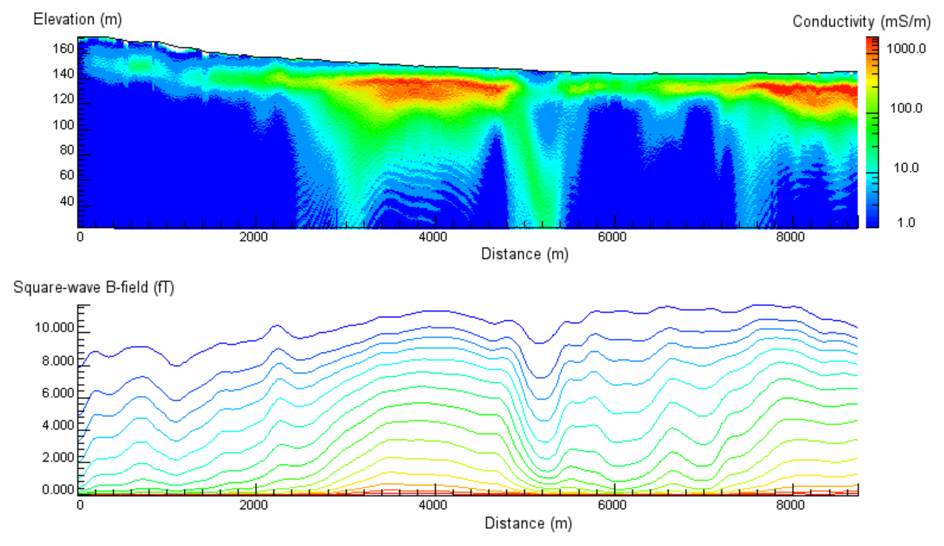

Figure 15. CDI conductivity section and TEMPEST X component window response amplitudes for line 20510, Lake Harris, South Australia. The 1D assumption in the CDI calculation results in edge artifacts at strong lateral contrasts in conductivity. A good example is evident at a distance of 5,000 m along this line. Features extending to depth around 3,000 and 7,500 m distance along line are more subtle edge effects. "Ribbing" or repeated steps present in low conductivity values at depth in the intervals 2,500-4,500 m and 7,400-8,800 m distance along line are artefacts of the conductivity transformation.

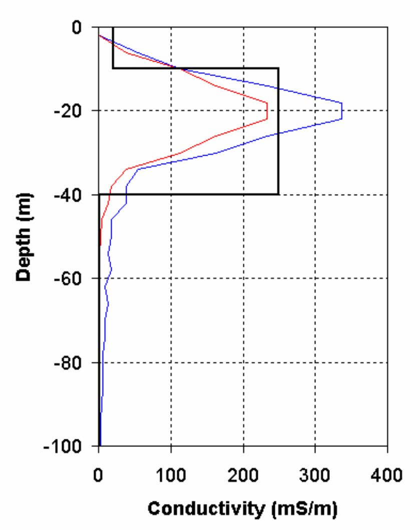

Figure 16. Example of 3 layer conductivity model (black) and EMFlow CDI conductivity soundings obtained after converting the forward model response of the 3 layer model to conductivity. The red sounding curve was obtained with halfspace basis functions whilst the blue curve was obtained with exponential basis functions. This example demonstrates some typical behaviour of the CDI algorithm used in EMFlow. Total anomalous conductance is reasonably well predicted whilst sharp conductivity boundaries are smoothed, and an overshoot is present below the top of the most significant near-surface conductive layer.

Despite the limitations noted above, it must be reiterated that in many regolith applications, conversion to conductivity is highly beneficial in reducing the complexity of the system response, in facilitating integration with other subsurface information, and in developing an appreciation of the 3D conductivity distribution.

Interpretation

Artifacts due to noise and assumptions made during data processing can be difficult to recognise. The residual imprint of the acquisition system characteristics (eg. bandwidth, footprint) and the processing that is applied to the data (eg. along line processing functions applied to AEM data) must be constantly borne in mind when interpreting the data. Relatively few detailed studies of the conductivity of regolith materials that could serve as a guide for interpretation have been published. Since, conductivity is a function of several parameters (eg. conductivity of solid material, arrangement of pores, saturation, conductivity of fluid, clay content), unravelling the relationship between conductivity and geological units is not always straightforward. In regolith applications, interpretation of EM information (ie. establishing the relationship between conductivity and geological units) is significantly aided by detailed surface mapping and judicious use of drilling. Used in this fashion, EM methods provide an objective basis for interpolating between relatively widely spaced boreholes and/or small areas of detailed surface mapping.

8. ACKNOWLEDGMENTS

The following organisations are thanked for supplying data; Fugro Airborne Surveys, Cooperative Research Centre for Australian Mineral Exploration Technologies (CRC AMET), Cooperative Research Centre for Landscape Environments and Mineral Exploration (CRCLEME), Office of Minerals and Energy Resources (MER) in Primary Industries and Resources South Australia (PIRSA), Metex Resources NL, Southern Geoscience Consultants. The assistance of Ross Brodie, Nick Direen, Jayson Meyers, Éva Papp, Bill Peters, Melissa Spry, Greg Street and Lisa Worrall in preparing this article is gratefully acknowledged.

REFERENCES

Archie, G.E., 1942. The electrical resistivity log as an aid in determining some reservoir characteristics. Transactions American Institute of Mechanical Engineers (AIME) 146: 54–67.

Bell, B., Fullagar, P.K., Paine, J., Whitaker, A. and Worrall, L., 2001. Exploring through cover. The integrated interpretation of high resolution aeromagnetic, airborne electromagnetic and ground gravity data from the Grant’s Patch area, Eastern Goldfields Province, Archaean Yilgarn

Craton. Part B: Gravity inversion as a bedrock and regolith mapping tool. Exploration Geophysics 32: 194-197.

Bennett, D.L., George, R.J. and Whitfield, B., 2000: The use of ground EM systems to accurately assess salt store and help define land management options for salinity management. Exploration Geophysics 31: 249-254.

Bishop, J., Sattel, D., Macnae, J. and Munday, T., 2001. Electrical structure of the regolith in the Lawlers District, Western Australia. Exploration Geophysics 32: 20-28.

Bonwick, C., 1997. Discovery of the Challenger Gold Deposit - Implications for future exploration on the Gawler Craton. New Generation Gold Mines '97, Case Histories of Discovery. Australian Mineral Foundation (AMF), unpaginated.

Boyd, G., 2001. Normandy heli-borne time domain EM system. Extended Abstract, Australian Society of Exploration Geophysicists (ASEG) 15th Geophysical Conference and Exhibition, August 2001, Brisbane (CD ROM).

Braine, M.F. and Macnae, J., 1999. Removing the regolith: EM defined structure fails to correct gravity at Elura. Exploration Geophysics 30: 115-122.

Carter, W., Shrestha, R., Tuell, G., Bloomquist, D. and Satori, M., 2001. Airborne laser swath mapping shines new light on Earth's topography: EOS 82(46): 549-555.

Cook, P.G. and Kilty, S., 1992. A helicopter-borne electromagnetic survey to delineate groundwater recharge rates. Water Resources Research 28: 2953-2961.

Cook, P.G., Walker, G.R., Buselli, G., Potts, I. and Dodds, A.R., 1992. The application of electromagnetic techniques to groundwater recharge investigations. Journal of Hydrology 130: 201-229.

Dentith, M.C., Frankcombe, K.F., Ho, S.E., Shepherd, J.M., Groves, D.I. and Trench, A., (Editors), 1994. Geophysical Signatures of Western Australian Mineral Deposits: Geology and Geophysics Department (Key Centre) and UWA Extension Publication No.26, Australian Society of Exploration Geophysicists Special Publication 7, 454 pp.

Duncan, A., Amann, W., O'Keeffe, K., Williams, P., Tully, T., Wellington, A. and Turner, G., 1998. Examples from a new EM and electrical methods receiver system. Exploration Geophysics 29: 347-354.

Emerson, D.W., Macnae, J.C. and Sattel, D., 2000. The petrophysics of the Lawlers regolith, Western Australia. Exploration Geophysics 31: 229-235.

Emerson, D.W. and Macnae, J., 2001. Further physical property data from the Archaen Regolith, Western Australia. Preview June 2001: 33-37.

Farquharson, C.G. and Oldenburg, D.W., 1993. Inversion of time-domain electromagnetic data for a horizontally layered Earth. Geophysical Journal International 114: 433-442.

Fitterman, D.V. and Deszcz-Pan, M., 2001. Using Airborne and Ground Electromagnetic Data to Map Hydrologic Features in Everglades National Park. Symposium on the application of geophysics to engineering and environmental problems (SAGEEP) March 4-7 2001, Denver (CD ROM).

Gettings, M.E., Bultman, M.W., and Wynn, J.C., 1999. An interpretation of the 1997 Airborne Electromagnetic (AEM) survey, Fort Huachuca vicinity, Cochise County, Arizona: U.S. Geological Survey Open-File Report 99-7-B. (http://caldera.wr.usgs.gov/OF99-7-B/).

George, R.J., Beasley, R., Gordon, I., Heislers, D., Speed, R., Brodie, R., McConnell, C. and Woodgate, P., 1998. The national airborne geophysics project, national report. Evaluation of airborne geophysics for catchment management (draft). (Unpublished). (http://www.ndsp.gov.au/NAGP/nagp_nr.htm).

Green, A., 1998a. Altitude correction of time domain AEM data for image display and geological mapping using the Apparent Dipole Depth ADD) method. Exploration Geophysics 29: 87-91.

Green, A., 1998b. The Use of Multivariate Statistical Methods for the Analysis and Display of AEM data. Exploration Geophysics 29: 77-82.

Huang, H. and Fraser, D.C., 1999. Airborne resistivity data leveling. Geophysics 64: 378-385.

Huang, H. and Fraser, D.C., 2001. Mapping of the resistivity, susceptibility, and permittivity of the earth using a helicopter-borne electromagnetic system. Geophysics 66: 148-157.

Hunter, D. and Macnae, J., 2001. Subsurface conductivity structure as approximated by conductivity-depth transforms. Extended Abstract, Australian Society of Exploration Geophysicists (ASEG) Conference, Brisbane, August 2001 (CD ROM).

Jenke, G. and Cowan, D.R., 1994. Geophysical signature of the Ellendale lamproite pipes, Western Australia. In: Dentith, M.C., Frankcombe, K.F., Ho, S.E., Shepherd, J.M., Groves, D.I. and Trench, A., (Editors), Geophysical signatures of Western Australian mineral deposits. Geology and Geophysics department, University of Western Australia publication 26: 403-414.

Lane, R., 2000. Conductive unit parameters: summarising complex conductivity distributions. 70th Meeting, Society of Exploration Geophysicists (SEG), Calgary, Expanded Abstracts 1, Section EM4.2, pp. 328-331.

Lane, R. and Pracilio, G., 2000. Visualisation of sub-surface conductivity derived from airborne EM. Symposium on the application of geophysics to engineering and environmental problems (SAGEEP) 2000, 20-24 February 2000, Arlington, Virginia pp. 101-111.

Lane, R., Green, A., Golding, C., Owers, M., Pik, P., Plunkett, C., Sattel, D. and Thorn, B., 2000. An example of 3D conductivity mapping using the TEMPEST airborne electromagnetic system. Exploration Geophysics 31: 162-172.

Lane, R., Heislers, D. and McDonald, P., 2001. Filling in the gaps, validation and integration of airborne EM data with surface and subsurface observations for catchment management, an example from Bendigo, Victoria, Australia. Exploration Geophysics 32: 205-215.

Lawrie, K.C., Munday, T.J., Dent, D.L., Gibson, D.L., Brodie, R.C., Wilford, J., Reilly, N.S. and Chan, R.A., 2000. A 'Geological Systems' approach to understanding the processes involved in land and water salinisation in areas of complex regolith - the Gilmore Project, central-west NSW. AGSO Research Newsletter 32: 13-15, 26-32.

Leggatt, P.B., Klinkert, P.S. and Hage, T.B., 2000. The Spectrem airborne electromagnetic system - Further developments. Geophysics 65: 1976-1982.

Liu, G. and Becker, A., 1990. Two-dimensional mapping of sea-ice keels with airborne electromagnetics: Geophysics 55: 239-248.

Macnae, J., 1995a. Applications of Geophysics for the Detection and Exploration of Kimberlites and Lamproites. Journal of Geochemical Exploration 53: 213-243

Macnae, J., 1995b. Esoteric and mundane geophysics for diamondiferous pipe exploration. Exploration Geophysics 26: 131-137.

Macnae, J. and Bishop, J., 2001. Simplified electrical structure models at AEM scales, Lawlers, Western Australia. Exploration Geophysics 32: 29-35.

Macnae, J.C., King, A., Stolz, N., Osmakoff, A. and Blaha, A., 1998. Fast AEM data processing and inversion: Exploration Geophysics 29: 163-169.

McIntosh, S. M., Gill, J. P. and Mountford, A. J., 1999. The geophysical response of the Las Cruces massive sulphide deposit. Exploration Geophysics 30: 123-134.

McNeill, J.D., 1980. Electromagnetic terrain conductivity measurement at low induction numbers. Geonics Technical Note TN-6: 15 pp.

McNeill, J.D., 1986. Geonics EM39 borehole conductivity meter, theory of operation. Geonics Technical Note TN-20: 17 pp.

Meyers, J., Worrall, L., Lane, R. and Bell, B., 2001. Exploring through cover – the integrated interpretation of high resolution aeromagnetic, airborne electromagnetic and ground gravity data from the Grant's Patch area, Eastern Goldfields Province, Archaean Yilgarn Craton. Part C: Combining geophysical methods for a holistic exploration model. Exploration Geophysics 32: 198-202.

Munday, T.J., Macnae, J., Bishop, J. and Sattel, D., 2001. A geological interpretation of observed electrical structures in the regolith: Lawlers, Western Australia. Exploration Geophysics 32: 36-47.

Paine, J.G., Dutton, A.R., Mayorga, J.S. and Saunders, G.P., 1997. Identifying oil-field salinity sources with airborne and ground-based geophysics: a West Texas example. The Leading Edge 16(11): 1603–1607.

Paine, J.G., Angle, E.S. and Petrossian, R., 2000. Identifying and assessing ground water in the Lower Rio Grande Valley, Texas, using airborne electromagnetic induction. Proceedings of Symposium on the application of geophysics to engineering and environmental problems (SAGEEP) 2000, 20-24 February 2000, Arlington, Virginia pp. 83–93.

Palacky, G.J., 1989. Advances in Geological Mapping with Airborne Electromagnetic Systems. Exploration '87 Proceedings - Third Decennial International Conference on Geophysical and Geochemical Exploration for Minerals and Groundwater pp. 137-152.

Peters, W.S., 1996. A rough guide to transient electromagnetics (TEM). Geophysics for Geologists and Engineers. AIG Bulletin 19: 21-47.

Peters, W.S., 2001. Ground electromagnetics: the basics and recent developments. Recent Developments and Future Directions in Geophysics. AIG Bulletin 33: 15-32.

Poikonene, A., Sulkanen, K., Oksama, M. and Suppala, I., 1998. Novel dual frequency fixed-wing airborne EM system of Geological Survey of Finland (GTK). Exploration Geophysics 29: 46-51.

Potts, I.W., 1990. Use of the EM-34 instrument in groundwater exploration in the Shepparton Region. Australian Journal of Soil Research 28: 433-442.

Rodriguez, B.D., Deszcz-Pan, M., Grauch, V.J.S., Doucette, J.P., Sawyer, D.A. and Stone, B.D., 2001. Mapping Grain Size Facies for the Hydrogeologic Model of the Middle Rio Grande Basin, New Mexico Using Airborne Time-domain Electromagnetic Data. Proceedings of Symposium on the application of geophysics to engineering and environmental problems (SAGEEP) March 4-7 2001, Denver (CD ROM).

Rutherford, J., Munday, T., Meyers, J. and Cooper, M., 2001. Relationship between regolith materials, petrophysical properties, hydrogeology and mineralisation at the Cawse Ni laterite deposits, Western Australia. Implications for exploring with airborne EM. Exploration Geophysics 32, 160-170.

Sattel, D., 1998. Conductivity information in three dimensions. Exploration Geophysics 29: 157-162.

Sauer, M.C., Southwick, P.F., Spiegler, K.S. and Wyllie, M.R.J., 1955. Electrical conductance of porous plugs. Industrial and Engineering Chemistry 47: 2187-2193.

Skirrow, R., 2001. Under cover work in Gawler to penetrate mineral sectrets. AGSO Geoscience Australia. AUSGEO News 61: 3-5.

Slavich, P.G. and Petterson, G.H., 1990. Estimating average rootzone salinity from electromagnetic induction (EM38) measurements. Australian Journal of Soil Research 28: 453-463.

Smith, R.S., Annan, A.P. Lemieux, J. and Pedersen R.N., 1996. Application of a modified GEOTEM system to the reconnaissance exploration for kimberlites in the Point Lake area, NWT, Canada. Geophysics 61: 82-92.

Smith, R.S., Annan, A.P. and McGowan, P.D., 2001. A comparison of data from airborne, semi-airborne, and ground electromagnetic systems. Geophysics 66: 1379-1385.

Strack, K.M., 1992. Exploration with deep transient electromagnetics. Elsevier Science Publications, Amsterdam 374 pp.

Street, G.J., 1992. Airborne Geophysical Surveys, Applications in Land Management. Exploration Geophysics 23: 333-338.

Stone, P.M. and Simsky, A., 2001. Constructing high resolution DEMs from airborne laser scanner data. Extended Abstract, Australian Society of Exploration Geophysicists (ASEG) Conference, Brisbane, 2001 (CD ROM).

Valleau, N.C., 2000. HEM data processing, a practical overview. Exploration Geophysics 31: 584-594.

Wolfgram, P. and Golden, H., 2001. Airborne EM applied to sulphide nickel, examples and analysis. Exploration Geophysics 32: 136-140.

Worrall, L., Lane, R., Meyers, J. and Whitaker, A., 2001. Exploring through cover, the integrated interpretation of high resolution aeromagnetic, airborne electromagnetic and ground gravity data from the Grant's Patch area, Eastern Goldfields Province, Archaean Yilgarn Craton, Part A: Mapping geology using airborne electromagnetics (TEMPEST). Exploration Geophysics 32: 190-193.

Wynn, J.C., Pool, D., Bultman, M., Gettings, M. and Lemieux, J., 2000. Airborne EM as a 3-D aquifer-mapping tool. Proceedings Symposium on the application of geophysics to engineering and environmental problems (SAGEEP) 2000, 20-24 February 2000, Arlington, Virginia pp. 93-100.

Zhang, Z. and Oldenburg, D.W., 1999. Simultaneous reconstruction of 1-D susceptibility and conductivity from electromagnetic data. Geophysics 64: 33–47.

APPENDICES

Appendix 1 - Survey Costs

For surveys carried out by contract crews, costs are generally broken down into 3 categories; 1) mobilisation / de-mobilisation, 2) a daily (ground EM) or line km (airborne EM) rate; and, 3) standby. The rates depend on factors such as the system involved, product requirements, timing requirements, location, distance between base of operations and the survey area, size (ie. number of days or line km) and the line configuration (eg. length, separation). The survey organisations can generally provide a quotation fairly readily upon receipt of a survey proposal.

For airborne surveys, the line km rate can vary from over A$100 per line km for small areas to less than A$50 per line km for very substantial surveys (10's of thousands of line km). Rates for fixed wing and helicopter surveys are similar.

For TD ground EM surveys, the daily rate for a 3-person crew is typically A$1000 to A$2000. Production varies considerably depending on the terrain and the configuration. These costs are likely to amount to A$250 to A$1000 per line km.

Standby charges (for bad weather, client delays etc) are typically less than A$1000 per day for a ground EM crew and several thousand dollars for an airborne EM system.

Single-frequency ground EM instruments can be hired for less than a few hundred dollars per day. Production depends on access and sample interval, but can be 5 to 10 km per day. Some of these systems have been fitted to all-terrain vehicles and incorporate a GPS antenna for location. Productivity is higher, as are the costs.

Appendix 2 - Survey Organisations

Airborne Electromagnetic Systems

Fugro Airborne Surveys
65 Brockway Road, Floreat, WA 6014
Telephone: +61 8 9273 6400

UTS Geophysics
Valentine Road, Perth Airport
P O Box 126, Belmont, WA 6014
Telephone: +61 8 9479 4232

Ground Electromagnetic Systems

Fugro Ground Geophysics
65 Brockway Road, Floreat, WA 6014.
Telephone: +61 8 9273 6400

McSkimming Geophysics Pty. Ltd
30 Needham Court, Kiels Mountain, QLD 4559.
Telephone +61 7 5450 8100

Outer-Rim Exploration Services
PO Box 1754, Aitkenvale, QLD 4814.
Telephone +61 7 4725 3544

Solo Geophysics
3A McInnes St, Ridleyton, SA 5008.
Telephone +61 8 8346 0924

Zonge
98 Frederick St, Welland, SA 5007.
Telephone +61 8 8340 4308

Appendix 3 - Associations

Assistance with EM methods can be obtained through a number of professional geophysical organisations.

Australian Society of Exploration Geophysicists (ASEG) (http://www.aseg.org.au/)
Society of Exploration Geophysicists (SEG) (http://www.seg.org/)
The Environmental and Engineering Geophysical Society (EEGS) (http://www.eegs.org/)
Symposium on the Application of Geophysics to Engineering and Environmental Problems (SAGEEP) (http://www.sageep.com/).

Appendix 4 - General Texts and Further Reading

Cook, P.G. and Williams, B.G., 1998. Studies in Catchment Hydrology. The Basics of Recharge and Discharge. Part 8. Electromagnetic Induction Techniques. CSIRO Land and Water, CSIRO Publishing, Canberra 16 pp.

Fitterman, D., (Editor), 1990. Developments and Applications of Modern AEM Surveys: USGS Bulletin 1925: 216 pp.

Nabighian, M., (Editor), 1988. Electromagnetic Methods in Applied Geophysics: Society of Exploration Geophysicists. Volume 1, Theory. Volume 2, Applications, 528 pp. and 992 pp.

Palacky, G.J., (Editor), 1986. Airborne resistivity mapping. Geological Survey of Canada Paper 86-22: 195 pp.

Spies, B., (Editor), 1998. AEM 98. The International Conference on Airborne Electromagnetics, Sydney, Australia, February 23-25, 1998. Exploration Geophysics 29: 1-271.

Ward, S.H., (Editor), 1990. Geotechnical and Environmental Geophysics. Society of Exploration Geophysicists. Volume I, Review and Tutorial. Volume II, Environmental and Groundwater. Volume III, Geotechnical, 1050 pp.

GROUND PENETRATING RADAR

Stephen Griffin[1] and Timothy Pippett[2]

[1] Geophysical Technology Limited. 15 Jedda Street, Tallebudgera, QLD 4228. E-mail: stevegriffin@geotec.com.au

[2] Alpha Geoscience Pty. Limited. Suite 7, 852 Princes Highway, Sutherland, NSW 2232. E-mail: tpippett@alpha-geo.com

1. INTRODUCTION

Ground penetrating radar (GPR) also known as ground probing radar, impulse radar or subsurface interface radar, is a geophysical method used for high resolution imaging of shallow subsurface features. It is similar to air-directed radar in that it transmits a burst of electromagnetic energy and then waits for reflections from targets to be received before repeating the process continuously. However, it differs significantly from that better known form by transmitting the energy instantaneously over a wide frequency range, utilising a very short transmission pulse and a broadband antenna design. The usual operating frequency varies between about 25 MHz and 1000 MHz (covering the VHF/UHF bands).

The energy is transmitted into the ground using antennas that are in direct contact with the surface, and as this energy propagates to greater depths, a series of reflections are directed back to the surface where they are detected by the receiving antenna. The method is only suitable for shallow investigation (up to tens of metres in the best conditions) because the ground absorbs the energy at a rapid rate, and as it propagates to greater depths. Eventually there is insufficient energy to generate a reflection from a deep target that can be redirected back to the surface and detected by the receiver.

Although the GPR method has been widely applied to a range of applications in Australia, there are only a limited number of applications where it can be regarded as having been successful, compared to the extent in which it is used in say Europe and the USA,. The main reason for this is the occurrence of soils that are generally more conductive than those in other countries. Despite this fact, there are at least four groups in Australia who have designed and built world class systems for specialised applications. All of the commercially available systems are well represented by a sales agents and consultants, and the number of practitioners has risen greatly in the twenty years since it was first introduced here.

2. DESCRIPTION

The GPR method provides a high-resolution image of subsurface features in the form of a cross-section view that is essentially a map of the variation in ground electrical properties. These can be correlated with physical changes such the soil/bedrock interface, the boundary between different soil types, the water table, underground structures such as pipes, cables and tunnels as well as voids and cavities. Features in the GPR section will correlate with geological cross-sections if for instance stratigraphic boundaries representing different rock types correspond to significant variations in the electrical properties, but not necessarily to other physical properties such as density, grain size or chemical composition.

The short pulses of RF energy are radiated into the ground from a transmitting antenna placed either on the ground surface or in close proximity. Energy reflected back to the surface from subsurface targets is detected by the receiving antenna, also located in close proximity to the surface. The antennas physical size or dimension limits the frequency (or wavelength) of the transmitted pulse. A high frequency waveform (short wavelength) will provide a more detailed or higher resolution image than a low frequency waveform, but the higher frequencies are attenuated or absorbed at a greater rate

In Papp, É. (Editor), 2002, *Geophysical and Remote Sensing Methods for Regolith Exploration*, CRCLEME Open File Report 144, pp 80-89.

so the penetration depth is not as great as lower frequencies. For any specific application, the appropriate choice of antenna frequency involves a compromise between resolution (or size of objects/features to be detected) and the depth of interest.

The transmission is characterised as a single burst of energy after which the receiver then 'listens' and records any reflected energy such that the recording time (from the point of transmission) represents the depth to the source of the reflection. That is, a reflection from a deeper target will appear later in time in the GPR section since the energy has travelled further than for the shallower targets. At any instance, the receiver is only on for a finite period of time (of the order of several hundred nanoseconds) after which another pulse is transmitted to repeat the process. The GPR section is actually a time section, however with knowledge of the propagation velocity, time is converted to depth.

The two most important soil and rock electrical properties are the dielectric constant and conductivity. Both are greatly influenced by water (eg. soil moisture content) therefore water has a significant influence on GPR performance overall. Soil conductivity limits the maximum depth of energy penetration (or target detection depth) since it influences the rate at which the energy is absorbed. A more conductive soil (one that is wetter and/or has a higher clay content) will absorb the energy at a far greater rate than a low conductivity soil such as dry sand. The penetration depth in dry clay soils will typically be in the range of one or two metres and a wet clay will reduce penetration to less than one metre, whereas dry sandy soils will allow penetration to more than 10 metres. Rock types with low conductivity (high resistivity) include limestone, coal, granite and other crystalline rock, whereas rock types that are more conductive include basalt, shales and mudstones or any weathered terrain with reasonably high porosity.

The RF energy propagates through the ground at about one-third the speed of light or 10 $cm.ns^{-1}$ (the units are chosen for convenience only, and some people may prefer to express this velocity as 0.1 $m.ns^{-1}$). The velocity of propagation will vary for different earth materials, but will generally be within the range $8 \rightarrow 12$ $cm.ns^{-1}$ and is determined by the relative dielectric constant (expressed as a quantity relative to the value of air). All materials of interest will vary between the range 1 (for air) and 81 (water). Geologic materials will generally fall within the range 5 - 15.

A reflection will occur in response to changes in the dielectric constant, and this may not necessarily correlate with properties such as density, which most people intuitively understand from their experience with seismic methods. However, the dielectric constant or electrical permittivity is analogous to the acoustic impedance in seismics, in a mathematical sense. That is, as well as determining velocity, the change or contrast in the dielectric constant with different earth materials will cause a reflection whose strength (or amplitude) is dependent on the magnitude of that contrast.

To summarise the importance of water in understanding GPR performance, a higher moisture content in the soil will reduce the possible depth of penetration, but may provide for a stronger reflection (since the presence of water will increase the dielectric constant significantly. This will therefore also cause the velocity of propagation to be higher, which in itself will influence resolution through its relationship with frequency and wavelength.

3. FIELD PROCEDURES

Most GPR antennas are able to be easily man-handled, and the usual method of operation is to drag the antennas slowly across the ground surface in a straight line traverse, transmitting and receiving continuously, so that a profile picture builds up (referred to as a GPR section). This represents the accumulation of reflections that have been received. The series of single waveforms combine together to give the effect of mapping layers and objects in the ground. The receiving antenna and circuitry records for a finite period of time, so that the derived time record or waveform has an early time period corresponding to reflections from shallow targets and later time corresponding to deeper targets, with amplitude representing the strength of the reflection. For this reason the GPR sections can be thought of as a depth section or profile view of the subsurface conditions below the traverse line.

Generally, operation of a commercial GPR system requires two operators, one to drag the antennas along the ground, the other to control the instrument operations from a console which is often simply a laptop personal computer and another electronic module connected to the antennas by cable or optic fibre. Many commercial operators may use vehicles such as 4WD's or 4-wheeled motorbikes to assist with both instrument carriage and antenna mobility.

Instrument configuration and survey design is determined by the survey objectives and physical factors such as the terrain and site layout - especially the roughness of the ground surface and the presence of obstructions such as water courses, trees, gullies, rocks or man-made structures.

Distance control along a traverse line can be provided by a range of means that include odometers attached to wheels or cotton on a spool tied off at the starting point, fiducial marking (manually inserting a mark into the data say with an electronic push-button, corresponding to known points along the traverse), and differential GPS.

To a great extent, the appropriate field procedures are determined by the actual system being used, and while the commercial systems have certain similarities, there are some that are better suited to particular applications than others. For example, to gain data quality improvements using the low frequency antenna it is recommended that the antenna should be manhandled to each measurement point and kept stationary for the duration of the recording time in order to obtain the best possible result. They can be used by continuous dragging across the ground, either by man or vehicle, however the data quality will be reduced. Such as system might be more time consuming but the tradeoff is the best possible result.

The survey objective has a significant impact on instrument configuration as well as field layout by determining in the first instance the appropriate antenna frequency. Other factor such as the target size determine line spacing and number of samples required along the traverse line in order to satisfy basic spatial sampling criteria, according to such factors as target depth, antenna frequency, reflector geometry and instrument measurement parameters (pulse characteristics and high frequency signal sampling).

4. INSTRUMENT TYPES AND CONFIGURATIONS

The following is a list of commercially available systems in Australia, with a brief summary of the key similarities and differences, and how this relates to certain limitations.

1. Geophysical Survey Systems, Inc. of Burlington, New Hampshire, GPR system includes the SIR2000, SIR10 systems. These systems have a range of in-house and third party antennas ranging in frequency from 40 to 1500 MHz and all being shielded antennas.

2. Mala Geosciences Inc. of Mala, Sweden, have the RAMAC/GPR system. The RAMAC system has a full range of antennas from 25 to 1,000 MHz including borehole probes, either 100 or 250 MHz. The RAMAC system console controls both the unshielded and shielded antennas and the borehole probe with a PC Notebook computer as the acquisition, display and storage device. The Mala range of antennas include 25, 50, 100 and 200 MHz unshielded and 100, 250, 500, 800 and 1,000 MHz shielded.

3. Sensors and Software, Inc. of Toronto, Canada, includes the pulseEKKO100 and pulseEKKO1000 systems and the Nogun systems. The pulseEKKO100 system is designed for low frequency systems using unshielded antenna and the pulseEKKO1000 system is for the higher frequency applications using shielded antennas from 200 MHz to 900 MHz. The Nogun systems are a single

frequency unit with either 250 or 500 MHz. Both pusleEKKO and the Nogun systems use a PC Notebook computer as the acquisition, display and storage device.

5. DATA PROCESSING

One of the great advantages of the GPR method is the fact that the raw data is acquired in a manner that allows it to be easily viewed in real time using a computer screen. Often very little processing is required for an initial interpretation of the data, with most of the effort directed towards data visualisation. On the other hand, depending on the application and target of interest, it may be necessary to perform sophisticated data processing, and many practitioners find that the techniques common to seismic reflection such as deconvolution and migration can be successfully applied.

As stated earlier, the basic form of the data is a profile or section view of subsurface features beneath a straight-line traverse, with the vertical dimension being two-way travel time (usually expressed in nanoseconds) just like seismic sections. However, because most people are interested in converting this to a depth section, it is necessary to have some knowledge of the propagation velocity through the soil and rock in order to rescale the data appropriately. Depending on the required accuracy, this can be as simple as applying a nominal velocity based on textbook data and some knowledge of the likely soil/rock type and moisture content. Alternatively it can involve simple data processing using seismic processing techniques such as common mid-point and velocity analysis of a normal moveout section. Calibration through direct measurement of the depth to certain recognisable features using either drilling or trenching is also commonly applied.

6. DATA INTERPRETATION

GPR sections can be presented as greyscale or colour images that use the different shades of grey or colours to represent the variation in the signal amplitude. The examples shown in the Applications Section illustrate some of the various displays available to the interpreter.

Although it is generally assumed that at any instance the recorded waveform is composed of reflections from targets located directly below the antenna, the image is often complicated by the fact that the waveform spreads out on a spherical wavefront, so that strong reflectors off to the side will be superimposed over other weaker reflections from another location. Another complication will occur when reflections from above ground sources may be superimposed on the below ground reflectors.

7. APPLICATIONS

Figures 1-5 illustrate some of the various applications that the GPR technique can be used for.

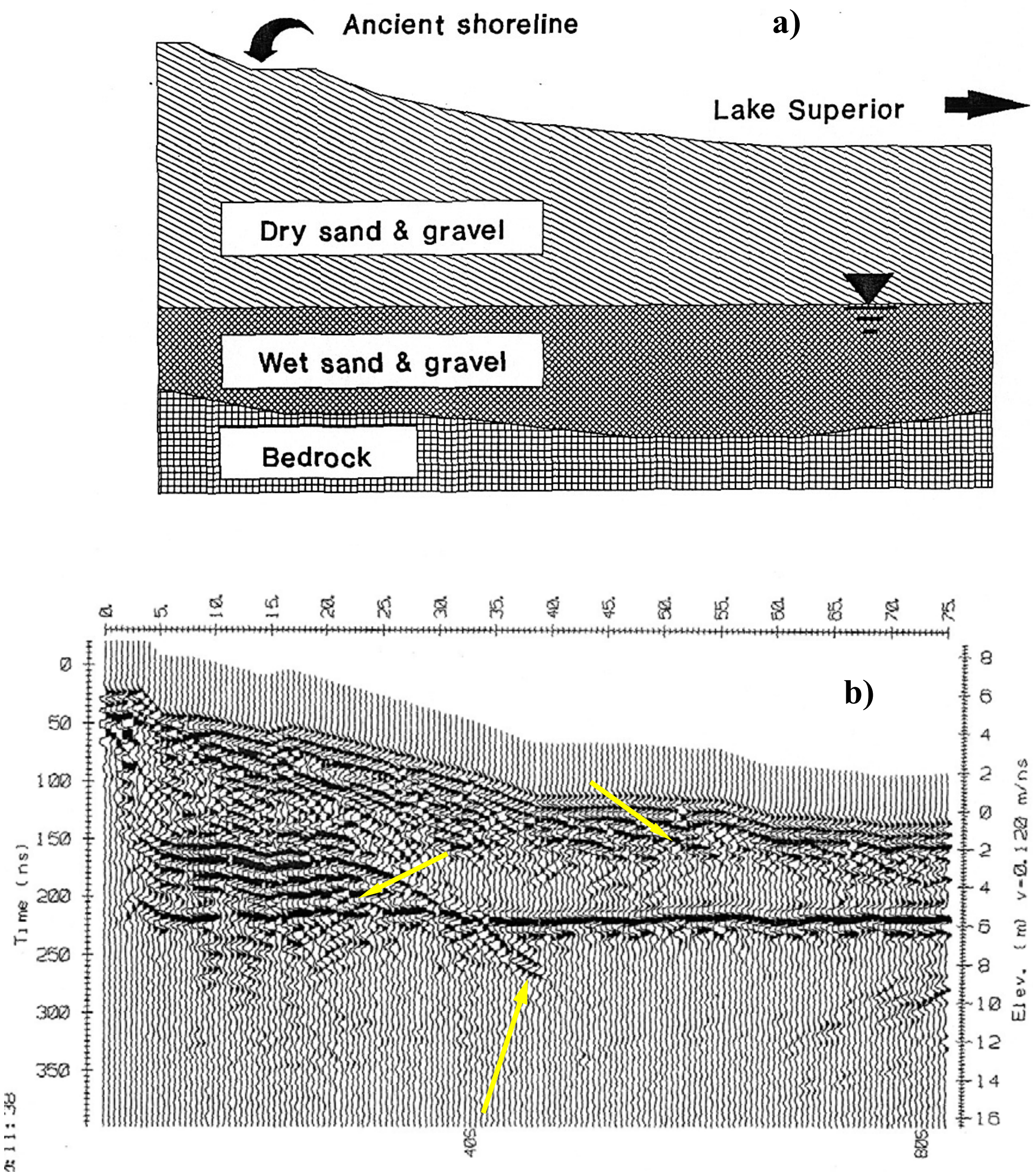

Figure 1 a and b. An application of using the GPR technique to map the groundwater surface and the sand / gravel-bedrock interface (Scaife and Annan, 1991).

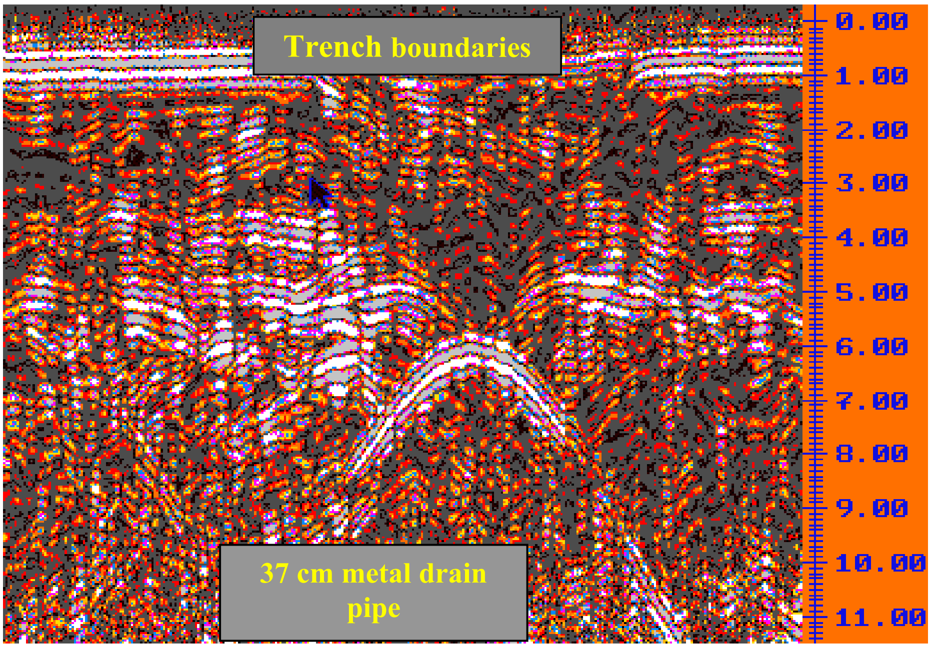

Figure 2. This section illustrates the use of GPR for the location of underground services and in this case a pipe buried at approximately 2 metres (Courtesy of Mala Geoscience).

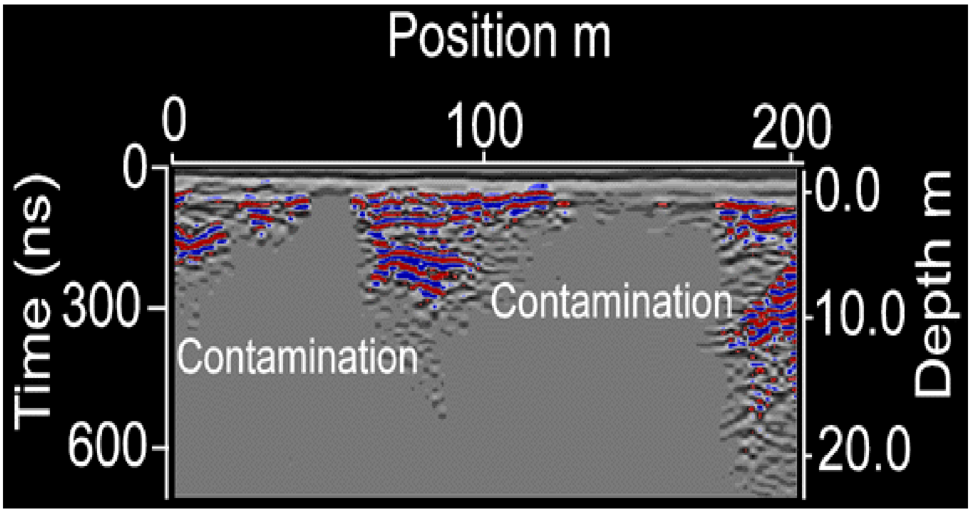

Figure 3. Radar section across an area that has two plumes of contaminated groundwater present. Note the lack of GPR signal penetration due to the contamination having a much higher conductivity than the surrounding ground (Davis and Annan, 1989).

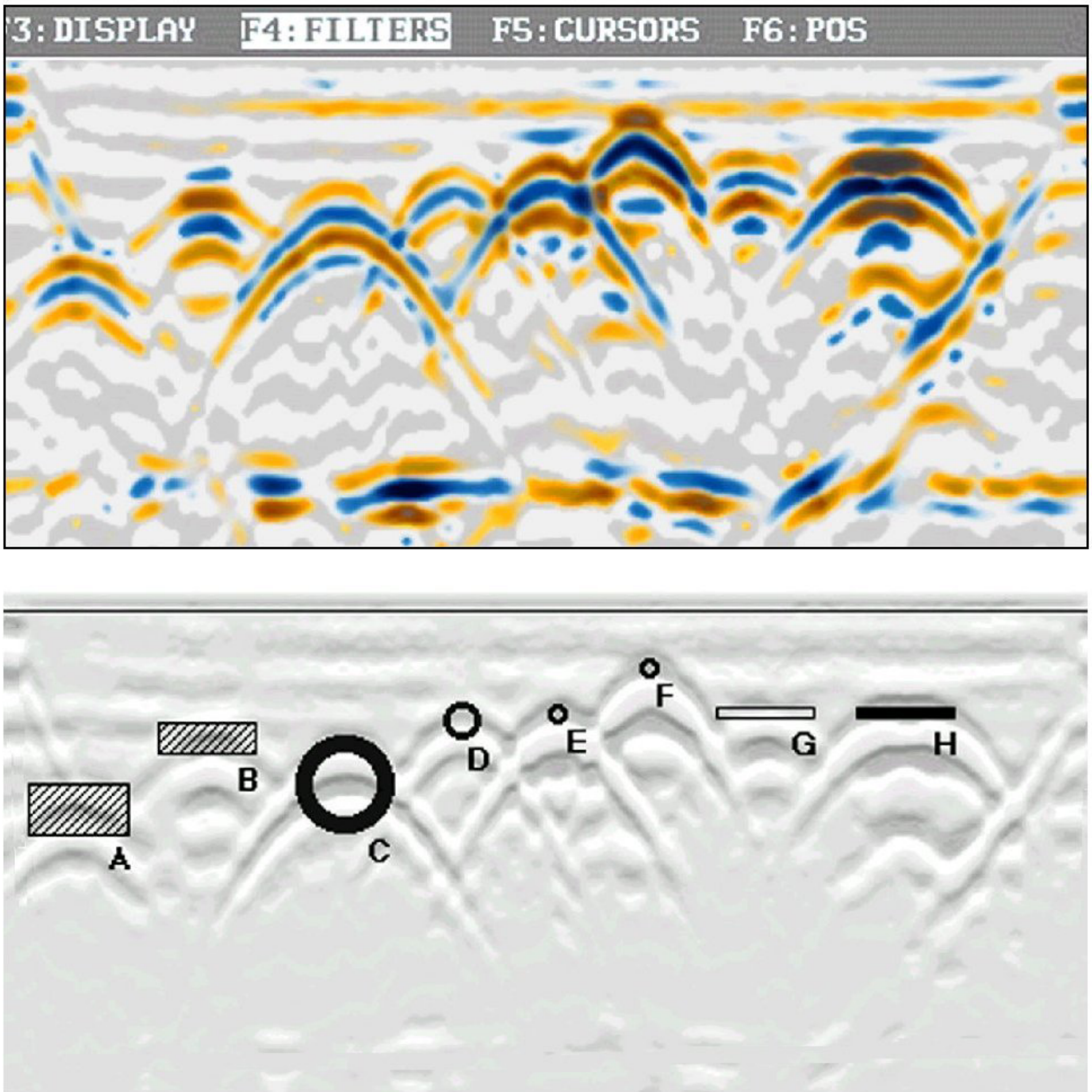

A) Polystyrene disc ø60 cm, H: 30 cm, Appr. depth: 100 cm (top)
B) Polystyrene disc ø60 cm, H: 15 cm, depth: 60 cm (top)
C) Concrete tube ø60 cm, Appr. depth: 100 cm (center)
D) PVC tube ø20 cm, Appr. depth: 60 cm (center)
E) Iron tube ø6.35 cm, Appr. depth: 60 cm (center)
F) Iron tube ø6.35 cm, Appr. depth: 30 cm (center)
G) Wood disc ø60 cm, H: 4 cm, Appr. depth: 60 cm (top)
H) Iron disc ø60 cm, H: 4 cm, Appr. depth: 60 cm (top)

Figure 4. This illustrates the versatility of the GPR system to locate various different items made of different material at various depths (Courtesy of Mala Geoscience).

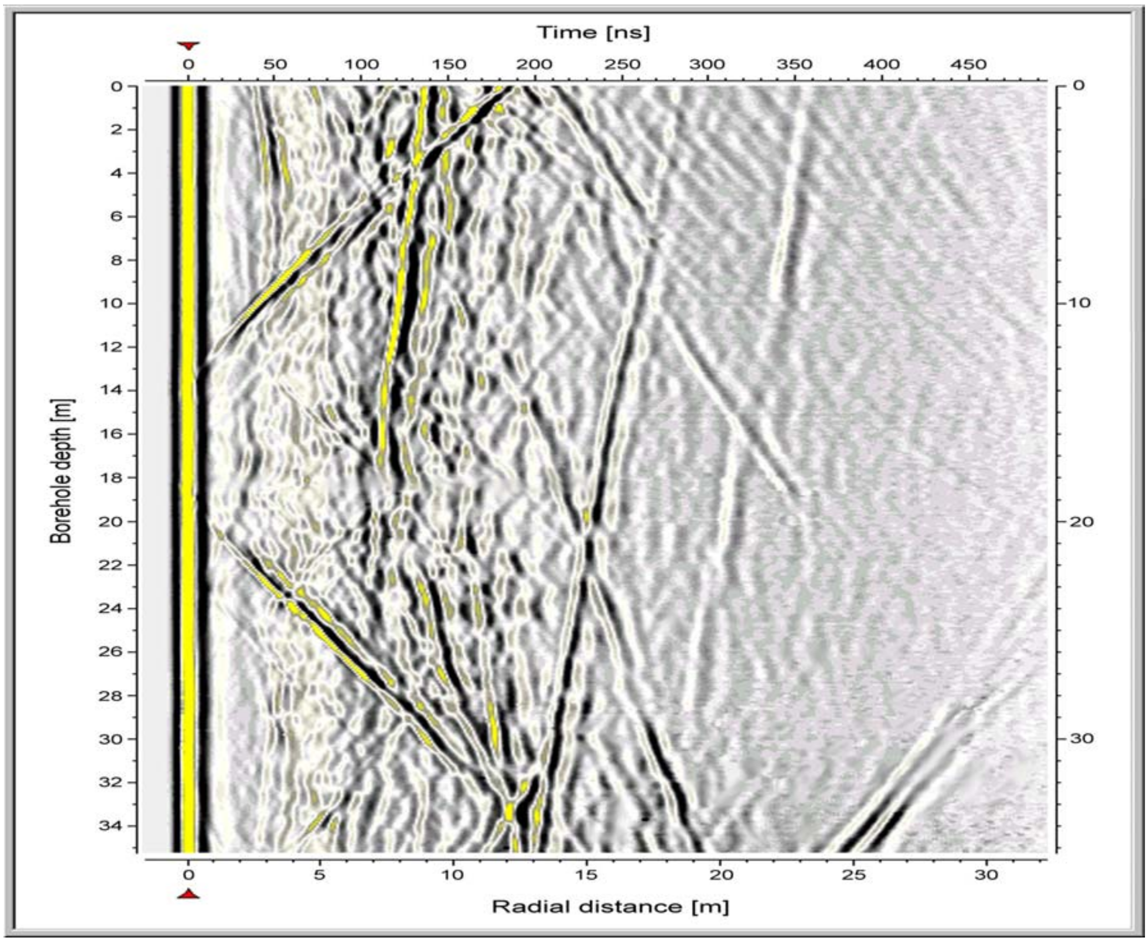

Figure 5. An example of a borehole radar section obtained with a Mala Geoscience borehole probe. Note that the probe is omni-directional and the reflector coming in at approximately 45° is the same one that is going out at 45° but the other side of the borehole (Courtesy of Mala Geoscience).

8. LIMITATIONS AND PROBLEMS

There are a number of limitations and problems for the GPR technique. These include:

1. Ground conductivity – which will limit the overall depth of penetration and thus the usefulness of the technique;

2. Time consuming;

3. Large quantity of data is accumulated - makes processing and interpretation task difficult without the right software tools;

4. Competing with intrusive methods, ie. backhoe, and thus the technique needs to produce results on the spot and at an economic price;

5. Suitability of instrument available for particular applications, different units are more suitable for particular applications and ground conditions than others;

6. Need to dig holes to 'have a look' in order to get best possible calibration or correlation; and,

7. Frequency dependent dispersion - spreading of pulse to reduce resolution - because different portions of the energy will slow down, increasing the wavelength.

9. SURVEY ORGANISATIONS

Groups who manufacture GPR systems in Australia for specialised applications include Monash University, Queensland University (CSSIP), CSIRO and Sydney University.

The following is a list of agents for the commercially available systems in Australia and New Zealand:

- **GSSI Systems**

Detection Solutions
P.O. Box 38-061
Howick, Auckland. New Zealand.
Tel: 0-9-576-8000
Fax: 0-9-576-4641
Mobile: 025-327 292
Contact: Mr. Steve Simmons
E-mail: detectso@ihug.co.nz

Geophysics Australia
3061 Great North Road
New Lynn, Auckland, New Zealand.
Contact: Mr. Grant Roberts
Tel: 64-9-826-0700
Fax: 64-9-826-0900
E-mail: g.roberts@geophysical.com.au
Website: www.geophysical.com.au

- **Mala Geoscience**

Alpha Geoscience Pty. Limited
Suite 7, 852 Princes Highway
Sutherland, NSW. 2232. Australia.
Tel: 61-2-9542-5266
Fax: 61-2-9542-5263
Mobile: 61-412-663-541
Contact: Mr. Timothy Pippett
E-mail: sales@alpha-geo.com
Website: www.alpha-geo.com

- **Sensors and Software**

Fugro Instruments
21 Mellor Street
Sydney, NSW. 2114. Australia.
Tel: 61-2-8878-9000
Fax: 61-2-8878-9012
Contact: Mr. Simon Stewart
E-mail: sales@fugroinstruments.com
Website: www.fugroinstruments.com

10. COSTS

The cost of the various systems depends very much on the antennas selected, the range of investigations required, and the processing software required. The pricing of the systems will also depend on the country of manufacture as the prices have been affected by the exchange rate, ie. the $US has been more affected than the Euro.

To gain up to date pricing, it is recommended that an approach be made to the manufactured representative in Australia or New Zealand.

1. The cost to rent the radar systems will again depend on the configuration selected but would be in the vicinity of $ 350 to $ 500 per day or $ 1,750 to $ 2,500 per week.

2. A professional consultant to run the radar system or train operators on the use of the system would be in the vicinity of $ 500 to $ 750 per day (depending on experience).

REFERENCES

Annan, A.P. & Cosway, S.W., 1991. Ground Penetrating Radar Survey Design. 53rd Annual Meeting of the European Association of Exploration Geophysicists. Florence, May 1991.

Davis, J.L. and Annan, A.P., 1989. Ground penetrating radar for high-resolution mapping of soil and rock stratigraphy. Geophysical prospecting 37: 531-551.

Scaife, J.E. and Annan, A.P., 1991. Ground penetrating radar - a powerful, high resolution tool for mining, engineering and environmental problems. In: 93rd CIM Annual general meeting, Vancouver, British Columbia, April 1991, 6 pp.

GROUND ACOUSTIC PENETRATION

Bronislav A. Koulmametiev and Boris V. Matveev

InterGeoRAP Consulting. 8 Hartleap Lane, Beldon, WA 6027. E-mail: tchern@iinet.net.au

1. DESCRIPTION

Ground Acoustic Penetration (GAP) is a new ground geophysical method based on modern approaches to the interpretation of acoustic signals.

Soil/upper regolith layers are comparatively thin and their response to acoustic pulses has a very complex nature. Responses from different layers/borders are close in time, and as they interfere with each other, they create complex oscillations. To interpret this wave pattern, two significantly different approaches are used. One of them is based on the study of the frequency spectra of waves and is described in some detail by Houdzinsky (1962). The spectrum of a wave S(f), reflected from a layer, can be determined from the following equation:

$$S(f)=q(f)p(f)K(f)e^{-a(f)}k(f),$$

where q(f) is the spectrum of the impact pulse; p(f) is the filtering influence of the upper stratified medium on the waves that are going through; a(f) is the dependence of the absorption index on frequency; K(f) is frequency characteristic of the registering device, including geophone station characteristics.

The major problem of this approach is to accurately determine spectral characteristics for each of the adjustments and the problem was resolved by the developers of GAP. At present it is this approach that is used for processing and interpreting field data based on research carried out in Russia (Brekhovskikh and Godin, 1989) and other countries (Bath, 1974, Aki and Richards, 1980). The data are presented as cross-sections, which show the distribution of acoustic impedance of studied media.

Modern powerful computing equipment makes it possible to use another approach - complicated from the point of view of mathematics but more appropriate for the physics of the studied processes. It is based on finding and analysing the response from each of the reflecting borders in the time domain. At present this approach has got complete experimental verification and software for its practical implementation is being developed.

The GAP method is implemented with modern hardware and software backing, based on National Instruments' products.

2. FIELD PROCEDURES

GAP surveys are carried out along profiles with 1 to 20 m spacing between measuring stations depending on clients' requirements and local geology. The major considerations when planning the location and spacing of the stations are the size and depth of target geological features.

Subject to the spacing and ground conditions, a 2-person field team makes a few hundred measurements per day. Very portable field equipment (~6 kg including 12V batteries) makes it possible to use GAP in remote areas without expensive ground clearing and gridding. Profile and station positioning may be arranged using some standard portable GPS equipment.

Basic calibration for the area specific geology may be carried out in the field based on available geological and other data to better interpret variations in acoustic properties.

In Papp, É. (Editor), 2002, *Geophysical and Remote Sensing Methods for Regolith Exploration* CRCLEME Open File Report 144, pp 90-94.

Field quality control includes two steps:

1. evaluation of acoustic noise and spectral patterns at each station; and,

2. preliminary processing and visualisation in a field camp using laptop computers. The preliminary visualisation is available for inspection a few hours after finishing field measurements.

3. DATA PROCESSING AND INTERPRETATION

GAP profiles are presented as raster images compiled by the correlation of processed discreet records into continuous cross-sections. The cross-sections show variations in acoustic properties and may be calibrated for real depths and interpreted on the basis of available drilling data or other geological and hydro-geological information for example.

Certain processing and interpretation algorithms have already been developed for some typical geological situations and target features, eg. for diatreme structures. Such algorithms make it possible to successfully use GAP in grass-roots exploration with very limited geological information on a survey area.

4. APPLICATIONS

The technique has already been successfully used in primary and alluvial diamond exploration in Russia, Ukraine, Africa and Australia, as well as on a number of environmental and geotechnical projects, including for example, radioactive waste control and geohazard studies.

The GAP depth range is from less than 1 m to approximately 300 m. Resolution depends on surface conditions and geology, and may be adjusted for different depths using available acoustic sensors and various recording time/frequencies. The adjustment allows an indication of the general thickness of regolith and deep bedrock relief features (Figure 1) as well as internal regolith irregularities (Figure 2).

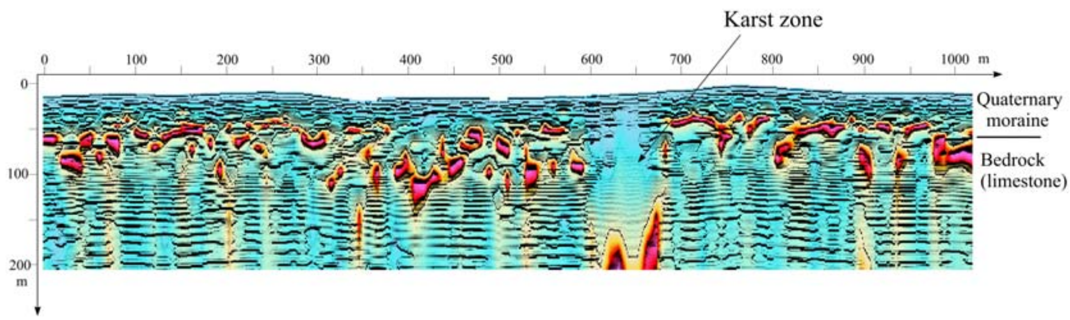

Figure 1. Regolith thickness and bedrock relief: geotechnical regolith study along the Moscow - St. Petersburg Highway 1997.

GAP may be used as a cost-effective alternative/support to traditional geophysical techniques and drilling in mining and exploration projects, in particular for the delineation of discovered geological bodies and search for their extensions, in testing magnetic/EM anomalies and palaeochannel exploration. There are also obvious GAP applications in geotechnical regolith studies (Figures 1 and 2).

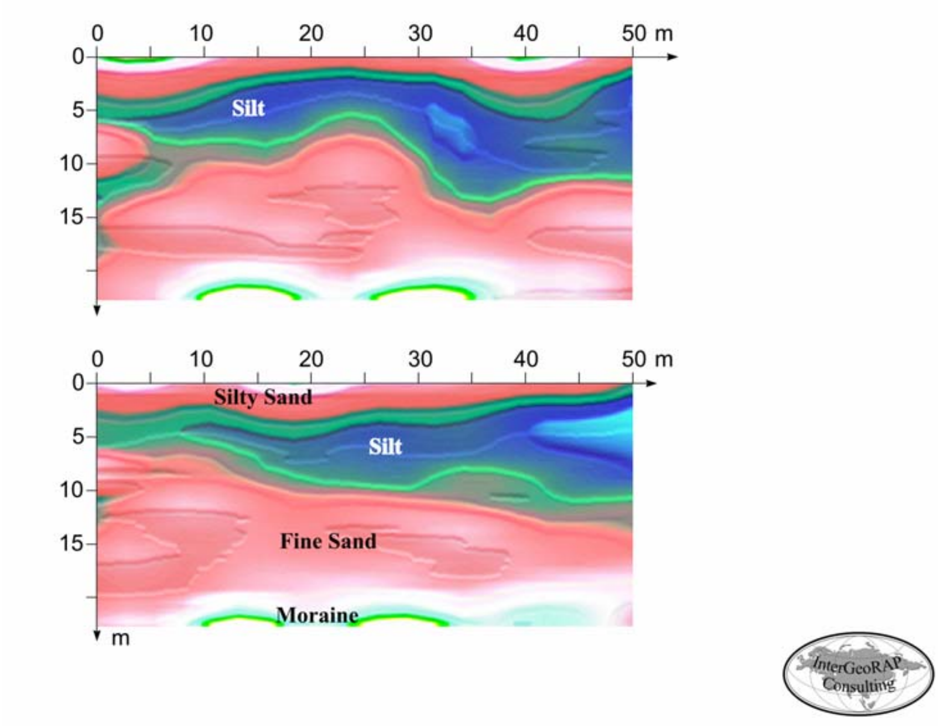

Figure 2. Regolith structure. Geotechnical regolith study at a construction site, St. Petersburg 1999.

GAP may be used in areas where conventional EM techniques and Ground Penetrating Radar fail to provide reliable results due to soil salinity and unfavourable hydrogeological conditions. Good resistance to interference makes it possible to use GAP in urban environments.

Extensive GAP trials were carried out in Australia in November-December 1999. The trials were hosted by the Cooperative Research Centre for Landscape Evolution and Mineral Exploration (CRC LEME) and sponsored by Geoscience Australia and 7 major mining and exploration companies; Anaconda Nickel; Ashton Mining; Astro Mining; Great Central Mines; PacMin Mining; Placer (Granny Smith) and WMC. The technique was tested at a few regolith projects (palaeochannels, alluvial terraces, laterites and deep weathering profiles) as well as on bedrock geology (gold, diamonds) and geotechnical projects.

Following the trials, InterGeoRAP started commercial surveys in Australia in 2000. At this stage the completed commercial surveys include primary and alluvial diamond exploration, gold exploration projects and a hydro-geological study. Further geotechnical studies were carried out on laterite profiles (Figure 3).

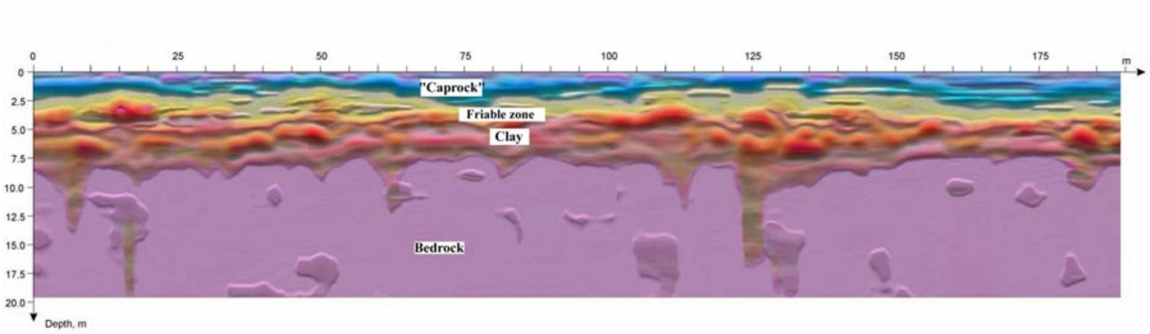

Figure 3. Example of GAP laterite geotechnical studies.

5. PROBLEMS, LIMITATIONS

GAP provides good resolution down to approximately 300 m depth. At this stage GAP involves mechanical sources of acoustic signals (eg. geopick, sledge hammer) and therefore depends on the surface conditions. Accumulating and averaging of measurements as well as additional filtering are necessary for surveys over a loose sandy or soft wet ground and heavily disturbed areas (eg. dumps, pits, rehabilitated areas) as well as over areas close to sources of acoustic disturbances. A non-mechanical source of signals is supposed to help to overcome these limitations at the next stage of the development of the technique.

6. SURVEY ORGANISATIONS

The GAP technique has been developed up to the stage of industrial applications by an independent geophysical consulting firm, InterGeoRAP Consulting, established in 1996 in St. Petersburg, Russia. The firm employs a group of geophysicists and software specialists, formerly involved in major Russian mining and exploration companies. InterGeoRAP has been developing the new ground acoustic technique and implements innovative approaches and software for the processing and interpretation of ground and airborne magnetic data. It also specialises in ground and airborne radiometrics, EM and gravity surveys.

At this stage InterGeoRAP does not sell or rent out its proprietary GAP equipment. The firm carries out field surveys and consulting assignments in Russia and internationally.

Additional information on the firm and some examples of GAP applications are presented at InterGeoRAP's web site: http://www.iinet.net.au/~tchern

Any inquires about InterGeoRAP may be addressed to firm's overseas agent in Australia:
Dr Boris Matveev
8 Hartleap Lane, Beldon, WA 6027.
Tel: (+61 8) 9307 6607
E-mail: bmatveev@iinet.net.au

7. COSTS

The GAP survey costs depend on the station spacing and ground conditions and are in the order of a few hundred dollars/ line kilometre. The survey costs include both fieldwork and interpretation/reporting.

REFERENCES

Aki, K. and Richards, P.G., 1980. Quantitative seismology. Theory and methods. W.H. Freeman and Co. San Francisco. Vol. 1 and 2 880 pp.

Bath, M., 1974. Spectral analysis in geophysics. Elsevier Scientific Publishing Company, Amsterdam 387 pp.

Brekhovskikh, L.M. and Godin, O.A., 1989. Acoustics of stratified media. (In Russian). Nauka Publishers, Moscow 416 pp.

Houdzinsky, L.L., 1962. On determining some spectral characteristics of stratified media. (In Russian). Proceedings of the USSR Academy of Sciences. Geophysics Series 3: 281-297.

SEISMIC SURVEYS FOR IMAGING THE REGOLITH

Barry Drummond

Geoscience Australia. PO Box 378, Canberra, ACT 2601. E-mail: barry.drummond@ga.gov.au

1. INTRODUCTION

Seismic reflection and refraction imaging are geophysical methods widely used for investigating the structure of the Earth's crust. They are used, particularly, in sedimentary basins for finding geological structures where oil and gas might be accumulated. Both reflection and refraction imaging are techniques that can be scaled to the structure of interest, and are therefore useful for imaging the regolith.

Seismic energy generated as shock waves at the surface of the Earth travel outwards in all directions through the layers below the surface (Figure 1).

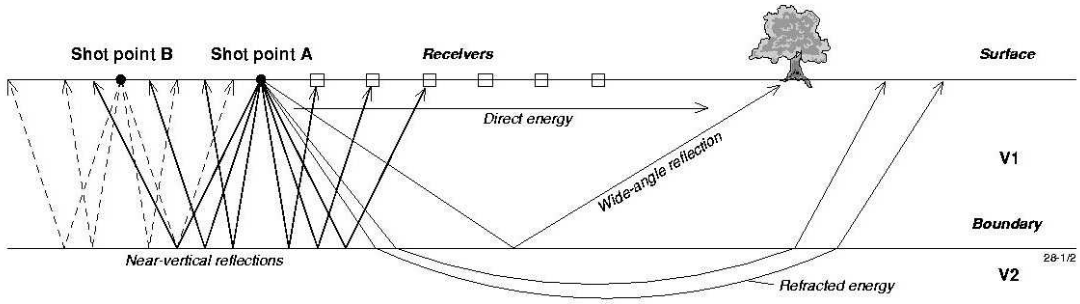

Figure 1. The seismic energy travels along several paths at and below the surface.

Any energy returning to the surface is detected as minute ground vibrations by geophones, which are similar to sensitive microphones. The geophones are connected by lightweight cables or by radio to a recording system. The time between the generation of the shock waves at the surface and their arrival at the geophones is measured and used to create images of the subsurface.

The principles of seismic reflection and refraction are shown in Figure 1. Figure 2 is a seismogram showing both reflected and refracted energy. Each "wiggle" trace shows the energy recorded at a geophone. The energy source, or shotpoint[1], was mid-way along the line of geophones.

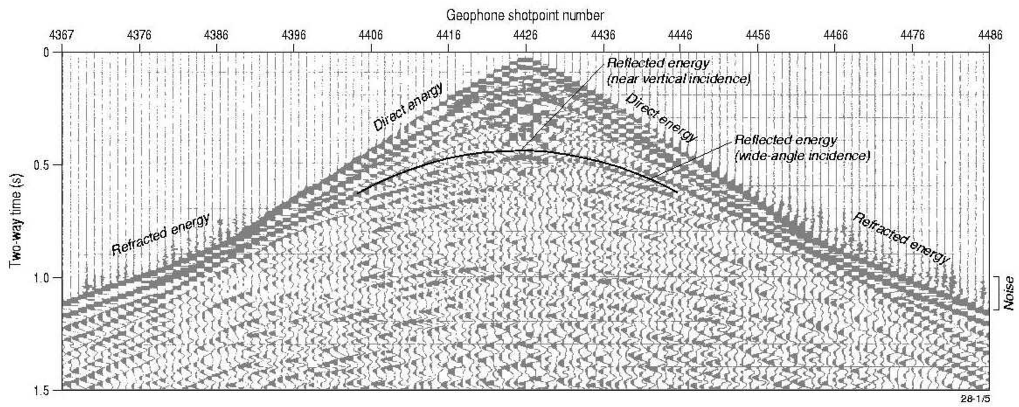

Figure 2. A seismogram showing both reflected and refracted energy.

[1] The term "shotpoint" is traditionally used for the point where seismic energy is generated. Early seismic surveys used explosive sources, hence the name. In recent times, mechanical sources such as ground vibrators and weight drops have been used.

In Papp, É. (Editor), 2002, *Geophysical and Remote Sensing Methods for Regolith Exploration*, CRCLEME Open File Report 144, pp 95-99

The propagation of energy from a shotpoint is best described in terms of the distance of the geophones from the shotpoint. The first energy recorded by geophones close to the shotpoint will be energy travelling directly through the near surface rocks. It will be followed by reflections from boundaries directly underneath the shotpoint. These energy phases have a distinctive appearance in seismograms (Figure 2). On the left hand side of Figure 1, which has two layers, energy from shotpoints A and B is shown reflected back to the surface at near vertical incidence to the boundary between two layers. This is the energy used for reflection profiling.

Other energy from shotpoint A (Figure 1) is shown reflected back to the surface at wider angles of incidence. Refracted energy, which has passed through the boundary into the deeper layer, propagates to greater distances before returning back to the surface at the right hand end of the diagram. Wide angle reflected and refracted energy are used in refraction profiling. These energy phases are shown in Figure 2. Note that the direct energy is the first phase recorded for most of the geophones both to the right and left of the shotpoint, but at greater distances the refracted energy is recorded first. Although it has a longer travel path than the direct energy because it has to reach and penetrate the deeper boundary before it travels sub-horizontally, it travels faster in the deeper layer, and eventually overtakes the shallower direct energy. In the seismogram, wide angle reflections join the near vertical reflections to the refracted energy.

2. REFLECTION PROFILING

Seismic reflection surveys are used where the primary information required is the geometry of interfaces in the regolith and the underlying basement.

For seismic surveys that study the regolith, the seismic energy can be produced by a variety of means. Mechanical sources are preferred because of their low environmental impact. These include vibrator trucks, which vibrate a heavy mass on the surface of the ground (Figure 3), hammers used to thump the ground, and accelerated weight drop tools which use hydraulic rams or heavy springs to accelerate weights downwards onto the ground. Explosive sources can also be used. They include explosive charges down drill holes and shotguns that fire vertically at the ground.

Figure 3. The truck on the right has a large pad mounted at the back. It is lowered to the ground, and the weight of the truck used to hold the pad firmly on the ground. Hydraulic rams are then used to send vibrations through the pad. Because the pad cannot move up and down, the vibrations are transmitted into the ground. The instruments used to record the reflected energy are in the back of the vehicle on the left.

In reflection surveys of the regolith, up to 48 geophones[2] might be arrayed at 1–2 m intervals either side of the shotpoint. Once the energy is recorded, the shotpoint is moved further along the line and the process repeated. This is done in such a way that at least some of the energy from one blast is reflected off the same part of boundaries at depth as the energy from the blasts either side. In a typical survey using, say, 96 geophones, each point in the subsurface would be sampled 12, 24 or 48 times. This is called multi-fold recording using the Common Mid Point Method, and is done to allow higher fidelity images of the subsurface to be created in the data processing centre after the field survey. Very few seismic surveys produce a final image of the subsurface in the field in real time. Most require extensive post-field processing using specialist software.

In seismic reflection surveys, the structure of subsurface geological formations is mapped by the variation in the time taken for the reflected shock waves to return to the surface. The information is usually displayed as continuous reflection-time cross-sections, which are really pictures of the geological structure at depth. Figure 4 gives an example (Courtesy of Christopher Leslie, CRC LEME). It shows the geometry of transported material and a basement high to the right. The time for the seismic energy to travel to the reflectors and back (two-way time) is shown as a linear scale on the left. Two-way time can be converted to depths using estimates of seismic velocities generated during the data processing stage. Depths are shown on the right. Note that a linear two-way time scale does not convert to a linear depth scale.

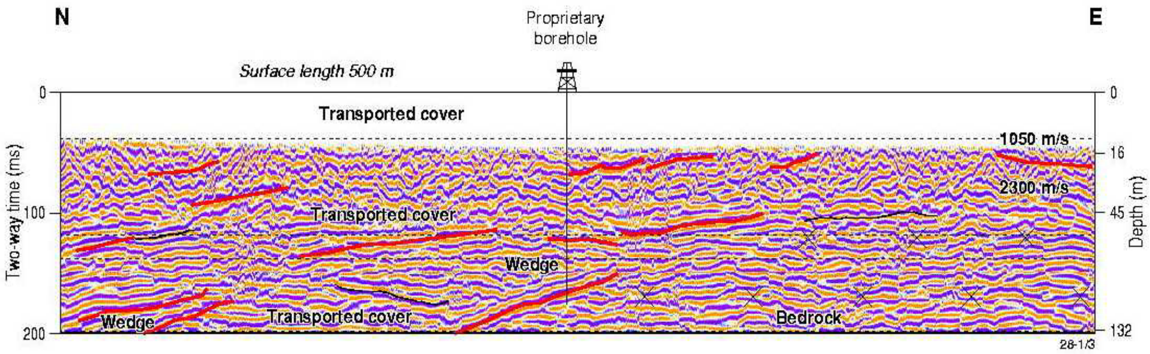

Figure 4. An example of continuous reflection-time cross section, picturing geological structure at depth (Courtesy of Christopher Leslie, CRCLEME).

The most used information in sections like this is the structural information. The amplitude, frequency, phase, and other characteristics of the reflected waves can also provide information on the likely physical characteristics of the boundaries. For example, stronger reflections come from boundaries where the seismic impedance contrast[3] is high compared to boundaries where the impedance contrast is low. Reflections from a boundary where the impedance increases from the upper layer to the lower layer will have the same phase as the energy source, whereas those from boundaries where the deeper layer has a lower impedance will have the opposite phase to the energy source.

[2] The optimum number of geophones depends on the problem to be solved. However, the number of channels and how far they are arrayed each side of the shotpoint can also be limited by the depths of the surfaces to be imaged. Practical limitations of field deployments can limit the number of channels for regolith work to around 48. The type of recording system can also limit the number of channels. Instruments that send analog signals from the geophones to the recording system are limited by the practical number of wires that can be built into the cables; they usually have 24, 48 or 96 channels although larger numbers are possible. Systems that use digital telemetry between the geophones and the recording system can effectively have unlimited numbers of channels.

[3] Seismic impedance is the product of the density of a rock and the velocity at which seismic waves travel in the rock. Impedance contrast is the contrast in the seismic impedances of the rocks on either side of a boundary.

3. REFRACTION SURVEYS

Seismic refraction surveys are used when variations in the composition of the regolith or the underlying basement are the targets, and not the detailed geometry of interfaces. This is because seismic refraction profiling provides a robust image of the variation in the velocity at which seismic waves travel through rocks. Seismic velocity is often an indicator of composition. However, refraction surveys usually provide a less detailed geometrical image than reflection profiling.

The primary data used for refraction interpretation are the direct and refracted phases and often the wide angle reflections. The data are generated using field practices similar to reflection profiling, with the exception that the length of the array of geophones is typically at least 5 times the depth to the target layer. Figure 2 illustrates how non-intuitive these data can be when viewed for the purpose of generating subsurface models. Typically the data have to be forward or inverse modelled. Figure 5 shows one form of output from an inversion (Courtesy of GA). The lower part shows the thickness of regolith along a 120 km profile from the Broken Hill Block into the Murray Basin. It has considerable vertical exaggeration. It was derived from 30,000 traces similar to those in Figure 2 (Figure 2 is from the right hand end of the profile shown on Figure 5).

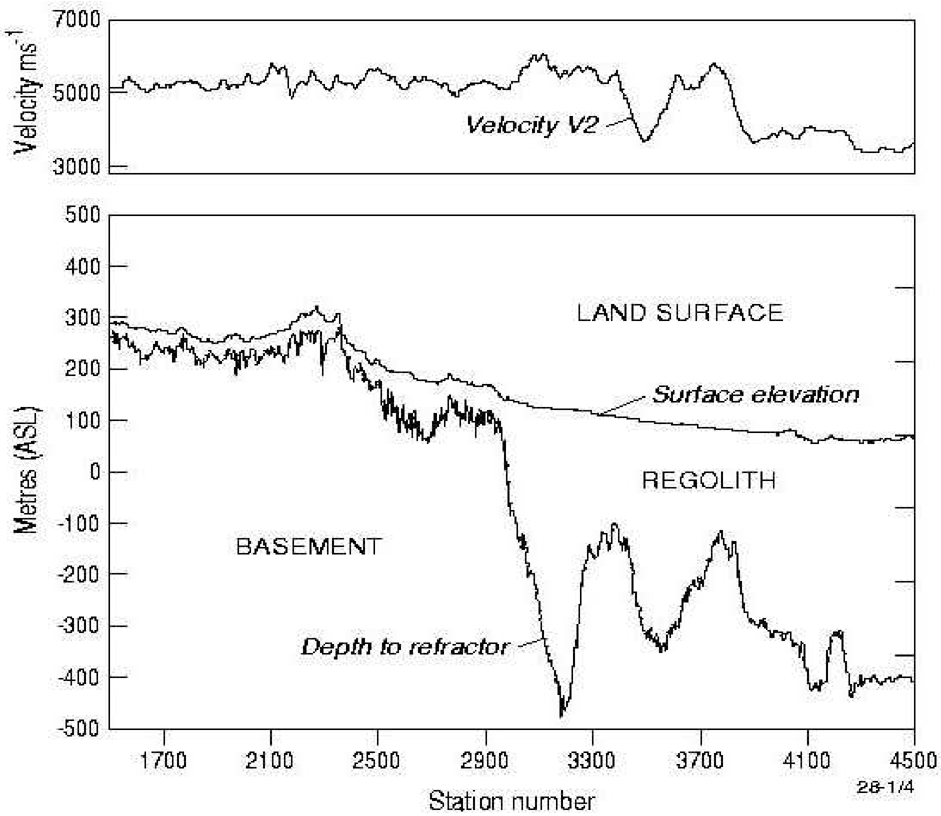

Figure 5. Results of a seismic inversion (Courtesy of GA). The lower part shows the thickness of regolith along a 120 km profile from the Broken Hill Block into the Murray Basin. The section has a considerable vertical exaggeration.

The style of presentation depends on the purpose for which the study was undertaken. In this example, the top of the basement is highlighted. The lower part of the figure shows the regolith thickening because of the transported material of the Murray Basin, to the right of Station 2900. The graph at the top shows the velocity at which seismic energy travels in basement. It shows velocities near 5000 ms^{-1}

on the left, typical of Proterozoic metamorphic rocks in the region. East of about station 2900, the velocities are higher, and are probably basement consisting of rocks of the Delamerian Orogenic Belt. A sharp drop in velocities between stations 3300 and 3700 corresponds to a small ?Mesozoic basin underlying the Murray Basin, and the steady drop to the right of station 3900 correlates with the Palaeozoic Darling Basin.

Just as this example was used to extract information on the nature of the basement, seismic refraction profiling could be used at higher resolution to determine variations in the seismic velocities within the regolith, and thereby map indirectly variations in regolith density.

4. OPPORTUNITIES AND LIMITATIONS

Seismic techniques are extremely flexible, and in their reflection or refraction forms can usually be adapted to image most kinds of features in and below the regolith. The cross section in Figure 4 is an example; palaeochannels would be another.

Seismic techniques are limited in their resolution by the wavelengths of seismic signals that are generated at the surface, passed through the regolith and returned to the surface. This is usually determined by the regolith, because although seismic sources are available to generate most frequencies, the regolith can severely attenuate high frequency signals, which have the greatest resolving power. It is not possible to calculate a nomogram that demonstrates the resolution of seismic techniques for a particular region without specific details of the depths of the surface to be imaged and the velocities at which seismic waves travel in the region. Any field survey should therefore undertake a range of tests at the beginning to ascertain the seismic frequencies generated, the frequencies recorded by the geophones, and therefore whether the survey will provide suitable resolution.

5. COSTS

The cost of seismic imaging varies considerably, depending on the nature and size of the target, the amount of resolution required, and the logistics of working in the area concerned. Data processing costs should also be considered. A seismic survey crew can have as few as 3-4 people or as many as 30. People who wish to use seismic imaging techniques should clearly define their target in geological terms, and then seek professional guidance from a qualified geophysicist.

6. MORE INFORMATION

Please contact:
Dr Barry Drummond
Director
Australian National Seismic Imaging Resource
c/- Geoscience Australia
GPO Box 378
Canberra ACT 2601.
E-mail: Barry.Drummond@ga.gov.au
Telephone +61 2 6249 9381
Facsimile +61 2 6249 9972

GRAVITY

Raymond M. Tracey and Nicholas G. Direen

Geoscience Australia. PO Box 378, Canberra, ACT 2601. E-mail: ray.tracey@ga.gov.au, nick.direen@ga.gov.au

1. DESCRIPTION

Gravity surveys measure variations in the gravitational attraction of the earth. These minute changes are caused by local variations in the densities of rocks near the surface (Telford, et al., 1990), as well as a variety of known factors. These factors include the latitude and elevation of the observation point, topography of the surrounding terrain and the tidal effect of the sun and the moon. Corrections can be made for known causes of the variations and the anomalies that remain provide the information about the changes in density that are of interest to explorers (Telford, et al., 1990).

These anomalies in the earth's gravitational field can in some cases be used to define the thickness and extent of the regolith, due to the strong contrast in density between the regolith (including *in situ* weathered bedrock) and fresh bedrock, and in defining regolith features such as palaeochannels. Further contrasts may occur between regolith materials that are developed *in situ* versus those that have been transported, due to the expected increase of porosity in the latter.

Berkman (1995) quotes examples of typical bulk densities for a variety of transported materials including alluvium, gravels (≈ colluvium), loess (≈ parna), sand, mixed sand and clay, and soils; values range from 1.00 to 2.20 t/m^3.

Clays, which represent several types of regolith materials, have a range of 1.63 to 2.60 t/m^3 (Berkman, 1995), which is considerably higher than many other types of transported regolith. Silcrete has a density of 2.45 to 2.60 t/m^3 (Direen, 1999), whereas bauxite is in the range of 2.30 to 2.55 t/m^3. The two main types of ferricretes ("laterites") are pisolitic, and massive-ferruginous (Ollier and Pain, 1996, Butt, 1990). These types correspond to two reported densities for these materials: 1.00 to 2.60 t/m^3 for the poorly consolidated pisolitic ferricrete (Emerson, 1990, Butt, 1990), and densities up to 3.00 t/m^3 for the massive ferruginous variety (Butt, 1990).

No direct bulk density data are available for the other two widespread specific types of duricrusts- Regolith Carbonate Accumulations (RCA) and gypcrete- highlighting a need for further petrophysical research to be undertaken on these materials. The upper limit on densities of these types of regolith is provided by assuming a composition of 100% of the constituent mineral phases, calcite and gypsum, which have grain densities averaging 2.70 t/m^3 and 2.35 t/m^3 respectively. Mann and Horwitz (1979) showed variable compositions for RCA in Western Australia, containing gypsum, dolomite, calcite and quartz in variable abundances. They likened the composition of RCA to limestone, implying densities of 1.74-2.76 t/m^3 (after Berkman, 1995). P-wave velocities of > 5 500 m/s for RCA (quoted by Hawkins & Whitely, 1979) are consistent with densities of 2.65 t/m^3 using empirical conversion methods (eg. Direen, 1999).

A graphical summary of the bulk density data is provided in Figures 1a and 1b. The averaged properties (Figure 1b), taking into account both the dry density minima likely to occur in regolith above the water table, as well as the higher bulk wet values, show a strong difference between transported and residual regolith varieties. The transported varieties have lower average densities of 1.67 to 1.95 t/m^3, whereas average residual regolith densities vary between 2.35 and 2.80 t/m^3.

In Papp, É. (Editor), 2002, *Geophysical and Remote Sensing Methods for Regolith Exploration*, CRCLEME Open File Report 144, pp 100-104.

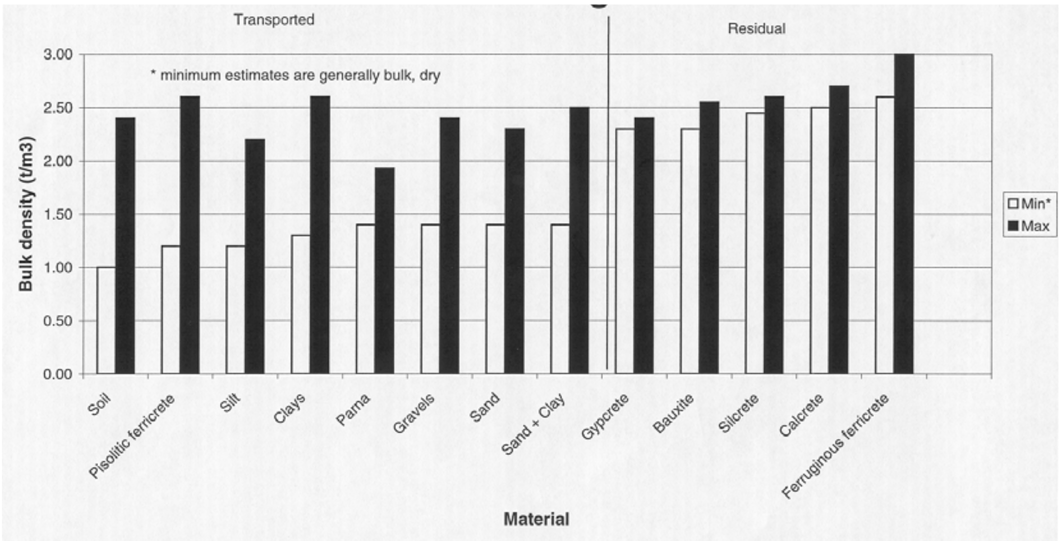

Figure 1a. Bulk density ranges for some common Australian regolith materials.

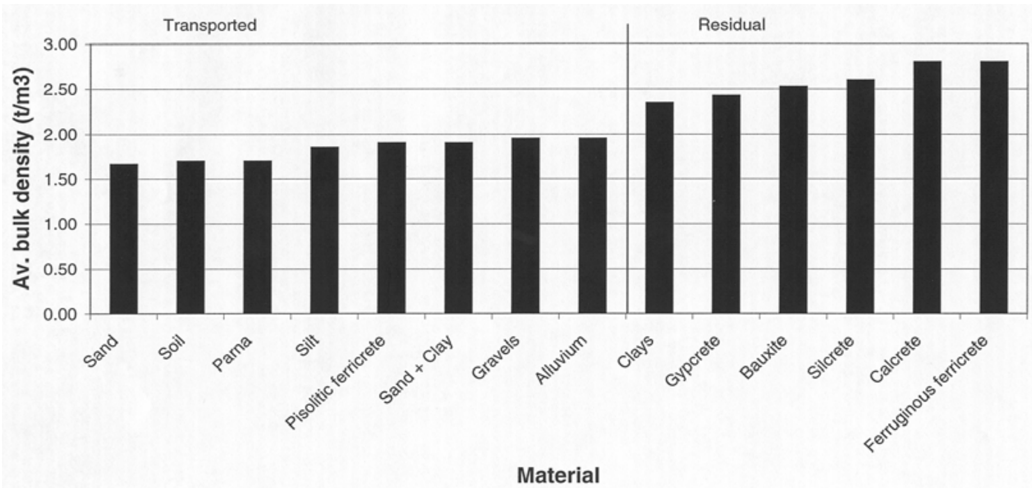

Figure 1b. Average bulk density ranges for some common Australian regolith materials.

2. FIELD PROCEDURES

The major consideration when planning a gravity survey is the location and spacing of the stations. The size, type, depth and density contrast of the feature being defined will determine if the survey is laid out as a grid, a traverse or a series of traverses. These factors will also determine the extent of the grid or traverse and the station spacing. For example, sampling theory dictates that station spacing should be no greater than half the expected width of any bodies being defined. In the case of a 100 m wide palaeochannel, the absolute maximum station spacing which could expect to define the position of the feature is 50 m; obviously, if more detail is required, a closer station spacing would be used.

Another consideration is the horizontal and vertical positional accuracy of the gravity stations. The vertical accuracy of the stations is most important because an error of $0.3 \mu m/s^2$ will be caused by each decimeter of error in the height estimate. This scale of error may be greater than the size of the anomaly of interest. To obtain this level of accuracy it is necessary to use optical (spirit level) surveying or precise differential GPS (Global Positioning System) techniques.

General field procedures for gravity surveys involve taking readings in loops where the first station is repeated after a few hours to quantify the drift of the gravimeter and allow for correction of this in post processing. These techniques are described in most geophysics texts such as Telford, et al. (1990).

3. DATA PROCESSING

The acceleration due to gravity depends on latitude, elevation, topography of the surrounding terrain, tides, and density variations in the subsurface (Telford, et al., 1990). Corrections are made during processing to remove the effects of latitude, changes in elevation and topographic effects. The effect of tides can be mathematically modelled and removed during processing, or they can be assumed to occur as a linear drift over a few hours and removed along with the instrumental drift as mentioned previously in the field procedures. The anomalies in the earth's measured gravity acceleration remaining after these corrections have been applied are due to density variations in the earth's crust and can provide information about the regolith. Further descriptions of the standard corrections and how they are applied can be obtained from texts such as Blakely (1996), Telford, et al. (1990).

4. DATA INTERPRETATION

Gravity anomalies remaining after appropriate corrections have been applied represent the superimposed effect of density changes at various depths. The smoothness or apparent wavelength of the anomaly is generally an indication of the depth of the source of the anomaly: the smoother the anomaly, the deeper the source. In regolith studies it is necessary to separate these longer wavelength anomalies from the sharper, shorter wavelength anomalies that are due to near surface sources. Telford, et al. (1990) describes methods to remove the longer wavelength deeper anomalies, known as the regional, leaving the shorter wavelength residual anomalies.

For a given gravity anomaly, an infinite number of density distributions can be found to produce the same anomaly. Hence some knowledge of the geology of the area is necessary for a good interpretation of the data.

5. APPLICATIONS

The gravity method can be applied to many problems in regolith studies such as determining depth to bedrock or depth of weathering, defining palaeochannels and mapping sinkholes and collapse structures. Smyth and Barrett (1994) described how gravity can be used to define palaeochannels in the search for gold and uranium in the Yilgarn Block of Western Australia. They concluded that gravity, followed by EM soundings and drilling, proved to be a cost-effective exploration approach.

Qureshi (1979) used a detailed gravity survey of the Woy Woy district in NSW to determine the thickness of young unconsolidated sediments overlying bedrock. This study showed the applicability of the gravity method in a built-up area where many other geophysical methods cannot be applied.

Figure 2 shows how a gravity profile measured along a seismic line in the Broken Hill region of NSW has been modelled to estimate the thickness of the weathered zone. The broken line joining the square symbols in the top half of Figure 2 is the observed gravity profile. The solid line is the profile calculated from the model in the bottom half of Figure 2. The model can be derived from whatever information may be available such as surface mapping, drill hole data, seismic data or other geophysical information. In this example seismic refraction and drilling data were used to constrain the model. The observed gravity low is interpreted to be due to a zone of weathered material that has a lesser density than that of the fresh bedrock.

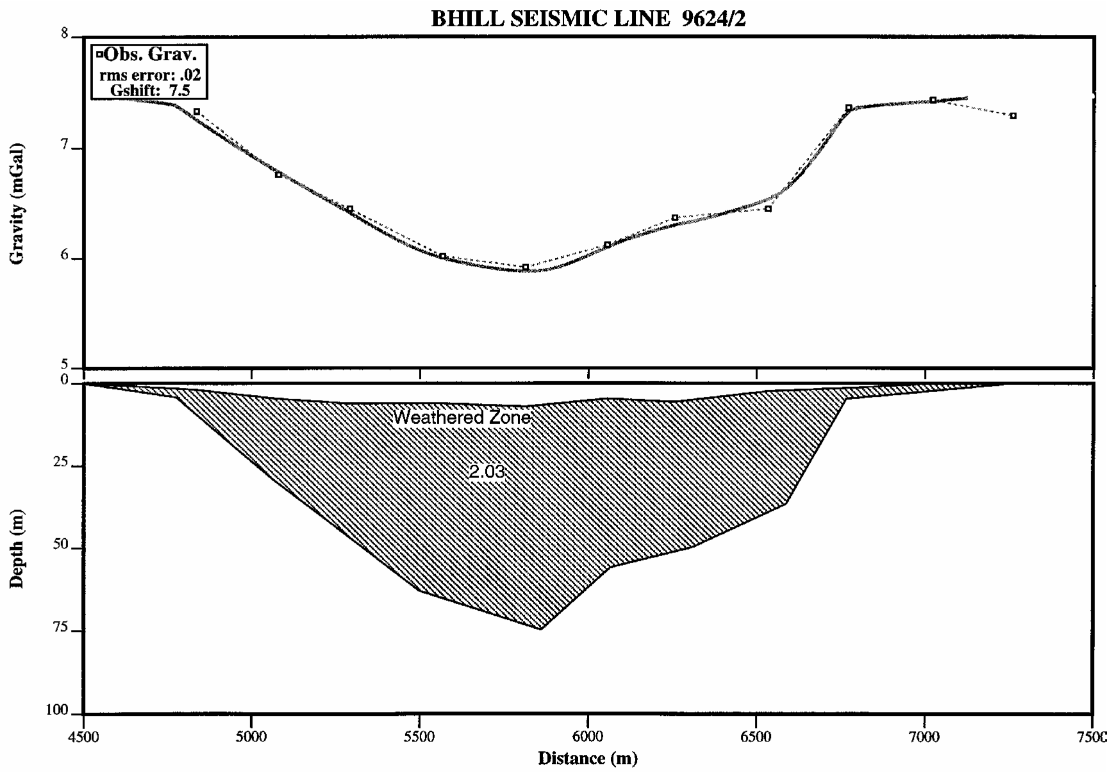

Figure 2. Gravity profile and 2D model of a palaeochannel filled with alluvium of density 2.03 t/m^3 showing the depth to fresh bedrock of density 2.67 t/m^3. This example is from GA seismic line 9624/2 south of Broken Hill, described by Gibson, et al. (1997) and Foster and Shirtliff (1998).

6. PROBLEMS, LIMITATIONS

Many geological conditions can complicate the gravity response (Smyth and Barrett, 1994). These can include insufficient density contrast between bedrock and the regolith, local variations in bedrock density and high regional gravity gradients. In addition, poor field technique and data reduction methods can introduce errors that may obscure many geological features of interest.

7. SURVEY ORGANISATIONS

Many geophysical contracting companies provide gravity surveying services. With the advent of GPS surveying, a number of geodetic survey companies have also specialised in gravity surveying.

Geoscience Australia (GA) maintains the reference standards for gravimetry in Australia through the Australian Fundamental Gravity Network. This is a network of about 800 gravity observations at about 250 locations throughout Australia. These observations are the reference values used as control for exploration surveys and engineering standards. GA also maintains the Australian National Gravity Database of gravity surveys carried out in and around Australia. Information on gravimetry in Australia can be obtained from GA's website at http://www.ga.gov.au.

8. COSTS

Prior to the introduction of GPS technology, it was necessary to use optical surveying techniques to obtain the height accuracy necessary for detailed gravity surveys. This was costly and time consuming. GPS surveying has greatly reduced the cost of detailed gravity surveys in many cases by allowing one observer to obtain a gravity measurement and an accurate position and height at the same time.

Current costs (as of April 2002) for gravity surveys range from $10/station for surveys with station spacing in the order of tens of metres to $100/station for surveys with station spacing in the order of a number of kilometres and where helicopter transport is involved.

REFERENCES

Berkman, D. A., 1995. 9.2 Gravity survey methods and tables. In: D. A., Berkman (Editor), Field geologists manual. 3rd edition. Australian Institute of Mining and Metallurgy Monograph 9: 324.

Blakely, R. J., 1996. Potential theory in gravity and magnetic applications. Cambridge University Press, Cambridge, 439 pp.

Butt, C. R. M., 1990. The nature and origin of the lateritic weathering mantle, with particular reference to Western Australia. In: H. A., Doyle, J. E., Glover and D. I., Groves (Editors), Geophysical prospecting in deeply weathered terrains. Publications of the Geology Department & Extension Service, University of Western Australia 6: 11-24.

Direen, N. G., 1999. Geology & geophysics of the Koonenberry Belt, far western New South Wales, and eastern Australian correlates. PhD thesis (Unpublished), University of Tasmania, 303 pp.

Emerson, D. W., 1990. Notes on mass properties of rocks- density, porosity and permeability. Exploration Geophysics 21: 209-216.

Foster, K. & Shirtliff, G., 1998. Correlation and distribution of regolith materials and landforms in the Balaclava area, Broken Hill. In: G. M., Gibson (Editor), Broken Hill Exploration Initiative: Abstracts from 1998 Annual Meeting. AGSO Record 1998/25: 36.

Gibson, G. M., Maidment, D., Peljo, M., Gibson, D., Owen, A., Fomin, T., Drummond, B. and Wake-Dyster, K., 1997. Broken Hill Exploration Initiative: A transect of the Broken Hill Inlier Workshop Notes. Broken Hill, 29 May, 1997, pp. 39-43.

Hawkins, L.V. and Whiteley, R.J., 1979. Estimation of rippability and excavation conditions in calcrete deposits with seismic refraction methods. Bulletin of the Australian Society of Exploration Geophysicists 10(3): 223-224.

Mann, A.W. and Horwitz, R.C., 1979. Groundwater calcrete deposits in Australia: some observations from Western Australia. Journal of the Geological Society of Australia 26: 293-303.

Ollier, C.D. and Pain, C.F., 1996. Regolith, Soils and Landforms. John Wiley & Sons Ltd, Chichester, 316 pp.

Qureshi, I.R., 1979. A gravity survey of Woy Woy district and its local and regional significance, Bulletin of the Australian Society of Exploration Geophysicists 10(3): 198-199.

Smyth, E.L. and Barrett, D.M., 1994. Geophysical characteristics of the tertiary palaeochannels in the Yilgarn Block, Western Australia. Geophysical Signatures of Western Australian Mineral Deposits. Geology and Geophysics Department (Key Centre) & UWA Extension, The University of Western Australia, Publication 26: 417-425.

Telford, W.M., Geldhart, L.P. and Sheriff, R.E., 1990. Applied Geophysics. 2nd edition. Cambridge University Press, Cambridge, 770 pp.

GEOPHYSICAL WELL LOGGING

Prame Chopra[1], Éva Papp[2] and David Gibson[3]

[1] Department of Geology, Australian National University, Canberra, ACT 0200. E-mail: prame.chopra@geology.edu.au

[2] Cooperative Research Centre for Landscape Environments and Mineral Exploration. Department of Geology, Australian National University Canberra, ACT 0200. E-mail: eva.papp@geology.anu.edu.au

[3] Cooperative Research Centre for Landscape Environments and Mineral Exploration, Geoscience Australia. PO Box 378, Canberra, ACT 2601. E-mail: dave.gibson@ga.gov.au

1. DESCRIPTION AND HISTORY

Logging is a general term which means to "make a record" of something. Geoscientists use many types of "logging" including core-logging, cuttings-logging, petrophysical logging and geophysical well logging.

Geophysical well logging was first developed for the petroleum industry by Marcel and Conrad Schlumberger in 1927 (Figure 1).

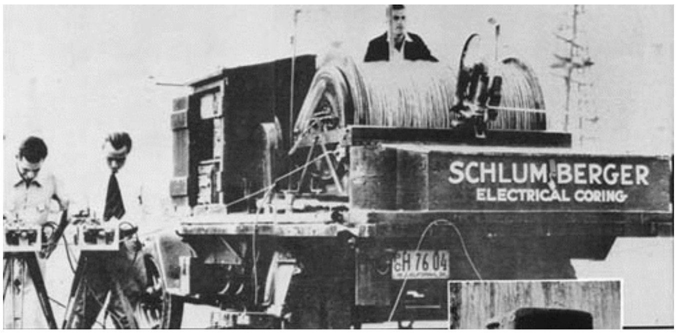

Figure 1. The original geophysical logging equipment used by the Schlumberger brothers in the late 1920's (Schlumberger, 2000).

The Schlumberger brothers developed a resistivity tool to detect differences in the porosity of the sandstones of the oilfield at Merkwiller-Pechelbronn, in eastern France. Part of the Schlumberger brother's original log is shown in Figure 2.

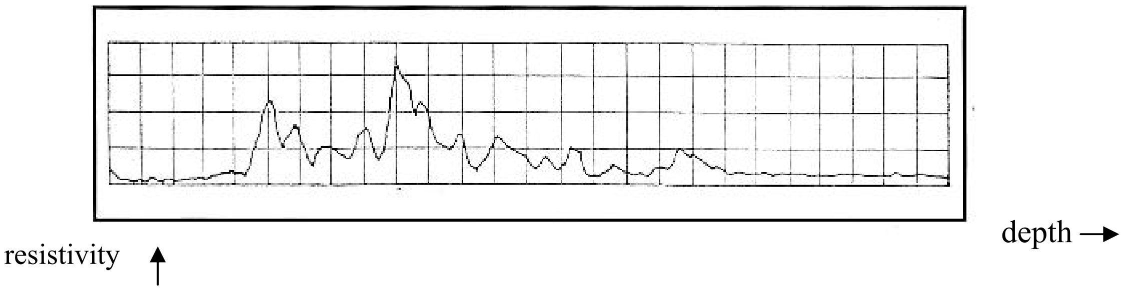

Figure 2. Part of the first geophysical log obtained by the Schlumberger brothers in 1927.

Since this first log was run, geophysical well logging has developed into a billion-dollar global industry serving a wide range of industry and research activities. Geophysical well logging is a key technology in the petroleum industry. In the mineral industry, it is very widely used both for

In Papp, É. (Editor), 2002, *Geophysical and Remote Sensing Methods for Regolith Exploration*, CRCLEME Open File Report 144, pp 105-115.

exploration activities and for monitoring grade control in working mines. In groundwater exploration and assessment it is also central to the delineation of aquifers and producing zones. In regolith studies, geophysical well logging can provide unique insights into the composition, structure and variability of the subsurface, and is also widely used for ground truthing airborne geophysical data sets, such as airborne electromagnetics.

Geophysical well logging is a mature technology comprising many separate systems. It is well beyond scope of a short article like this to detail the science and the results of the many facets of geophysical well logging. What is intended here is just a short description of some of the more routine well logging methods. These methods are the ones most likely to be included in the suite of tools used for small well logging projects typical for regolith studies.

In geophysical well logging, many different physical properties can be used together to characterise the geology surrounding a borehole. This ability to sense various properties is the greatest strength of geophysical well logging. The different types of information obtained reflect on different aspects of the geology and are often complementary in nature. Thus the porous gravel bed of a palaeochannel, containing detrital maghemite, might have low density, low sonic velocity and natural gamma signal but high magnetic susceptibility and porosity.

2. WHY DO GEOPHYSICAL WELL LOGGING?

Knowledge of the subsurface comes primarily from drilling. This is at once an expensive technique and a limited one. Drilling costs invariably limit the number of holes that can be drilled.

Geophysical well logging offers the opportunity of determining the composition, variability and physical properties of the rocks around the borehole. The actual volume of material sampled in this way varies from technique to technique and with the geological conditions, but it is invariably much larger than is represented by just the borehole. Moreover, depth control with a modern geophysical logging system is often better than a few millimetres. This means that the depth resolution of borehole data, representing the subsurface structure, is generally better than can be obtained even with diamond coring, where core breakage and core loss can be a serious problem, especially in regolith.
Modern geophysical logging systems can be easily deployed from 4WD vehicles, using digital, computerised, small systems, such as the one shown in Figure 3.

Figure 3. Regolith logging with a small, easy-to-use geophysical logging system, mounted in a 4WD vehicle.

3. THE BOREHOLE ENVIRONMENT

The very act of drilling a borehole can perturb the physical properties of the rocks that have been drilled. Fluids and drilling additives can invade the surrounding formations changing resistivities, densities and electric potentials. Drill cuttings created by the drilling bit can plaster themselves over the walls of the hole as “mudcake” and can originate at quite different depths from where they are now found. For these reasons, drilling of regolith is often carried out using compressed air instead of drilling fluid to cool the drill bit and lift cuttings. While this minimises the introduction of drilling contaminants, it is still important to remember that the borehole environment will not always be strictly representative of the properties that you are trying to measure.

4. SOME SELECTED GEOPHYSICAL WELL LOGGING METHODS

Mechanical Methods

Caliper Logging

1. A caliper tool is used to measure the diameter of a borehole and how it changes with depth. It typically works by using one or more spring-loaded arms, which are pressed against the borehole wall as the tool is raised from the bottom of the borehole. Motion in and out from the borehole wall is recorded electrically and transmitted to surface recording equipment.

2. The simplest caliper tool uses just one arm to record diameter. More sophisticated tools may have four or more arms each independently measuring distance to the borehole wall. Multi-arm tools generally give better resolution of the borehole shape than a single arm tool.

Sonic Logging

Sonic tools work by transmitting a sound (ie. P waves) through the rocks of the borehole wall.

A basic sonic tool generally consists of two modules. One contains the transmitter and the other contains two or more receivers. The two parts separated by a rubber connector (Figure 4) to reduce the amount of direct transmission of acoustic energy along the tool from transmitter to receiver.

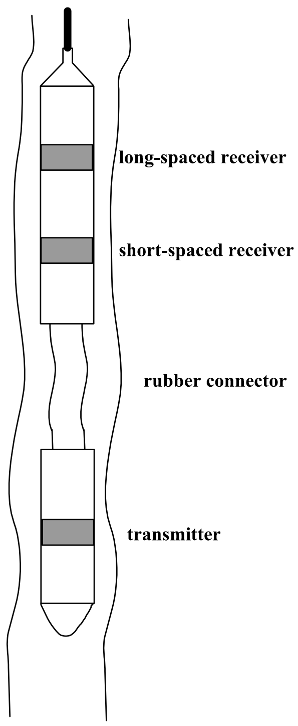

Figure 4. Schematic diagram of a sonic tool with the transmitter and two transceivers.

The transmitter injects a sinusoidal wave-train of acoustic energy into the formation. The detectors subsequently receive a complex signal, because of the multiplicity of ray paths that the wave-train can take through the formation. The fastest arrival (in uncased holes) will generally be through the rocks near the borehole wall.

Detection of this signal uses a signal processing algorithm involving cross-correlation between the original wave train generated by the transmitter and the coda received by the detectors.

In practice, sonic logging actually measures the "time of flight" along the fastest signal path. Because this time of flight is dependent on the density of the medium, it can be used to calculate the average density of the rocks through which the signal passed.

Sonic logging tools were initially developed for the petroleum industry as porosity measuring devices, and they have a similar use in regolith. In hard rock environments, where porosities are generally low, sonic logs can be very useful lithological probes.

A very important use of sonic logs is for the correcting of interval velocities used in seismic processing and interpretation. This leads to better velocity models for seismic processing and analysis. Sonic log data from shallow holes drilled in the regolith can also be particularly useful as inputs for *static corrections* in seismic processing. This can yield useful information about the depth of the regolith.

ELECTRICAL METHODS

Common electrical logs used in hard rock drilling include:

1. resistivity and conductivity;

2. spontaneous potential (SP), and,

3. induced polarisation (IP)

These methods are also used in regolith studies. In particular, conductivity logs are often used for ground-truthing airborne EM data, and resistivity and SP logs are recorded in some water bores.

The factors, which effect the electrical properties of rocks, are, in order of decreasing importance (Hallenburg, 1984):

1. porosity and water content;

2. water chemistry;

3. rock chemistry and mineralogy;

4. degree of rock alteration & mineralisation;

5. amount of evaporites;

6. amount of humic acids; and,

7. temperature.

Resistivity Logs

If a material containing unbound charged particles is subjected to a voltage difference then an electrical current will flow. The impedance to this flow is called the electrical resistance and it is a function of the geometry of the current flow and the intrinsic resistivity of the material. Some materials such as quartz and muscovite have high resistivities, while others have more moderate values (eg. sand) and for some the resistivity is low (eg. clay, saline groundwater).

The resistivity and conductivity of a material are inversely proportional quantities. The measurement is referred to as resistivity when measurements are made with a contact, or focused, resistivity probe by causing a current to flow in rocks. In these cases the resulting voltage drop is measured. (Keys, 1988)

Current flow in a porous clean sandstone (ie. shale-free) is mainly through the fluids within the pore spaces. Thus, in the absence of shale, the resistivity is mainly indicative of the characteristics of the pore spaces (for example pore volume, pore interconnectivity, pore fluid composition).

Pore space character tends to vary significantly from formation to formation. For this reason, resistivity logs are often useful tools for exploring stratigraphy and depositional history, and for the definition of different regolith units.

Simple "single point resistivity" logging typically uses a geometry like that shown in Figure 5. Note that resistivity logs only work if the downhole probe is below the water table. This can be a limitation for some shallow regolith studies unless water can be added to the borehole to artificially raise the level to the area of interest.

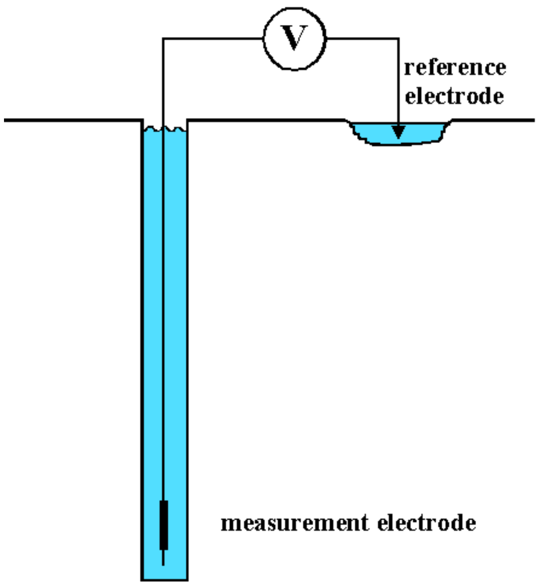

Figure 5. Schematic diagram of logging setup for resistivity and SP logging.

Single-point resistivity logging measures the resistivity between a single moving electrode downhole and an earth connection at the surface. Theoretical analysis and practical observation shows however that the bulk of the signal is in fact generated within a small volume surrounding the downhole electrode. Thus for a 5 cm diameter spherical electrode, 90% of the signal is generated within 50 cm of the electrode.

Electrical conductivity

The term conductivity generally is applied to measurements that are made with an induction probe, utilising principles of electromagnetic induction. These measurements can be made either in fluid-filled or dry holes.

Conductivity measurements are important for calibrating airborne EM data. Physical properties influencing conductivity are:

1. porosity and fracturing;
2. mineralogy;
3. alteration;
4. pore fluid % in pores;
5. salinity; and,
6. pore connectivity.

Knowledge of fluid conductivity and the borehole diameter enables application of corrections for borehole effects.

The accuracy of induction logging systems decreases for high resistivity rocks, often exhibiting a 50% error at 100 Ohm-meters and a 100% error at 200 Ohm-meter. Because of this characteristic, inductive conductivity logging is more often used in regolith than in fresh rock environment.

Self Potential (SP) Logs

SP logs use the same geometry as that shown in Figure 5 and for this reason they are normally run at the same time as resistivity logs, using a composite tool.

SP is one of the oldest applied logging methods and was developed by the Schlumberger company. SP logs measure small differences in potential (ie. voltage) between the downhole movable electrode and the surface earth connection. These potentials can arise from a wide range of electrochemical and electrokinetic processes. The SP method has been used in the oil industry for many purposes, but it is of a limited value in a fresh water environment. The factors that cause SP effects in a bore hole are extremely complex, not very well understood, consequently interpretation of SP logs in regolith can be a challenging exercise.

Electrochemical SP-s can for example arise from preferential diffusion and absorption of cations and anions on and through clays. Cations being much smaller than anions generally have a higher mobility through clays. Saline groundwater which is in contact with clay-rich materials often develop charge imbalances (ie. potentials) as a result of fluid flow. These potentials which are typically in the range of a few mV to a few tens of mV-s, can be measured in an SP log (Figure 6).

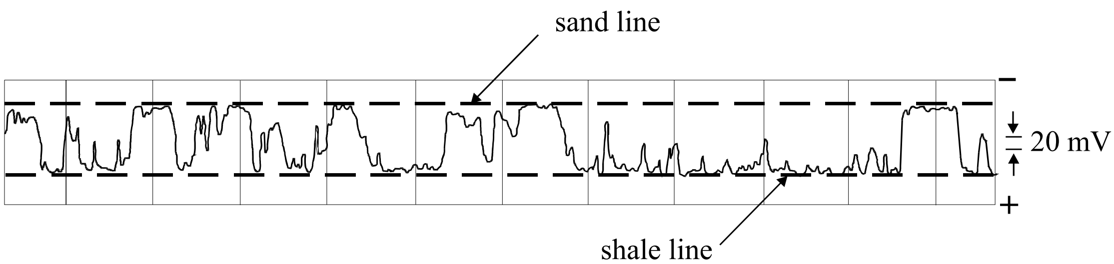

Figure 6. An SP log through interbedded sandstones and shales (modified after Sheriff 1991).

Induced Polarisation (IP) Logs

IP is a technique which is commonly used in surface prospecting for minerals but it can also be used in downhole applications. IP uses a transmitter loop to charge the ground with a high current. The transmitter loop is then turned off and the change in voltage with time is monitored using a secondary loop.

In borehole applications, the primary loop induces a current flow in the rocks beyond the borehole wall. This current flow can lead to a charge build-up on conductive particles such as sulphide ores and carbonaceous material such as coal (Figure 7). The time-dependent dissipation of this charge is reflected as a decaying voltage.

IP logging is widely used in mineral exploration, and has particular value in the exploration for disseminated sulphide targets such porphyry copper deposits.

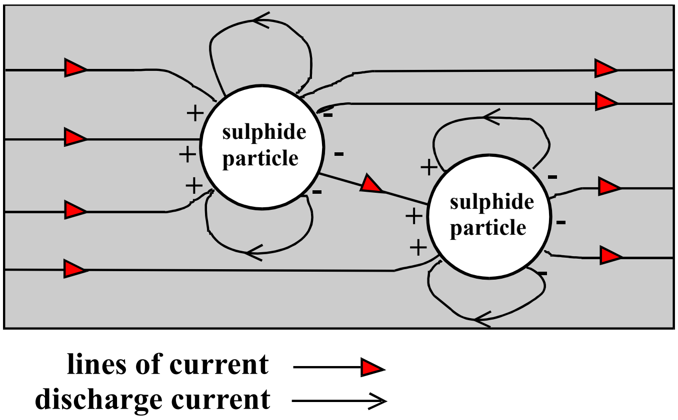

Figure 7. IP logging can be used to detect disseminated conductive grains (modified after Hallenburg, 1984).

The disseminated nature of these targets make them ideal for IP but otherwise difficult to detect. IP has also been used in the detection of zones of alteration and redox trends and it has been used successfully to determine the rank of coal *in situ*.

MAGNETIC SUSCEPTIBILITY LOGS

Magnetic susceptibility is the ratio of the intensity of magnetization of a magnetizable material to the intensity of an applied magnetic field. More formally it is a dimensionless quantity, which expresses the ease with which a substance may be magnetized.

The magnetic susceptibility sonde is similar to the induction conductivity sonde. A detailed description of the tool is given by McNeil, et al. (1996)

In practice, the magnetic susceptibility of a rock depends on the ferromagnetic mineral content. Magnetite is the most important ferromagnetic mineral, due to its widespread occurrence in nature and its high magnetic susceptibility, but other ferromagnetic minerals, such as illmenite, maghemite and pyrrhotite also cause magnetic susceptibility anomalies.

In sedimentary regolith, maghemite clasts are often present in gravelly beds, and so magnetic susceptibility logs can be particularly useful. They can be used to identify layer boundaries (eg. clay versus sand versus gravel. See for example the regolith log in Figure 9). The method is also useful in some cases for correlating lithological facies by identifying differing origins of similar materials, when for example some of the sediments are derived from mafic rocks.

It is important to note that magnetic susceptibility measurements taken in highly conductive material (>200mS/m) need to be corrected for conductive effects.

RADIOACTIVE METHODS

The principal radioactive emissions of interest in borehole geophysics are gamma rays and neutrons. Other radioactive products such as alpha particles (helium nucleii) and beta particles (electrons) can penetrate such small distances through rocks that they are not useful for logging.

Natural Gamma Logging

The simplest radioactive method in geophysical well logging is the natural gamma log. These logging tools record the level of naturally occurring gamma ray emissions from the rocks around a borehole. The simplest of these type of tools records only the total gamma ray signal. This signal is comprised essentially of gamma ray emissions at different energy levels from the radioactive isotopes of the elements potassium (^{40}K), Thorium (^{232}Th) and Uranium (^{238}U) and the daughter products in the decay series of each.

The distribution of K, Th and U (and their daughter products) varies widely in the continental crust and can also be significantly affected by regolith processes and by biological activity. As a result, logging of the gamma ray signal emanating from the rocks around a borehole can provide considerable information about the geology and the processes that have operated.

In sedimentary rock sequences, relatively high natural gamma counts are recorded in shales and other clay-rich sediments and relatively low counts are recorded in clean quartz sandstones and limestones. The high signals observed in clay-rich sediments are largely due to the affinity of clay minerals for potassium. However, many regolith clays are leached and do not contain substantial amount of potassium. Therefore, this interpretation is not always applicable for regolith units.

More sophisticated natural gamma logging tools separately record the gamma ray counts of the three decay series. In this way detailed information about the chemistry of the rocks in the borehole wall can be acquired. In practice, the sensors in these tools aren't directly measuring the parent nuclides ^{238}U and ^{232}Th, instead they record gamma ray emissions from the daughter products ^{214}Bi and ^{208}Tl.

The distance that an emitted gamma ray can travel through rocks is strongly dependent on the electron density of the medium because it is through scattering interactions with electrons that the gamma ray photons lose their energy. In practice, the gamma rays may penetrate as much as 1-2 metres through the rocks, though this depends strongly on their initial energy level and the rock density. Distances are greater in low density rocks such as highly porous sediments and coals and correspondingly much less in dense crystalline rocks. Gamma logs have been successfully used to search for roll front uranium deposits in regolith.

Because gamma rays can travel such distances through rock, the spatial resolution of the method is affected. Boundaries between widely differing natural gamma ray emitters can tend to be somewhat "smeared" in the gamma ray log results. Moreover, because the emission of gamma rays is a physical process with natural statistical variability, gamma response has a temporal variation. In logging, this effect is minimised by averaging response over a fixed time interval.

Neutron Porosity Logging

Neutron porosity logging uses an active neutron source to emit neutrons into the rocks around a borehole. Because free neutrons are almost unknown in the Earth, the flux of neutrons subsequently recorded at the detector in the tool can be used as an indicator of the conditions in the surrounding rocks.

The neutrons entering the rocks of the borehole wall from the tool are at high energy and generally have great penetrating power. The exception is when significant concentrations of hydrogen exist. In this case, the neutrons rapidly loose energy due to collisions with the hydrogen nucleii and become what are known as “thermal neutrons”. These thermal neutrons behave in many respects like a diffusing gas and form a spherical shell around the source in the probe. The radius of this sphere will depend primarily on the concentration of hydrogen in the environment around the probe.

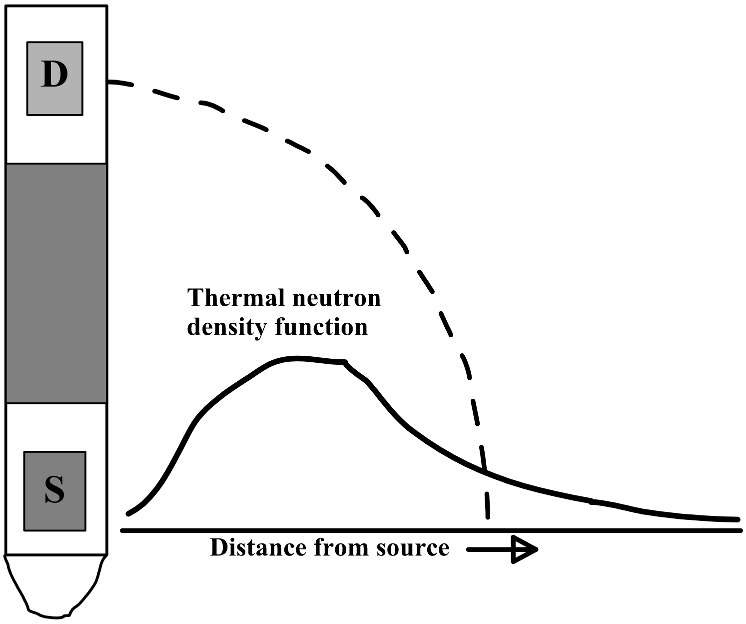

Figure 8. The density distribution of thermalised neutrons around a neutron tool

In general the neutron tool is a very useful tool for measuring “porosity” but it must be remembered that the measurements are model-dependent. In particular:

1. the pores are assumed to be completely water-filled;

2. any hydrogen structurally bound in minerals (eg. clays in the form of OH) will have the same affect of slowing neutrons down. Thus an independent estimate of “shale” content will be needed (eg. an SP or a resistivity or a natural gamma log);

3. the neutron tool only measures the properties of the rocks very close to the borehole (ie. there may be complications with drilling-induced changes); and,

4. the neutron log results are influenced by changes in borehole diameter.

Primary Calibration of the Instrument

Neutron porosity tools are traditionally calibrated in API test pits built from a sequence of limestone samples of differing water-filled porosity. Thus the porosity values obtained from neutron logs actually refer to *equivalent limestone porosities*.

In Australia, AMDEL maintain a series of these API test pits at its suburban Adelaide site and logging equipment is generally taken there on a regular basis to re-check the primary calibrations of the equipment.

In order to make sense of these equivalent limestone porosities, a series of curves are usually provided showing how the limestone porosities correlate with porosities in other rocks

Strengths of the Neutron Porosity Logging Technique

The neutron porosity log can be run in a hole, which has been cased with steel. Logging in shallow holes cased with PVC is a problem though because of the H in the PVC.

Because the technique is sensitive to lithological differences, neutron porosity logs can be very useful in cross plots with other log data to help determine lithology.

In mineral geophysical logging in hard rock environments (low porosities) the neutron porosity log can often be used in place of a resistivity log (since both actually measure water-filled porosity). In cases where the neutron porosity log indicates higher porosities than does the resistivity log, the cause could be hydrocarbons in the fluid, or lack of effective permeability (ie. the pores are not well interconnected).

5. EXAMPLE REGOLITH LOG

An example of wireline logs of a drillhole through regolith is shown in Figure 9. Other data included are grain size (visual estimate of combined one metre composite cutting samples) of the transported alluvial sediments which overlie weathered diorite, and mineralogy (as determined by quantitative XRD).

The magnetic susceptibility log shows several sharp spikes that correspond to the presence of detrital grains (and gravel clasts at 11-12 and 20-21 m) of maghemite in the sediment. The slightly higher readings in the weathered bedrock are probably due to disseminated magnetite.

The conductivity log shows higher conductivity in clayey units of the sediment, and in the clayey saprolite. Conductivity falls dramatically at the saprolite/saprock interface. The higher conductivity portions of the log may be due to more saline groundwater in the clay units, which have around 20% porosity, but low permeability.

The gamma log does not clearly reflect the sand/clay ratios of the sediment, in contrast to the usual responses in sedimentary rocks. This is a result of the predominance of kaolinite (which is devoid of potassium) in the transported regolith clays.

However, the four large spikes and the smaller anomaly at 45 m in the magnetic susceptibility log correspond to small local dips in the gamma log, indicating that these dips are associated with more sandy beds. Many local highs and lows in the conductivity log appear to correspond to local highs or lows in the gamma log. This probably reflects local changes in grain size and mineralogy that aren’t evident from the sampling techniques and laboratory methods used.

6. CONCLUSIONS

Geophysical well logging provides many different opportunities to investigate the material making up the walls of a borehole, be it regolith or crystalline rock. A wide range of different sensors provide information which is complementary in nature. Best results are obtained by running a suite of logs and analysing their similarities and differences.

7. PROBLEMS, LIMITATIONS

The biggest problem in using geophysical well logging is that you must have a “well” (ie. a borehole) in which to operate. The cost of drilling means that boreholes are not always available and hence geophysical well logging will not always be possible for a particular study. In regolith, it may be difficult to stop holes from collapsing while wireline logs are run. Two possible methods of stabilising holes are to drill with foam, which helps prevent collapse, or insert plastic casing into the hole, and log inside the casing.

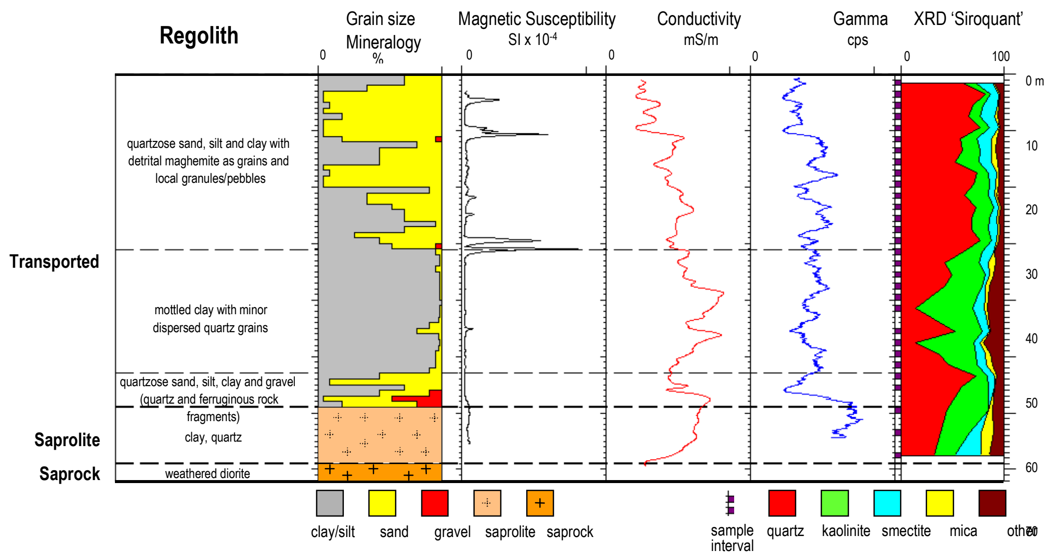

Figure 9. An example of wireline logs of a drillhole through regolith.

When geophysical well logging methods can be used, it is important to recognise that each method has its own particular strengths and weaknesses. The presence of PVC casing for example can prevent electrical logging but has little impact on natural gamma logs. Similarly, such casing presents a problem for neutron logging because of its hydrogen content whereas a steel casing generally does not. The specific problems and limitations vary from log to log and need to be understood on a case by case basis.

8. SURVEY ORGANISATIONS

Geophysical well logging is in many respects a mature technology and as a consequence it is available as a commercial service from many companies.

9. COSTS

Costs of geophysical logging vary depending on the depth of the borehole to be logged and the types of logs to be run. In the extreme case, log runs of exploration and production holes in the petroleum industry often cost upward of A$1 million, particularly in offshore operations. In the mineral industry and in groundwater applications, boreholes are normally much shallower and costs are consequently much lower.

REFERENCES

Hallenburg, J.K., 1984. Geophysical logging for mineral and engineering applications. PennWell Books, Tulsa, Oklahoma, 254 pp.

Keys, W.S., 1988. Borehole geophysics applied to groundwater investigations. U.S. Geol. Surv. Open File Report 87-539, Denver.

McNeill, J.D., Hunter, J.A. and Bosnar, M., 1996. Application of a borehole induction magnetic susceptibility logger to shallow lithological mapping. Journal of Environmental and Engineering Geophysics 2: 77-90.

Schlumberger, 2000. Beginnings. A brief history of Schlumberger wireline & testing, WWW site: http://www.1.slb.com/recr/library/wireline/brochure/beginnings.html

Sheriff, R.E., 1991. Encyclopedic Dictionary of Exploration Geophysics, Society of Exploration Geophysicists, Tulsa, Oklahoma, 376 pp.